THESIS FOR THE DEGREE OF DOCTOR OF PHILOSOPHY (PHD)

Genetic and epigenetic alterations of invasive melanoma cells

by Viktória Koroknai

Supervisor: Margit Balázs, PhD, DSc

UNIVERSITY OF DEBRECEN

DOCTORAL SCHOOL OF HEALTH SCIENCES

DEBRECEN, 2020

Table of contents

Abbreviations

CGH: comparative genome hybridization

AMT: amoeboid-mesenchymal transition

CAN: copy number alteration

CGI: CpG island

CHL1: cell adhesion molecule L1

CIMP: CpG island methylator phenotype

CN: copy number

CNV: copy number variation

DHS: DNAse I hypersensitivity site

DMP: differentially methylated probe

DMR: differentially methylated region

DNMT: DNA methyltransferase

ECM: extracellular matrix

EMT: epithelial-mesenchymal transition

EWAS: epigenome-wide association study

FBN1: fibrillin-1

GDNF: glial cell derived neurotrophic factor

GEO: Gene Expression Omnibus

GLIPR1: GLI pathogenesis-related 1

GPAA1: glycosylphosphatidylinositol anchor attachment 1

HM450K: Illumina Infinium II Human Methylation 450K

MAPK: mitogen-activated protein kinase

MAT: mesenchymal to amoeboid transition

MC1R: melanocortin receptor 1

MITF: microphtalmia-associated transcription factor

MMP: matrix metalloproteinase

MSH: melanocyte stimulating hormone

MTA: methylthioadenosine

NAV2: neuron navigator 2

ncRNA: non-coding RNA

NM: nodular melanoma

NNMT: nicotinamide N-methyltransferase

OS: overall survival

PAX3: paired box gene 3

PCA: principal component analysis

PD-1: programmed cell death protein 1

PLEC: plectin

qPCR: quantitative PCR

RA: retinol acid

RBP4: retinol binding protein 4

RGP: radial growth phase

SHARPIN: SHANK-associated RH domain interactor

SKCM: Skin Cutaneous Melanoma

SOX10: SRY-related HMG-box 10

SSM: superficial spreading melanoma

TCGA: The Cancer Genome Atlas

TSS: transcription start site

UHRF: ubiquitin-like protein containing PHD and RING finger domain

VGP: vertical growth phase

Introduction

Malignant melanoma is considered as one of the most aggressive human cancer with a very high metastatic potential [1-4]. Although it is a relatively rare type of skin cancer, it accounts for the majority of skin cancer death [5]. Global incidence of melanoma is about 230,000 new cases per year, with 55,000 deaths, however, the estimated age-standardized incidence (cases per 100 000 residents) varies widely (Figure 1, 2) [6, 7].

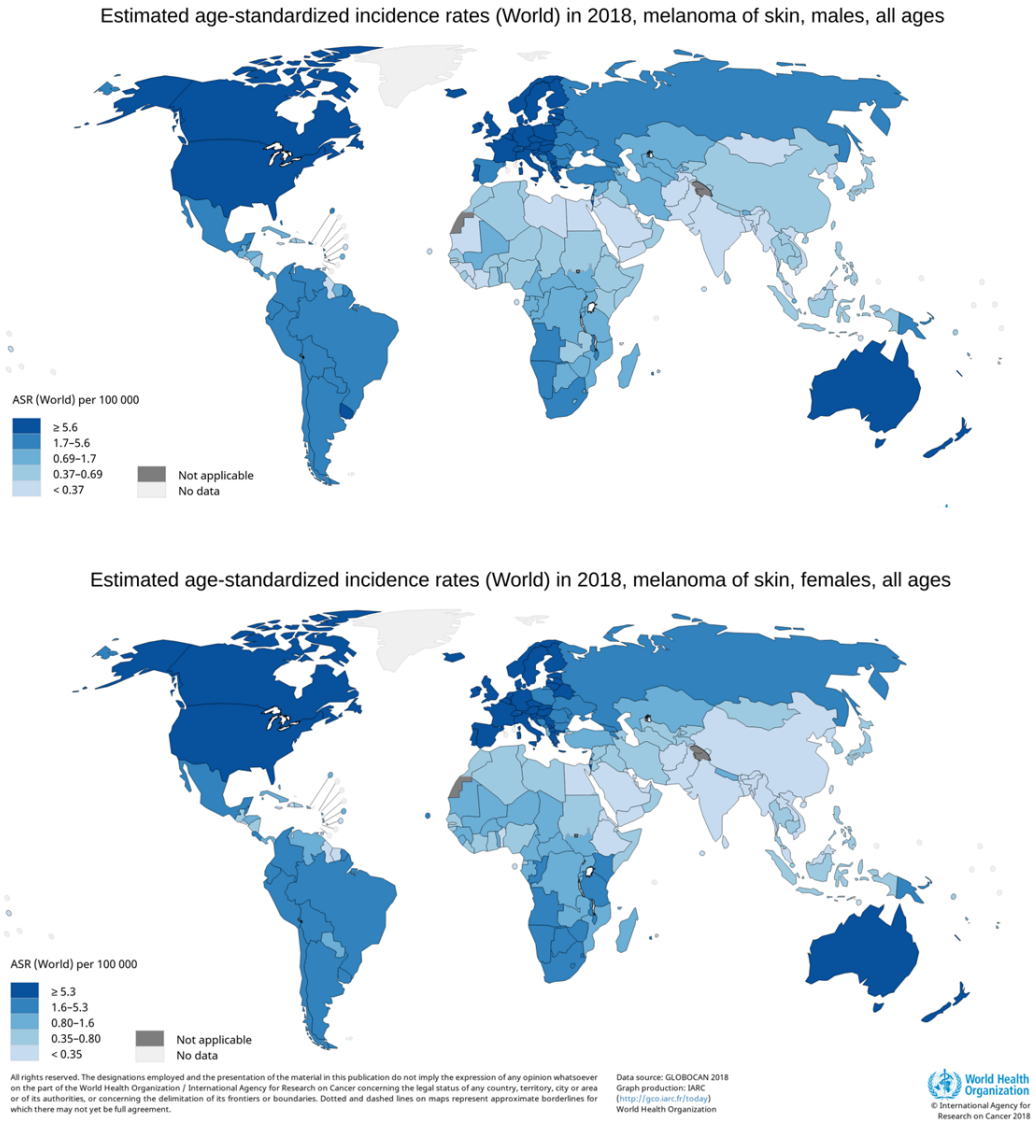

Figure 1. Global, estimated age-standardized incidence rate of melanoma of the skin. *Source: https://gco.iarc.fr/today [7].*

In Europe, the annual incidence is 13.5 new cases per 100,000, while the highest documented frequency is in Australia (56 cases per 100 000 per year for men, and 41 cases per 100 000 per year for women) [4, 8, 9]. Recently, the rapid rise in melanoma incidence appears to be slowing, specifically among younger age groups, it has been found that the long-term incidence is still increasing globally, including Hungary as well [10, 11].

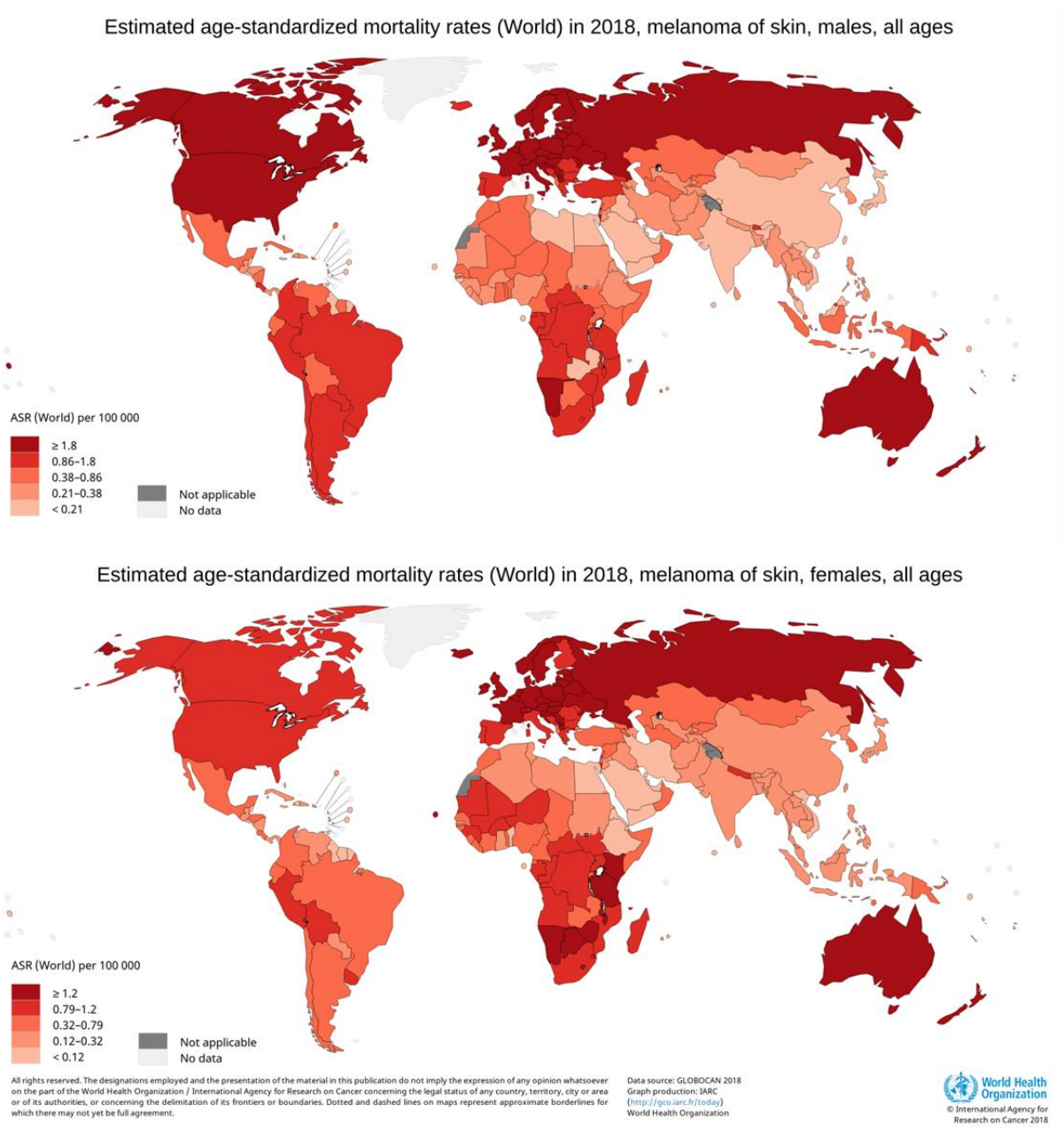

Figure 2. Global, estimated age-standardized mortality rate of melanoma of the skin
Source: https://gco.iarc.fr/toda [7].

The individual risk of emerging melanoma depends on factors such as the phenotype (fair skin, red or blond hair, blue eyes, increased number of nevi, and freckles), sun exposure, family history, and similar to other tumour types, accumulation of several molecular alterations can be observed [9, 12]. Epidemiological studies have indicated the relationship between ultraviolet-B (UVB) radiation exposure and melanoma development; moreover, Elwood et al. have pointed out that sunburns in childhood are associated with the highest risk [13, 14].

Patient survival with melanoma is still very poor, especially patients with metastatic tumour. Disease stage strongly determines the overall survival (OS), as the 5-years OS is estimated to be 94-100% for stage I melanoma, while only 9-28% for stage IV tumour [4, 5].

Despite the increasing treatment possibilities, early diagnosis and complete surgical excision still remain the best treatment for melanoma patients [8, 15, 16]. Until the discovery of new therapeutic approaches such as kinase inhibitors (BRAFV600E kinase inhibitors) and immune check point blockade therapies (CTLA-4 immunomodulatory antibody), chemotherapy with dacarbazine (DTIC) was the therapeutic standard, which had no clear survival benefit [17-19]. Anti PD-1 antibodies and their combinations with CTLA-4 treatment further improved the response rates for immunotherapies [20, 21]. Although these therapeutic approaches have significantly improved patient survival, resistance to kinase inhibitor therapy and side-effects of immunotherapies remain unsolved problems. Establishment of biomarkers for clinical benefit are especially important for treatment response and survival. Recent studies have underlined the significance of multiple parameters and their combinations to identify tumour-focused signatures [5, 20, 22]. Novel prognostic biomarkers are certainly needed to better identify primary melanoma tumours with metastatic capacity.

During our study we focused on to define the molecular background of invasion of melanoma cells, as an initial step of metastasis formation. Our main goal was to further advance the

understanding of the relationship between copy number alterations and the invasive behaviour of melanoma cells. In addition, we aimed to study the DNA methylation landscape and its effect on gene-expression of early invasion using a direct, *in vitro* selection of invasive melanoma cell subpopulation established from primary malignant melanomas.

Background

Cutaneous malignant melanoma and metastatic spread

Cutaneous melanoma develops from melanocytes, which originate from highly motile neural crest progenitors that migrate through the skin during embryonic development [3, 23-25]. The neural crest is an embryonic cell population that originates from the ectoderm, and after intensive migration, neural crest cells give rise to different cell types, including neural cells, smooth muscle cells, mesenchymal cells, and melanocytes [26, 27]. The differentiation of melanocytes and their progenitor cells, melanoblasts, is controlled by a complex network of transcription factors, including microphtalmia-associated transcription factor (MITF), which transcription is activated by the synergistic act of SOX10 and PAX3, and drives the expression of several genes essential for melanogenesis [26-28].

Melanin is a macromolecule produced by the melanocytes. In response to UV radiation, melanocyte stimulating hormone (MSH) is produced by keratinocytes of the skin, that stimulates melanin release of the melanocytes through melanocortin receptor 1 (MC1R) to prevent DNA damage [15, 29]. Primary melanomas can be originated from different types of precursor lesions, including benign naevi, dysplastic naevi and melanoma in situ [30].

The high metastatic potential and the resistance to many treatments make cutaneous melanoma the most life-threatening form of skin cancers [2, 30]. Metastasis is the escaping process of cancer cells from the primary tumours and the development of new tumour in other tissues [31].

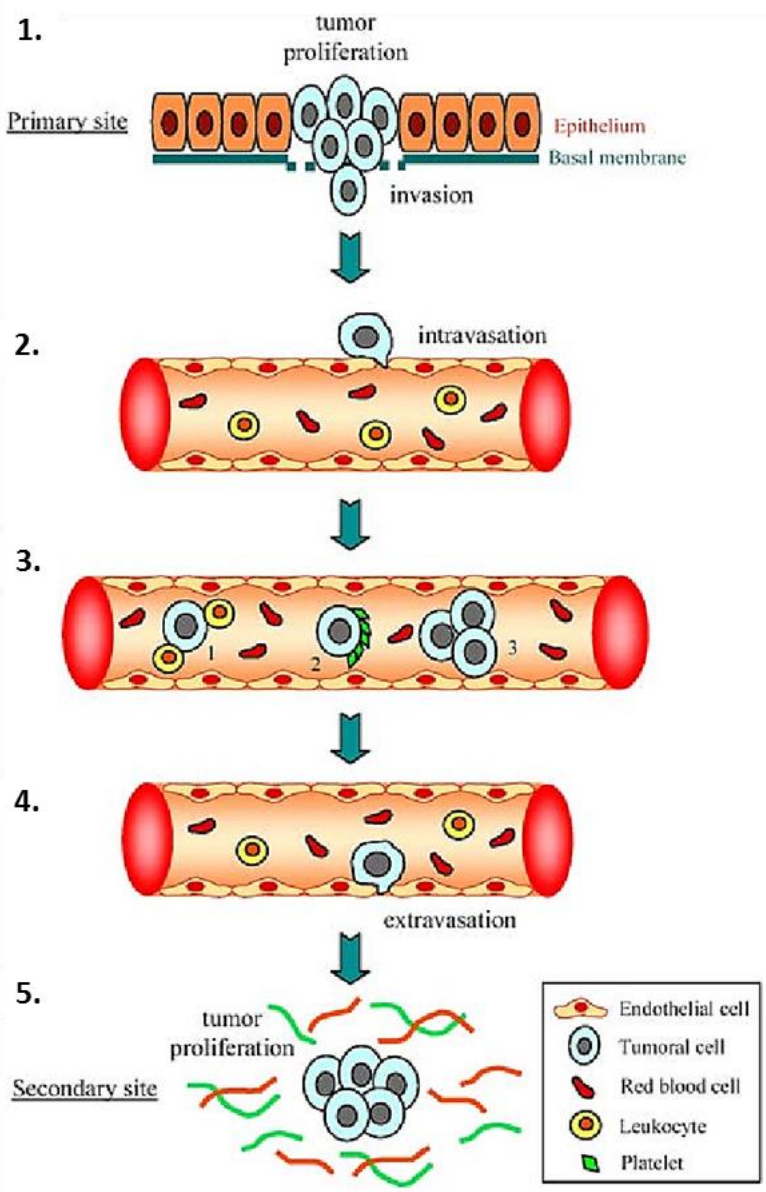

Figure 3. Metastatic cascade*. (1) Invasion of primary tumour cells. (2) Intravasation to vessels. (3) Survival in the circulation system. (4) Extravasation in target organ. (5) Proliferation and metastatic colonization (Gout et al in 2008 [32]).*

Metastasis formation is a multi-step process that includes (1) tumour cell invasion, (2) intravasation to vessels, (3) survival in the circulatory system, (4) extravasation and (5) proliferation, leading to metastatic colonization (Figure 3) [31, 33, 34]. To efficiently metastasize, invasive melanoma cells change their cytoskeletal organization and alter their contacts with the extracellular matrix (ECM) and the surrounding stroma [2]. In order to invade

the stroma, tumour cells have to pass through the basement membrane. Basement membrane is a specialized ECM which assembled from laminin and collagen type IV, and essential for tissue function and integrity as providing barrier to the migrating cells [35]. When invading, cells have broken through the basement membrane and cells enter the stroma [33].

The acquisition of invasive potential is one of the key transition in the progression of benign tumours to life-threatening metastatic melanoma [36]. Furthermore, the invasive strategy of melanoma cells depends on the microenvironment and the effects of therapeutic regimens [37-40].

Melanoma cell plasticity

The ability of melanoma cells to pass through the ECM and invade the surrounding tissues requires the transition of typical epithelial histologic features including apical-basolateral polarization, basement membrane integrity, and cell-cell adhesion to cells of invasive phenotype [41]. This transition is characterized by alterations in the cell shape; loss of epithelial cuboidal or columnar shape and gain of elongated morphology via increased expression of mesenchymal proteins and reduced expression of proteins maintaining epithelial integrity [41-43] (Figure 4). This phenotypical switch is termed as epithelial-mesenchymal transition (EMT). The disruption of actin cytoskeleton, remodelling cell-matrix adhesions, and loss of epithelial feature accompanied with the gene expression of invasive signature is characteristic of the progression to an invasive phenotype of most neoplasm, including melanoma [41, 44].

Tumour cells have different strategy of movement. Apart from the collective invasive strategy, where cells invade as multicellular units by forming strands or sheets, individual tumour cells can also migrate through tissue compartments separated by the basement membrane [2, 33, 34] (Figure 4).

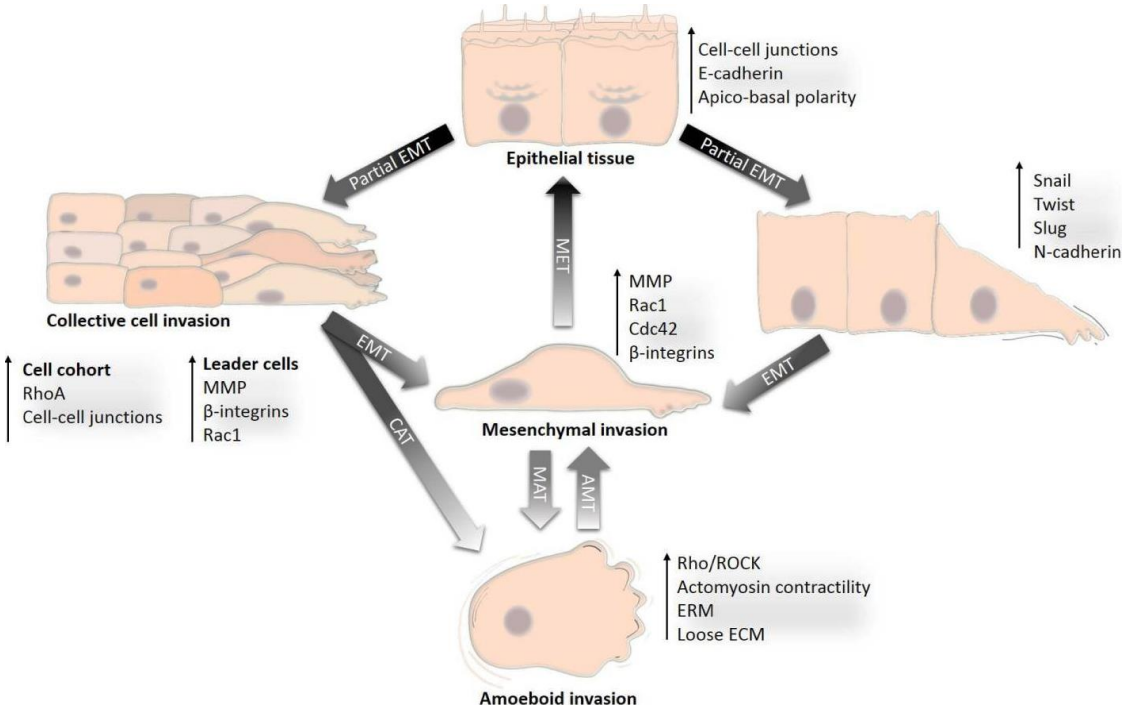

Figure 4. Switch between the different invasion modes (Gandalovicova et al. 2016 [41]).

Collective movement is sufficient only for entry into the lymphatic system, while individual cell movements enable for intravasation [45]. The main types of individual invasion are the elongated/mesenchymal and the rounded/amoeboid modes [2]. The morphology of the cancer cells is mainly depends on the actomyosin contractility, and the balance of adhesion and tension caused by the physical force [46]. During the amoeboid mode of movement, the actomyosin contractility leads to less adhesive and rounded cell shape. Actin assembly also contributes to generate protrusions and adhesion between cells and the extracellular matrix [47]. This type of motility does not require integrin signalling or degradation of the ECM by proteases [48]. In contrast, mesenchymal cells mediate adhesions via integrin molecules, and degrading the surrounding matrix by protease enzymes (e.g., matrix metalloproteinases: MMPs); Elongated movement also requires actomyosin contractility in retracting protrusions [37, 49].

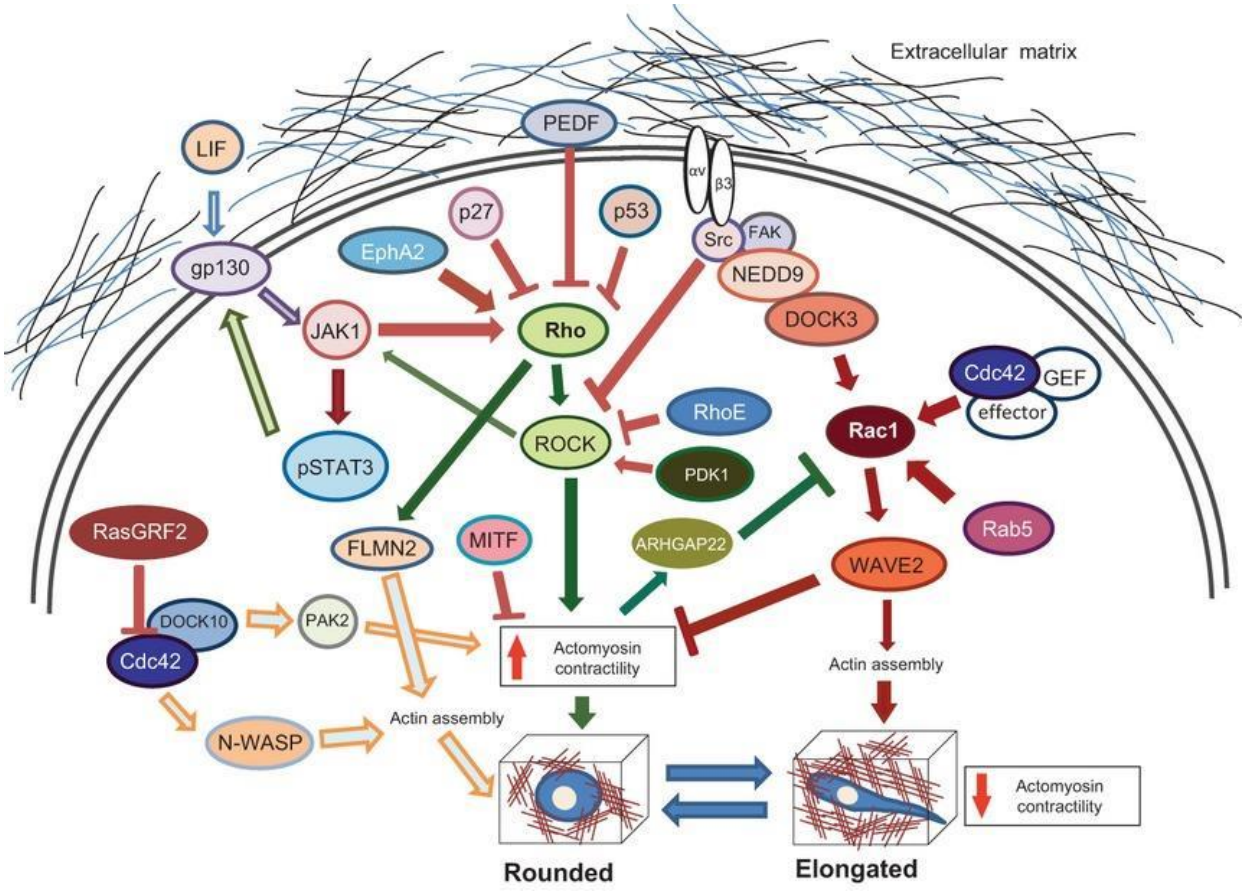

Figure 5. Signalling pathways that regulate plasticity in melanoma cell invasion (Orgaz et al. 2013 [2]).

Several studies have been carried out in the last decades focusing on the signalling pathways in association with invasive cell's plasticity. Rho GTPase signalling is one of the main molecular pathways of interest in this field, as Rho-family GTPases are key regulators of cytoskeletal motility, actomyosin contractility, adhesion, proliferation and survival [37, 38, 50]. Amoeboid type of movement is induced by Rho-ROCK and Cdc42 signalling generating actomyosin contractility, while Rac1 signalling is involved in the elongated movement through actin assembly (Figure 5).

Melanoma cells appear to be highly plastic and can change between amoeboid and mesenchymal movement during invasion (Figure 4) [37, 51]. Inhibition of proteases results in the activation of Rho-ROCK signalling and the switch of the type of movement from the

mesenchymal into the amoeboid mode via mesenchymal to amoeboid transition (MAT) [38]. Amoeboid cells can also switch to mesenchymal mode by amoeboid-mesenchymal transition (AMT), however, this process needs further investigations [41].

Histopathological studies have been described that the invasive front of the melanomas consists of round-shaped cells, while cells from the internal part of the tumour have elongated, spindle-shaped form [52]. Rounded tumour cells can move faster than the elongated cells, however, ECM remodelling is necessary to cross the barriers into the vessels; therefore, the ability to change the movement strategy during the invasion is essential [53, 54].

Genetic alterations in invasive melanoma

Accumulation of genetic alterations that lead to uncontrolled cell proliferation is involved in the development of different type of cancers including melanoma. Most of the investigations about these genetic alterations have been carried out on advanced melanomas; considering different types of precursor lesions and heterogeneity that are characteristic for melanomas, therefore it is difficult to summarize the order of mutations during melanoma progression [55, 56].

In the last decades, numerous studies have focused on the genetically disrupted signalling pathways affecting the pathogenesis of melanoma. Melanomagenesis can be associated with different somatic mutations affecting the MAPK signalling pathway activation, including KIT^{L5J6P}, $NRAS^{Q61K}$ or $BRAF^{V600E}$ mutations, or loss of tumour suppressor genes, e.g., *PTEN*, $P14^{ARF}$, or $P16^{INK4a}$, involved in cell cycle regulation [57-63] (Table 1). However, the association of mutations and/or copy number alterations with the invasive capacity of melanoma cells remain incompletely understood.

Table 1. Proto-oncogenes and tumour suppressor genes altered in cutaneous malignant melanoma by mutations or copy number alterations [64].

Gene type	Genes	Genetic alteration
Proto-oncogenes	*NRAS*	15–30% mutated
	BRAF	50–70% mutated
	KIT	<17% mutated
	MITF	10% mutated, 10% amplified
	AKT3	40–60% amplified
	CCND1	10–40% amplified
	CDK4	Rarely mutated, 5% amplified
	MDM2	5% amplified
Tumor suppressor genes	*PTEN*	10% mutated, 30–50% deleted
	TP53	10% mutated
	$P14^{ARF}$	40–70% mutated/deleted
	$P15^{INK4b}$	<5% mutated, 40–70% deleted
	$P16^{INK4a}$	30–70% mutated/deleted

$BRAF^{V600E}$ mutation (harboured by 50-70% of melanomas) is one of the most significant alteration in human cutaneous melanoma [59]. Braf is the member of Raf family of serine/threonine kinases, which have crucial role in the activation of ERK/MAPK pathway that involved in the regulation of cell growth, survival and differentiation [65]. The gain-of-function mutation of *BRAF* gene leads to increased proliferation and survival by constitutive activation of the ERK signalling [65]. Furthermore, $BRAF^{V600E}$ mutation is also involved in invasion and metastasis development of melanoma. *BRAF*-activating mutation can increase the expression of MMP1 protease via Raf/MEK/ERK pathway [66].

Mutations resulting in loss of the *PTEN* tumoursuppressor gene occur in 5-20% of advanced melanomas [55, 64]. *PTEN* loss of function leads to activation of AKT protein kinase, which inhibits RhoB in melanoma cells, promoting tumour cell invasion and metastasis formation [67]. On the other hand, a study by Dankort et al. has indicated the cooperation between *PTEN* loss and $BRAF^{V600E}$ in invasion and metastasis [68].

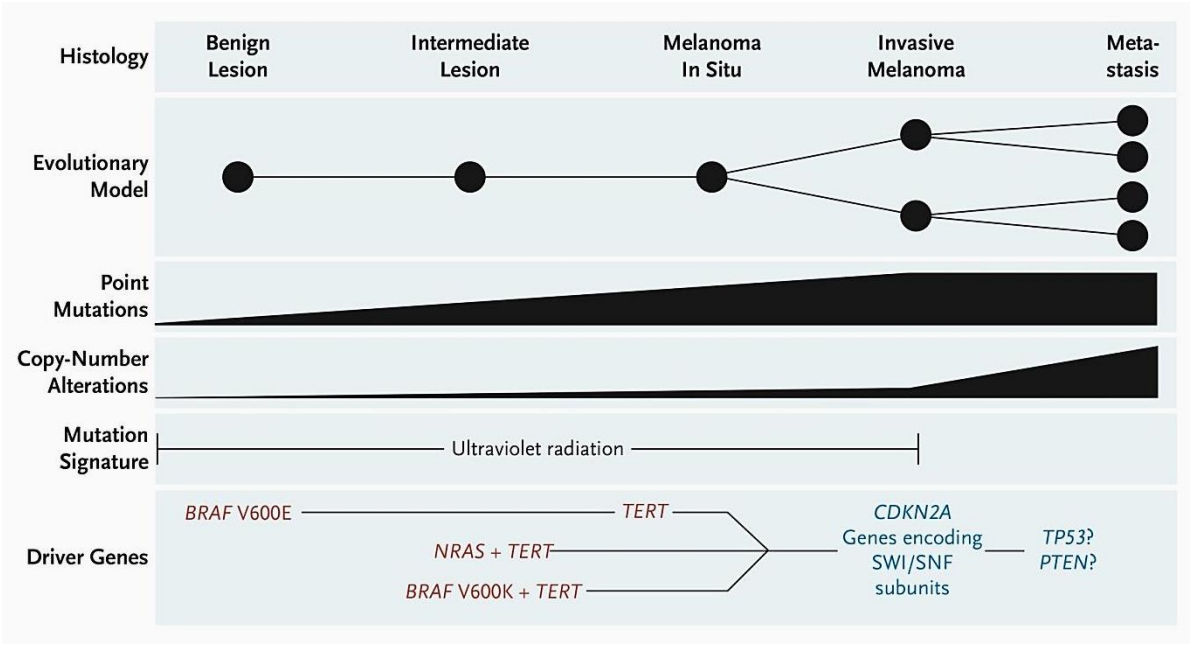

Figure 6. Proposed model for progression of melanomas (Shain et al. 2015 [55]).

Deletion of *CDKN2A* gene, which encodes $P14^{ARF}$ and $P16^{INK4a}$, has been described as a specific genetic event in invasive melanomas [55, 69, 70]. A progression cascade that was described by Shain et al. is based on the pattern of genetic changes associated with different stages during melanoma progression [55]. According to this proposed model, the cascade is initiated by mutations that trigger the MAPK signalling (*BRAF*, *NRAS*), while *TP53* and *PTEN* mutations were found only in advanced primary melanomas (Figure 6). The model indicates the role of biallelic inactivation of *CDKN2A* in the invasive phenotype of melanoma. Zeng et al. also observed that loss of $p16^{INK4A}$ promotes melanocyte migration and contribute to the invasive and metastatic capacity of melanoma cells through the activation of BRN2 (*POU3F2)* transcription factor [70]. Moreover, *RAC1* gain-of-function mutation has been identified in association with the motility of melanoma cells [71, 72]. RAC1 is a member of the Rho GTPase family that has important roles in the control of cell proliferation, cytoskeletal reorganization particularly in EMT and cell migration [73].

Gene expression signature of invasive melanoma

According to gene expression patterns of melanoma tissues, it can be categorized into different groups with different metastatic potential [74, 75] (Figure 7). One of these signatures (the so-called proliferative phenotype) is characterized by the overexpression of *MITF* and other melanocytic genes (e.g., *TYR*, *DCT*, and *MLANA*) along with several neural crest-related factors (e.g., *SOX10*, *TFAP1A*, and *EDNRB*). This signature is associated with high rates of proliferation among with low motility, and sensitivity to develop inhibition by TGF-β [74]. On the other hand, the second signature (the so-called invasive phenotype) downregulates the aforementioned proliferative gene signature and exhibits the upregulation of genes involved in extracellular matrix remodelling (TGFß-type signalling), and in the epithelial-to-mesenchymal transition (EMT) (e.g., *ZEB1*, *COL5A1*, *SERPINE1*, and *WNT5*). The invasive signature of the tumour is associated with lower rates of proliferation, high motility, and resistance to growth inhibition by TGF-β.

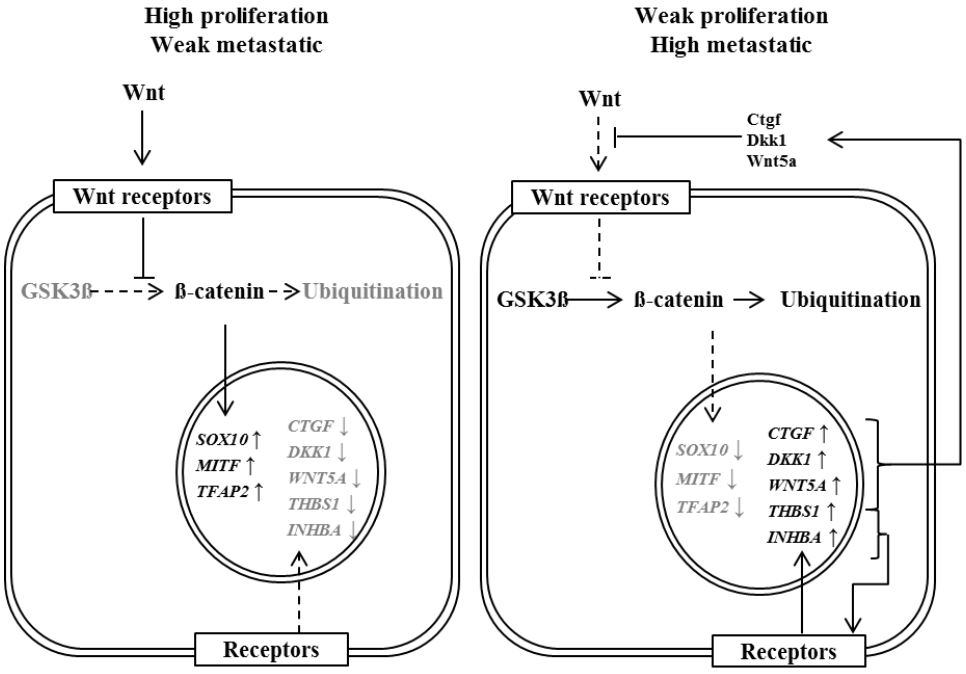

Figure 7. A gene regulation model for melanoma metastatic potential. *Adapted from Hoek et al. (2006) [75].*

Among upregulated genes in the invasive phenotype, there are several genes (e.g., *DKK1*, *CTGF* and *WNT5A*) which arrest Wnt signalling, suggesting that the activation of TGF-β pathway may accelerate the suppression of Wnt signalling [74-76].

Moreover, switch between invasive and proliferative phenotype has been described, which is ~~a~~ possibly the result of changes in the microenvironment during melanoma progression. This switch is coincident with an exchange in gene expression pattern from proliferative to invasive and vice versa (Figure 8) [74]. The exact definition of these specific microenvironmental indications remains incomplete, but hypoxia and inflammation can have effect on the phenotype switching of melanoma cells [77, 78].

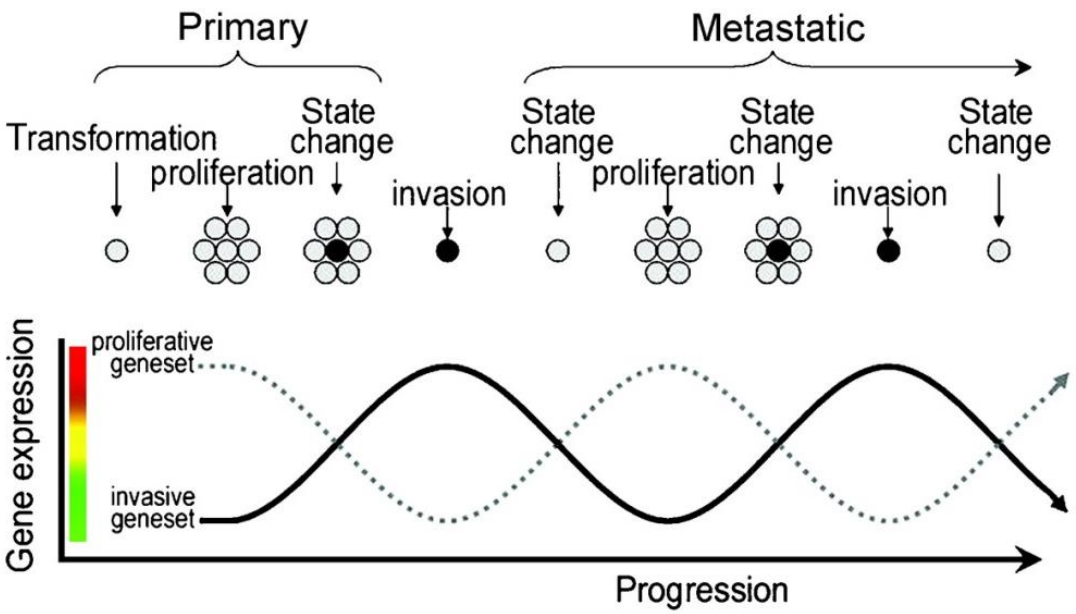

Figure 8. A model for gene expression changes occur in parallel with changes of metastatic potential and progression in melanoma (Hoek et al. in 2008 [74]).

Another important finding by Hoek et al. was that gene expression patterns exhibit correlation neither with the activating mutations of *BRAF* or *NRAS* nor with the consequent MAPK pathway components [75]. Due to the fact that the highly frequent *BRAF* mutation is one of the most promising therapeutic targets, the Hoek et al. study shed light into alternative molecular

pathways other than mutations. Verfaillie et al. developed a gene expression based prediction system in order to predict invasion according to the gene expression signature of melanomas [79]. The gene signatures distinct for proliferative and invasive cellular states were also described and extended into the gene regulatory landscape (Figure 9). Indeed, the proliferative cellular state is characterized by the expression of SOX10 and MITF transcription factors as master regulators of the melanoma-proliferative cell state. Both SOX10 and MITF are extensively studied in the context of neural crest cell development and melanocytic differentiation. On the contrary, invasive cells exhibit TEAD and AP1 expression. This study indicates that the gene regulatory network can be regulated into a different state by perturbing one of these master regulators and is consistent with the facility to switch from a proliferative to an invasive state through transcriptional reprogramming [79]. Furthermore, duplication of 7q34 was found to be enriched in the invasive melanoma samples including *BRAF* gene by Verfaillie and colleagues [79].

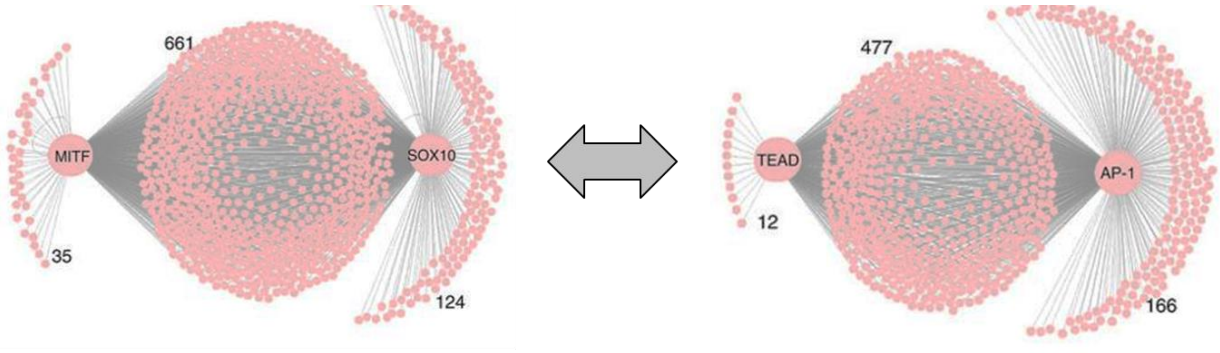

Figure 9. Predicted invasive (right) and proliferative (left) networks showing MITF/SOX10 and TEAD/AP-1 as master regulators, respectively (Verfaillie et al. in 2015 [79]).

Supporting the clinical relevance of studying invasion related transcriptomic and regulatory events, it seems that *TEAD* knockdown increases the sensitivity of invasive melanomas to MAPK-targeted therapeutic interventions [79]. Notably, the TEADs were previously shown

to be the key effectors of the Hippo pathway that is known to confer invasive properties in melanoma [80, 81].

DNA methylation pattern related to invasive behaviour

Epigenetic alterations of DNA, including DNA methylation, histone modifications, chromatin remodelling and non-coding RNA-mediated gene interference, do not modify the sequence code; however, they are heritable and involved in regulation of gene expression [82]. DNA methylation is the addition of a methyl group to the 5′-carbon of cytosine that results in 5-methyl-cytosine [83]. The localizations of methylated cytosines in the human genome are the so-called CpG islands (CGIs), which are CG-rich sequences of the genes [82]. CpG islands are generally located on the promoter region of genes, and they have a 60-70% overlap with transcriptional start sites (TSSs). Methylation of CGIs in the promoter site of genes is related to gene silencing, however, it can also have a gene-activating effect in specific cases [82]. Besides CGIs, CGI shores are located within 2 kb of islands upstream and downstream, CGI shelves are 2 kb regions upstream and downstream of the CpG island shores, and open seas are regions more than 4 kb distance from CGIs [84]. Methylation of CGI shores was found to be related to gene repression, while hypomethylated region in open sea areas are related to chromosomal instability, gene activation and tumorigenesis [85, 86].

The gene repression mechanism can be mediated by proteins harbouring methyl-CpG binding domain (MBD), which bind to methylated CpG islands leading to recruitment of histone deacetylases and chromatin compaction [87]. Another possible mechanism for gene silencing is the blocking of transcription factors binding to the promoter [88]. In contrast to CpG-rich promoter region, gene bodies are CpG-poor and highly methylated. The intragenic methylation has positive correlation with gene expression for CpGs outside CGIs, and it can correlate positively or negatively with gene expression when CpGs located within CGIs [88, 89].

DNA methylation pattern is regulated by DNA methyltransferases (DNMTs), which are responsible either establishing of the methylation (*de novo* methyltransferases, DNMT3a and DNMT3b) or the maintenance of the methylation (DNMT1) (Figure 10) [90, 91].

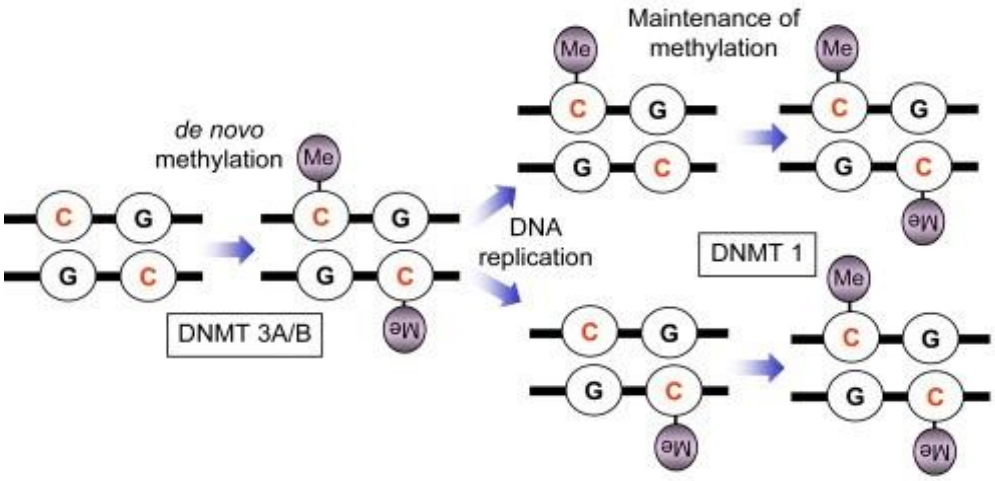

Figure 10. DNA methylation is established by de novo DNA methyltransferase (DNMT3A and DNMT3B) and maintained by DNMT1 after DNA replication (Herceg et al. in 2007 [91]).

Global hypomethylation has been observed in several different types of cancer, including melanoma [92, 93]. On the other hand, DNA hypermethylation at the transcriptionally active gene regions and promoters resulting in silencing of tumour suppressor genes [91]. Aberrant DNMT-regulated methylation results in the inactivation of different signalling pathways including MAPK, WNT, PI3K, pRB, and other pathways in cell cycle, apoptosis, invasion, and metastasis [94].

According to recent study, the proliferative vs. invasive transcriptomic signature is highly correlative with either permissive or repressive chromatin states underlying the importance of epigenetics regulation in the acquisition of invasive cellular state [79]. Due to the lack of direct genetic components in transcriptional reprogramming, studying the epigenetic factors that may promote cellular plasticity leading to increased invasion and metastasis is reasonable [95].

Based on the Cancer Genome Atlas Network (TCGA), the well-established mutational classifications of melanomas are not in agreement with gene expression patterns, which could explain not only the low response rate of therapies targeting the above-mentioned mutations but also the concerns raised against the durability of targeted therapies [96]. Nevertheless, the strong association between the mutations of chromatin remodelling genes (*ARID2* and *IDH1*) and the high degree of DNA methylation at several promoter regions described in melanoma (CpG island methylator phenotype; CIMP) suggest that epigenetic factors might play a pivotal role in cellular plasticity leading to increased invasion and metastasis [96, 97].

Recently, aberrant DNA methylation patterns have been observed in melanoma, suggesting that DNA methylation plays an important role in tumour formation and progression [94, 98]. While only a few genes were found to exhibit hypomethylated patterns, increased CpG island methylation levels have been described [64, 99, 100]. Recent improvements in epigenome-wide (EWAS) DNA methylation methods are allowed for the identification of potential biomarkers that could be exploited in clinical settings [93, 101-105]. However, in the case of earlier invasion steps in primary melanomas, insufficient data is available regarding the epigenetic mechanisms and especially the functionally relevant DNA methylation changes affecting gene expression patterns.

Of note, several genes of the melanocyte lineage differentiation pathway were found to be methylated such as *KIT*, *PAX3*, *SOX10*, different members of the HOX family genes and *MITF* [103, 106-108]. Remarkably, comparing matched primary and metastatic melanoma cell lines, Chatterjee et al. found *EBF3* promoter hypermethylation as a possible epigenetic driver of melanoma metastasis [109].

Importantly, EWAS on melanomas have more often focused on the metastatic tumours and therefore, the DNA methylation changes accompanying the early molecular invasion events

remain to be elucidated. A single study used cell lines derived from primary melanomas. Although the authors applied an indirect method (melanocytic markers) to distinguish between invasive and less invasive cell lines, the relevance of *SOX9* demethylation during metastasis formation well established and validated by an *in vivo* model [110].

Despite these essential therapeutic targets, effective treatment is still missing [111, 112]. Although our knowledge of melanoma cell motility has increased in the last decades, the complexity of the diverse invasive strategies requires further research [31, 37, 38, 113].

Objectives

The focus of this study was to discover the molecular background of melanoma invasion, as an initial step of metastasis formation. In order to better understand early metastasis-promoting genetic, epigenetic and gene-expression events, the main goal was to identify the relationship between copy number alterations, DNA methylation markers and gene expression alterations associated with the invasiveness of melanoma cells. We aimed to study the DNA methylation landscape and its effect on gene-expression of early invasion using *in vitro* selection of invasive melanoma cell subpopulation established from primary melanoma.

In our study we aimed to

1. investigate the relationship between copy number (CN) alterations and the invasiveness of melanoma cells using array CGH analyses, and to identify recurrent genetic regions related to invasiveness
2. define genetic alterations related to *BRAF* and *NRAS* mutation status of cell lines, and compare copy number changes associated with mutations of the invasive cell lines
3. establish selected invasive subpopulations of melanoma cells separated from the original cell lines in order to further analyse the invasion-related genetic and epigenetic alterations in melanoma cells by genetic and methylation profiling of the selected invasive cells and integrating methylation pattern with gene expression profiles that may render cellular plasticity towards increased invasion
4. characterize candidate genes with copy number alterations or methylation changes related to invasiveness in melanoma tumour tissue samples.

Materials and methods

Cell culture

Experiments were performed in primary tumour derived (WM35, WM1789, WM793B, WM3211, WM1361, WM902B, WM39, WM278, WM983A, WM1366, WM3248) and metastatic tumour derived melanoma cell lines (WM1617, WM983B, A2058, HT168, M24, M24met) obtained from the American Type Culture Collection (ATCC, Manassas, Virginia, USA) and from the Coriell Institute for Medical Research (Camden, New Jersey, USA). The HT199 melanoma cell line was developed in the Semmelweis University, Budapest, Hungary [114]. The clinicopathological characteristics of the cell lines are summarized in Table 2. The cells were cultured in RPMI 1640 medium (Lonza Group Ltd, Basel, Switzerland) or MCDB153-L15 medium (Sigma-Aldrich Co. LCC, St Louis, Missouri, USA) supplemented with 5–10% foetal bovine serum (Gibco, Carlsbad, California, USA, Cat. n.: 26140079) at 37°C in an atmosphere containing 5% CO_2.

Detection of BRAF and NRAS mutation

BRAF and NRAS mutation status of melanoma cell lines A2058, HT168, M24, M24met, HT199, WM902B) were determined, all the other cell lines were already tested for the mutations and the data were provided by ATCC or Coriell. Analysis of mutations in the BRAF codon 600 and in the NRAS codon 61 was performed on LightCycler real time PCR System (Roche Diagnostics GmbH, Mannheim, Germany) by melting curve analysis using fluorescent probes. Primers and probes were purchased from TIB Molbiol (Berlin, Germany). The reaction was performed as described previously [115].

Table 2. Characteristics of human melanoma cell lines.

Cell line	Origin[a]	Growth phase[b]	Histologic type[c]	BRAF mutation status[d]	NRAS mutation status[e]	Invaded cells/field (mean ± SD)[f]
WM35	primary	RGP	SSM	V600E	wt	0.0 ± 0.0
HT199	primary	RGP	NM	V600E	wt	15.0 ± 3.3
WM1789	primary	RGP/VGP	SSM	K601E	wt	0.0 ± 0.0
WM793B	primary	RGP/VGP	SSM	V600E	wt	1.5 ± 0.4
WM3211	primary	RGP/VGP	SSM	wt	wt	76.5 ± 29.5
WM1361	primary	VGP	SSM	wt	Q61L	0.0 ± 0.0
WM902B	primary	VGP	SSM	V600E	wt	0.0 ± 0.0
WM39	primary	VGP	NM	V600E	wt	0.0 ± 0.0
WM278[p1]	primary	VGP	NM	V600E	wt	0.0 ± 0.0
WM983A[p2]	primary	VGP	n.d.	V600E	wt	4.7 ± 2.0
WM1366	primary	VGP	n.d.	wt	Q61L	13.0 ± 1.4
WM3248	primary	VGP	n.d.	V600E	wt	0.0 ± 0.0
WM1617[m1]	metastasis	-	-	V600E	wt	0.0 ± 0.0
WM983B[m2]	metastasis	-	-	V600E	wt	3.3 ± 2.4
A2058	metastasis	-	-	V600E	wt	30.0 ± 3.6
HT168 [x1]	metastasis	-	-	V600E	wt	26.7 ± 5.2
M24	metastasis	-	-	wt	Q61R	27.0 ± 4.9
M24met[x2]	metastasis	-	-	wt	Q61R	74.0 ± 5.4

[a]tumor type of melanomas which the cell lines were derived from; [b]RGP: radial growth phase, VGP: vertical growth phase; [c]SSM: superficial spreading melanoma, NM: nodular melanoma, n.d.: no data; [d]V: valine, E: glutamic acid, K: lysine, wt: wild-type; [e]Q: glutamine, L: leucine, R: arginine; [f]data are presented as the mean ± SD of three independent invasion assay experiments; [p]primary tumor derived cell line with metastatic pair from the same patient; [m]metastatic pair of primary derived cell line; [x1]HT168 cell line originated from the A2058 cells after subcutan injection in immunsuppressed mouse [116]; [x2] M24met originated after in vivo injection of M24 cells into nude mice [117]

In-vitro invasion assay

The invasive potential of the melanoma cell lines was determined using BD Biocoat Matrigel invasion chambers (pore size: 8 μm, 24-well; BD Biosciences, Bedford, Massachusetts, USA). The upper chamber was filled with 500 μl cell suspension in serum-free media (5×10^4

cells/well). Medium containing 10% FBS was applied to the lower chamber as a chemoattractant (Figure 11). After the cells were incubated for 24 h at 37°C, cells in the lower layer were fixed with methanol and stained with hematoxylin–eosin. The invaded cells were counted using a light microscope in seven different visual fields at 200X magnification and the data are presented as the means ±SD of three independent experiments.

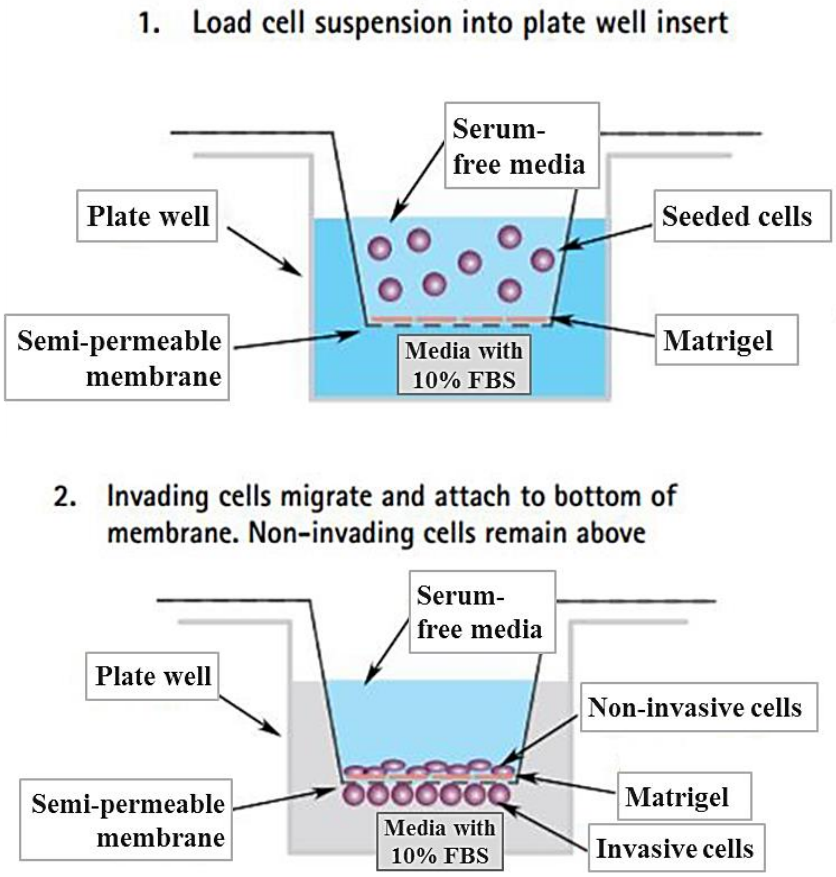

Figure 11. The cell invasion assay protocol based on Boyden Chamber technique. *Source: https://www.merckmillipore.com*

Selection of invasive cells

To select the invasive subpopulations from the original melanoma cell lines (WM983A, WM793B, WM1366 and WM3211), the invading cells in the lower chamber were treated with 0.5% trypsin/0.2% EDTA solution (Sigma-Aldrich Inc., St. Louis, MO, USA) for recovery

from the membrane. Selected invasive cells were cultured using standard protocol until DNA and RNA isolations. The selected subpopulations were labelled as WM983A-INV, WM793B-INV, WM1366-INV and WM3211-INV. In parallel with the nucleic acid preparation, the invasive capacity of the selected cells was detected.

Cell proliferation assay

Cell proliferation rate was determined using the WST-1 assay (Sigma-Aldrich Inc., St. Louis, MO, USA) according to the manufacturer's guidelines. Briefly, cells were seeded in 96-well plate in triplicate and cultured for 24, 48, 72 and 96 hours using standard protocol and 10 µl of WST-1 was added directly to the culture medium in each well, cells were incubated for another 3 hours. Absorbance was measured at 450 nm using a NanoDrop ND-1000 UV-Vis spectrophotometer (NanoDrop Technologies, Wilmington, Delaware, USA), while the reference absorbance was set at 700 nm.

Nucleic acid extraction

Genomic DNA was isolated using the G-spin Genomic DNA extraction kit (Intron Biotechnology Inc., Seongnam, Korea) according to the manufacturer’s protocol. The concentration and quality of the DNA were determined using a NanoDrop ND-1000 UV–visible spectrophotometer. The ratio of the absorbance at 260 and 280 nm was used to determine the purity of the DNA (a ratio≥ 1.8 was considered as high quality). The integrity of the DNA was verified by standard 1.2% agarose gel electrophoresis.

RNA was isolated using RNeasy Plus Mini Kit (Qiagen GmbH, Hilden, Germany) according to the manufacturer’s protocol. The concentration and quality of the RNA was assessed using NanoDrop and Bioanalyzer (Agilent Technologies, Palo Alto, CA, USA), and RNA samples

with 260/280 ratio ≥ 1.8 and with RNA integrity number ≥ 7.5 were involved in further analyses.

Array CGH and data analysis

DNA samples were hybridized to Cytochip ISCA 8 × 60 arrays (BlueGnome Ltd, Cambridge, UK). Array data were analysed using BlueFuse Multi v2.2 software (BlueGnome Ltd) and Nexus Copy Number 6.1 software (BioDiscovery Inc., Hawthorne, California, USA). To adjust the sensitivity of the segmentation algorithm, we determined a significance threshold of ~~1.0E−6~~ 10^{-6} and specified 1000 kbp as the maximum spacing between adjacent probes. To eliminate small copy number alterations (CNAs), we set the minimum number of probes per segment at 5. To detect gains and losses, ±0.3 log2 ratio thresholds were set, while 0.6 for high CN gains and −1.0 for homozygous deletions were adjusted. Significantly different CN events between invasive and non-invasive melanoma cell lines, and between selected invasive subpopulations and the original cell lines were identified using two-sided Fisher's exact test. The FDR adjustment was calculated to correct for multiple testing using the Nexus Copy Number 6.1 Comparison feature. To avoid sex bias, we excluded all probes on chromosomes X and Y.

Genome wide DNA methylation analysis

For methylation studies, bisulphite modification was performed on 600 ng of DNA using EZ DNA Methylation kit (Zymo Research, Irvine, CA, USA). We confirmed the quality of modification by PCR (HotStarTaq Master Mix kit; Qiagen GmbH, Hilden, Germany) using modified and unmodified primers for the *GAPDH* gene. To determine the DNA methylome profile, Illumina Infinium II Human Methylation 450K (HM450K) BeadChip assay was used (Illumina, San Diego, CA, USA), which contains more than 480,000 methylation sites (Figure 12) [118]. The array experiments were performed by the Epigenetics Group and the Core

Facility of the Genetic Cancer Susceptibility Group, International Agency for Research on Cancer (Lyon, France). The raw data were deposited in the Gene Expression Omnibus (GEO) repository (http://www.ncbi.nlm.nih.gov/gds) under accession number GSE115852.

The data pre-processing and all analyses were performed using several Bioconductor packages in R v.3.2.2 (http://www.r-project.org/) as follows: Following scanning, raw methylation data were imported and processed using the "Lumi v2.36.0", "wateRmelon v1.28" and "minfi v1.30" packages [119-121]. The DNA methylation level is described as the β-value, which is a continuous variable ranging from 0 (no methylation) to 1 (full methylation). The quality of data quality was checked in multiple steps: boxplots were used for the distribution of methylated and unmethylated signals, for inter-sample relationship, we used multidimensional scaling plots. As an additional quality control step, we used the inferred beta values to predict sex (getSex function of the "minfi" package). Then, a principal component analysis (PCA) was used to confirm the absence of batch effects.

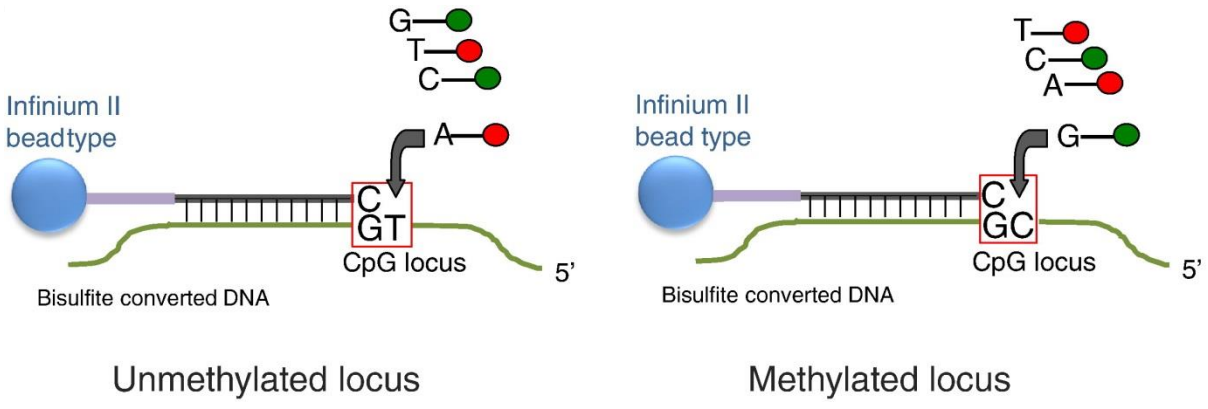

Figure 12. Infinium II methylation assay scheme on bisulfite converted DNA. *One bead type corresponds to each CpG sites Bibikova et al. 2011 [118]).*

Importantly, probes were filtered for low quality with the "pflter" function, additionally; known cross-reactive probes were also excluded from further analysis [120, 122]. Furthermore, probes

overlapping with known SNPs with a minor allele frequency ≥5% in the overall population (European ancestry) [122].

The remaining dataset was background-subtracted, and normalized using intra-array beta-mixture quantile normalization [123]. To follow the recommendation of the literature, methylation beta values were logarithmically transformed to M values before parametric statistical analyses, as recommended [124]. To define differentially methylated positions (DMPs) and differentially methylated regions (DMRs), first, we modelled the main variables (invasive capacity) as a categorical variable in a linear regression using the "limma v3.40.2" package an empirical Bayesian approach [125]. Since our cell lines were paired, to increase the statistical power, we included the cell line as a co-factor into the model. To infer the detected differentially methylated sites into DMRs, we used the "DMRcate v1.20" package with the recommended proximity based criteria: if a region harboured at least 3 probes spanning in 1kb [126]. DNA methylation changes were considered significant with an FDR-adjusted p value less than 0.05. Additionally, for a more stringent analysis, we defined those sites with a methylation difference (delta-beta) of 10% in any direction. For the annotations, to obtain information of the nearest gene and transcript of each the detected DMR, we used the FDb.InfiniumMethylation.hg19 v.2.2.0 package, using hg19 as a reference genome [127]. For the visualizations, we used either the DMRcate or coMET packages with the functionality of the Gviz package [128].

To determine the potential functional changes in the genes that were significantly differentially methylated as determined above, a pathway analysis was performed by Enrichr web application [129] (http://amp.pharm.mssm.edu/Enrichr/, RRID:SCR_001575) using WikiPathways June 2017 Release as an input that currently covers 11,532 human genes.

Correlation between gene expression and DNA methylation

To assess gene expression at genome-wide levels, we purchased Affymetrix Human Gene 1.0 microarrays (Affymetrix Inc., Santa Clara, CA, USA). The labelling, hybridization and imaging setup were performed in UD-GenoMedMedical Genomic Technologies Ltd. (University of Debrecen, Clinical Genomic Center, Debrecen, Hungary) using 500 ng of sample RNA. The raw CEL files were imported to R v.3.2.2 using the Oligo package. The filtering and normalization were performed using the Minfi and WateRmelon packages. We calculated the Pearson's correlation coefficients to correlate the gene expression $\log_2$ fold changes to the DNA methylation changes (Δß) in the genes belonging to the DMPs. The microarray data are available in the GEO (http://www.ncbi.nlm.nih.gov/gds) under accession number GSE114380.

The Cancer Genome Atlas (TCGA) data analysis

Detailed genomic analysis using array CGH data of melanoma samples was completed with the Skin Cutaneous Melanoma (SKCM) dataset: The Cancer Genome Atlas (TCGA, Provisional). The results are based upon data generated by the TCGA Research Network (http://cancergenome.nih.gov). Using the visualization tools of the cBioPortal, (http://www.cbioportal.org) we downloaded the melanoma dataset containing GISTIC-CNA results of 366 melanoma samples [130, 131]. All queries were carried out according to the cBioPortal's instructions.

On the other hand, we downloaded Illumina Methylation 450K data available for SKCM containing 437 tissues (88 primary and 349 metastatic melanoma samples) from the TCGA-GDC data portal (https://portal.gdc.cancer.gov/) by using the GDCquery and GDCprepare functions of the TCGAbiolinks R package [132]. The latter generated a summarized experiment object that we further analysed by using the TCGAanalyze_DMR function of the TCGAbiolinks package with a mean delta-beta cut-off 10% and a Benjamini-Hochberg

adjusted p-value of 0.05. The rest of the settings were the default options recommended by the developers of the package. We determined and compared to our results to the DNA methylation changes present in the TCGA metastatic melanomas versus tissues of primary sites. Tumours classified as "metastatic" vs "primary" according to the definition column of the clinical data available at the data portal. Afterwards, we added a variable to the colData data frame of the summarized experiment by using the addAnnotation function of the IntEREst R package [133], consisting of a merge of any Clark level below stage V into a single category to compare primary tumours by invasiveness (V vs not-V), and finally rerun the TCGAanalyze_DMR function as described above. We determined the methylation changes showing at least 10% differences for the mean beta values between the primary and metastatic samples; and the locally invasive primary (Clark stage V) vs. early stage primary (Clark levels below stage V) melanomas, respectively.

TaqMan Copy Number Assay

Real time quantitative PCR (qPCR) method was used on 18 melanoma cell lines to confirm the array CGH results. Copy numbers of *GLIPR1, COL1A2* and *RELN* genes were assessed using pre-designed TaqMan® Copy Number Assays on an ABI 7900HT instrument (Applied Biosystems Inc., USA) Predesigned TaqMan® Copy Number Assays were used to analyse copy numbers (Hs01421756_cn, Hs03071873_cn and Hs02363915_cn, respectively), and the *RNase P* gene was applied as a reference gene (Applied Biosystems Inc., USA). All assays were performed with TaqMan® Universal PCR Master Mix according to the manufacturer's protocol (Applied Biosystems Inc., USA). Ten µl reaction mixture consisted 4 ng of genomic DNA, 5 µl TaqMan® Universal PCR Master Mix of primers and probes. The experiments were performed in triplicate. The following thermal cycling conditions were used: 1 cycle of 95°C 10 min followed by 40 cycles of 95°C for 15 s and 60°C for 1 min [134]. Samples with *RNase*

P Ct value over 32 were excluded from further analysis. CopyCaller® Software v.2.0 was used to calculate copy numbers.

Real time quantitative PCR analysis

The relative expression level of the selected genes was determined by quantitative real-time PCR in 12 primary melanoma cell lines (WM35, HT199, WM1789, WM793B, WM3211, WM1361, WM902B, WM39, WM278, WM983A, WM1366 and WM3248) and in 4 selected invasive populations (WM983A-INV, WM793B-INV, WM1366-INV and WM3211-INV) using LightCycler® 480 Real-Time PCR System (Roche Diagnostics, GmbH, Mannheim, Germany). Reverse transcription was carried out on total RNA (600 ng) using the High Capacity cDNA Archive Kit (Applied Biosystems, Carlsbad, California, USA) according to the manufacturer's protocol. To perform qPCR reactions, SYBR premix Ex taq master mix was used (Takara, Japan). Primer sequences of the candidate genes are listed in Supplementary Table 1 (see Appendix).

Statistical analysis

SPSS 19.0 (SPSS Inc., Chicago, IL, USA) was used for statistical analyses. The Shapiro–Wilk test was used to evaluate the normality of the data. Pearson's correlation coefficient was calculated to correlate the array CGH and qPCR data. Mann-Whitney-Wilcoxon test was used to compare the mRNA expression of non-invasive cell lines to invasive ones. $P < 0.05$ was considered statistically significant.

Results

Invasive property of melanoma cell lines

To identify genomic alterations related to early invasive potential of primary melanoma cells, *in vitro* invasion assays were performed on cell lines derived from primary malignant melanomas (WM35, HT199, WM1789, WM793B, WM3211, WM1361, WM902B, WM39, WM278, WM983A, WM1366 and WM3248).

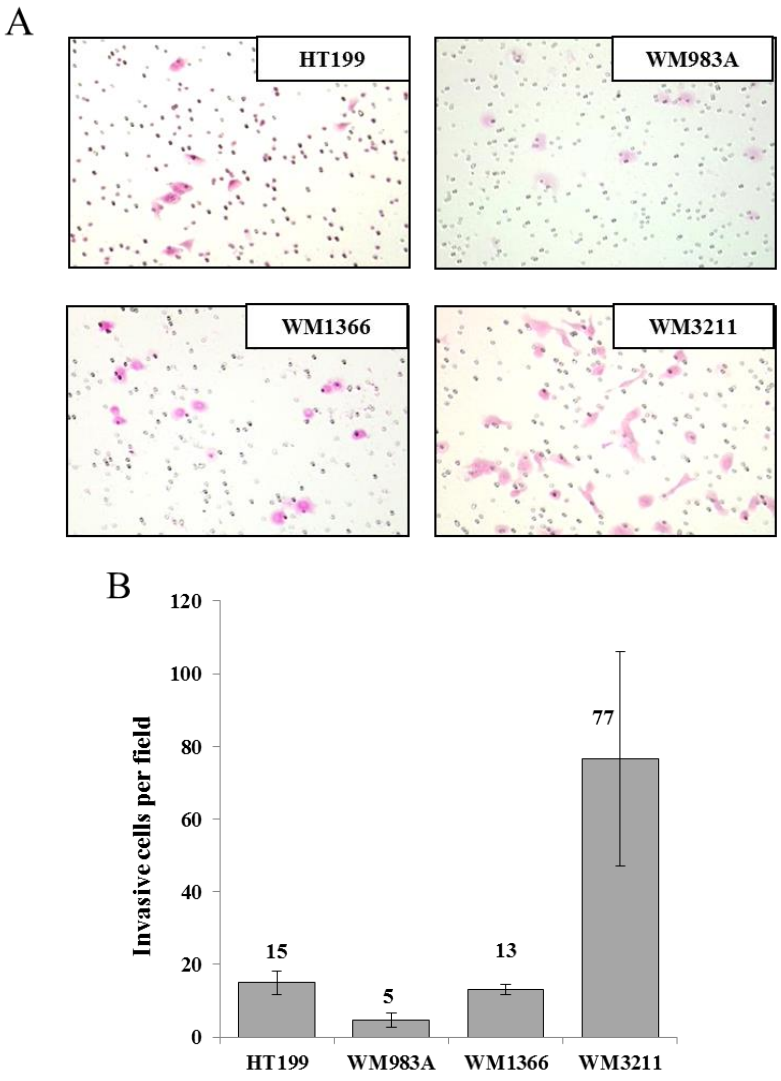

Figure 13. Invasive potential of primary tumour-derived cell lines. *(A) Representative images of cell invasion of four melanoma cell lines. Invasive capacity of melanoma cell lines was determined. Cells were cultured in Matrigel invasion chambers for 24 h. The invaded cells on the lower layer were fixed with methanol and stained with haematoxylin–eosin. (B) Quantification of the invasion assays. The invaded cells were counted in seven randomly selected microscopic fields on the membrane and the results are summarized and expressed as the mean number of invaded cells. The data for each cell line are presented as the mean ± SD of three independent experiments.*

According to the Matrigel invasion chambers, we observed invasive cells in five (HT199, WM793B, WM3211, WM983A and WM1366 out of the twelve primary tumour derived cell lines; however, for further array CGH analysis, we determined WM793B as non-invasive cell line according to the irrelevant number of invaded cells/field (1.5 ± 0.4) (Figure 13).

Genomic profiling of melanoma cell lines

Array CGH analysis

We performed array comparative genomic hybridization (CGH) analyses using the CytoChip ISCA array to identify chromosome copy number alterations in 18 human melanoma cell lines that originated from primary (n=12) and metastatic (n=6) tumours. A high degree of CN instability was identified across the genomes of all cell lines, involving CN gains in 1q, 6p, 7, 8q, 17q, 20 and 22q and CN losses in 6q, 9p and 10p (Figure 14). We observed CN alterations of several melanoma-related genes including *NEDD9, EGFR, BRAF* and *MYC* genes (Table 3).

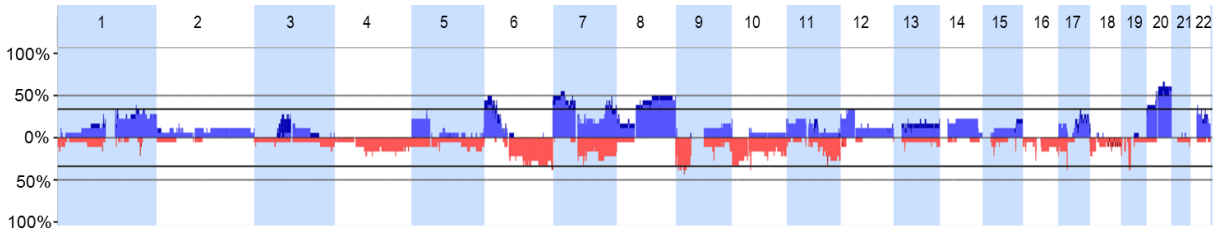

Figure 14. Frequency diagram of array CGH results obtained from individual chromosome profiles of melanoma cell lines. *Red indicates copy number (CN) losses and blue represents CN gains.*

Table 3. The most frequently altered chromosomal regions in 18 melanoma cell lines with melanoma related genes.

Cytoband location	Region Length (bp)	Event	No. of genes	Frequency (%)	Melanoma related genes
6p25.3	1,196,982	CN Gain	9	44.4	
6p24.3 - p22.3	10,532,509	CN Gain	56	50.0	NEDD9
6p22.3 - p22.1	3,868,451	CN Gain	36	44.4	
6p21.33	713,073	CN Gain	25	44.4	
7p22.3 - p21.1	18,809,250	CN Gain	133	50.0	
7p21.1 - p15.1	9,867,496	CN Gain	82	55.6	IL6
7p12.3	2,119,199	CN Gain	11	50.0	
7p12.1 - p11.2	4,554,834	CN Gain	24	44.4	EGFR
7q33	916,943	CN Gain	8	44.4	
7q34	3,391,177	CN Gain	39	44.4	BRAF
7q35	601,876	CN Gain	4	50.0	
8q12.1	1,282,511	CN Gain	8	44.4	
8q21.3 - q22.3	18,203,144	CN Gain	116	50.0	MMP16
8q22.3 - q24.23	32,930,000	CN Gain	139	50.0	MYC
8q24.3	882,425	CN Gain	46	50.0	
9p21.3	529,652	CN Loss	5	44.4	CDKN2A, CDKN2B
17p11.2 - q11.1	1,068,207	CN Loss	7	38.9	
20p11.21	2,098,960	CN Gain	22	55.6	
20q12 - q13.12	4,703,731	CN Gain	92	66.7	MMP9
20q13.32 - q13.33	5,535,582	CN Gain	120	61.1	

Invasive behaviour related recurrent genetic regions in melanoma cell lines

Comparison of the genomic alterations between *in vitro* invasive (n=4) and non-invasive (n=8) primary tumour derived cell lines, several CN alterations occurred at significantly higher frequencies in cell lines showing invasive behaviour (Table 4). Although a number of these altered regions mapped to known regions of germline copy number variation (CNV), we did

not exclude these from further analyses since well-validated cancer relevant genes have been known to locate in regions of germline CNV [56, 135].

Table 4. Chromosomal regions altered with significantly higher frequencies in the invasive cell lines

Cytoband location	Region length (bp)	Event	No. of genes	Frequency in non-invasive cell lines (%)	Frequency in invasive cell lines (%)	P-Value[a]	Candidate genes
4q22.1 - q22.2	1,063,318	CN Loss	2	0.0	75.0	0.018	n.c.
4q31.3	723,382	CN Loss	2	0.0	75.0	0.018	n.c.
4q35.1	722,510	CN Loss	4	0.0	75.0	0.018	n.c.
5p13.2	1,427,307	CN Gain	8	0.0	75.0	0.018	*GDNF*
7q11.23	59,511	CN Loss	2	0.0	75.0	0.018	n.c.
7q11.23 - q21.11	2,663,721	CN Loss	15	0.0	75.0	0.018	*PTPN12*
7q21.11 - q21.3	13,825,784	CN Loss	69	0.0	75.0	0.018	*ADAM22*, *FZD1*, *TFPI2*, *GNG11*, *COL1A2*
7q21.3 - q22.1	7,948,023	CN Loss	157	0.0	75.0	0.018	*SMURF1*, *VGF*, *RELN*
8q24.3	1,233,778	CN Gain	51	0.0	75.0	0.018	*GPAA1*, *PLEC*, *SHARPIN*

[a]P-Value was determined by a multiple corrected Fisher's exact test; CN: copy number; n.c.: no candidate gene.

Extended comparison including metastatic cell lines (n=6) revealed that copy number changes on 7q and 12q chromosomal regions appeared specifically in cell lines with invasive behaviour and were not detected in non-invasive and metastatic tumour derived cell lines (Figure 15). The targeted genes within these regions included the loss of several invasion-related genes such as *PTPN12*, *ADAM22*, *FZD1*, *TFPI2*, *GNG11*, *COL1A2*, *SMURF1*, *VGF*, *RELN* and *GLIPR1*. Additionally, the gain of 5p13 and 8q24 were present not solely in invasive cell lines but

occurred in metastasis-derived cell lines as well, harbouring *GDNF* (5p13.1), *GPAA1*, *PLEC* and *SHARPIN* (8q24.3) as invasion-related genes (Figure 16).

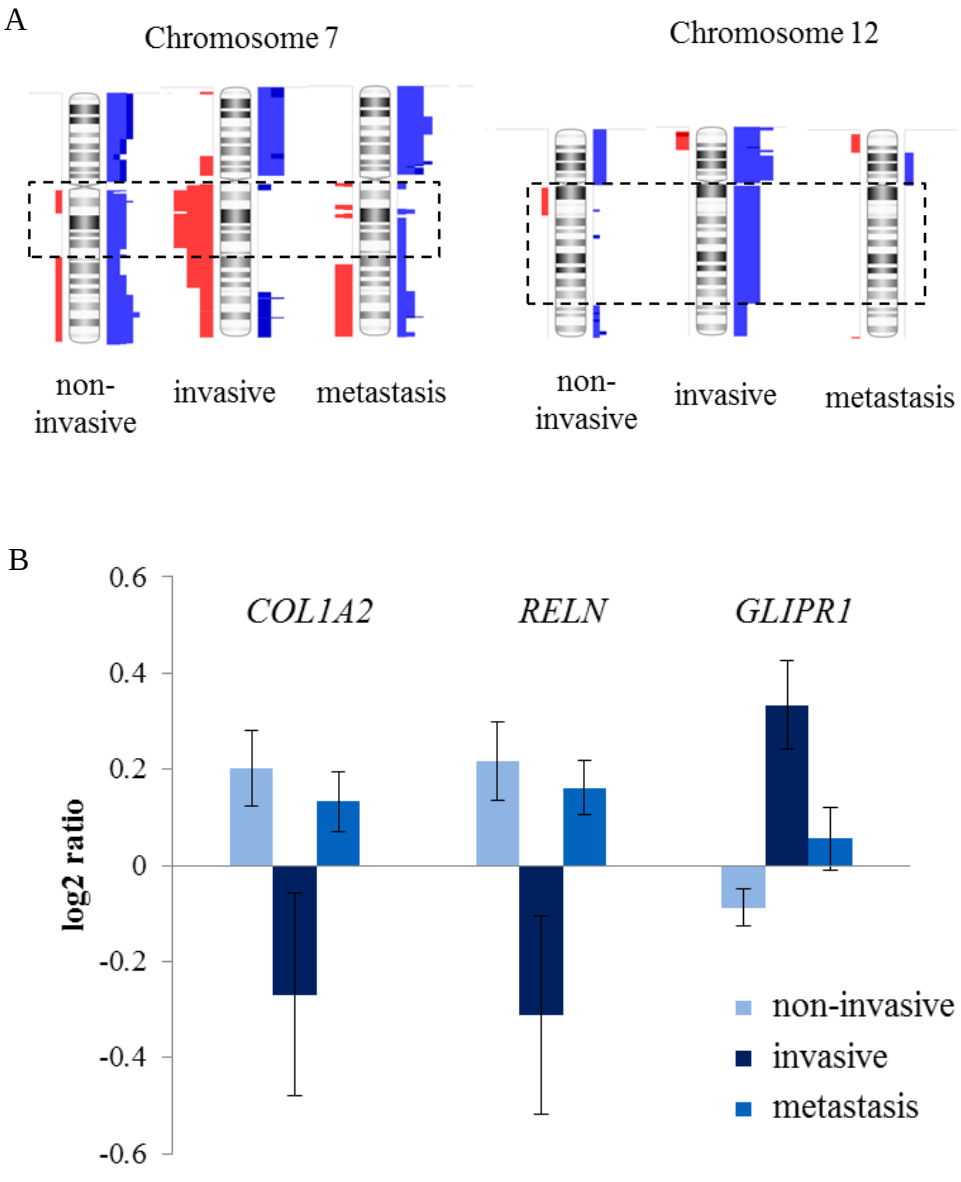

Figure 15. Summary of chromosome 7 and 12 copy number alterations in melanoma cell lines*. A.) Distribution of CN gains (blue colour) and CN losses (red colour) on chromosome 7 and 12 uniquely observed in non-invasive (WM35, WM1798, WM793B, WM1361, WM902B, WM39, WM278, WM3248), invasive (HT199, WM983A, WM1366, WM3211) primary- and metastatic tumour-derived (A2058, HT168, M24, M24met, WM1617, WM983B) melanoma cell lines. B.) Copy number alterations (log2 ratio) of COL1A2 (7q21.3), RELN (7q22.1) and GLIPR1 (12q21.2) genes.*

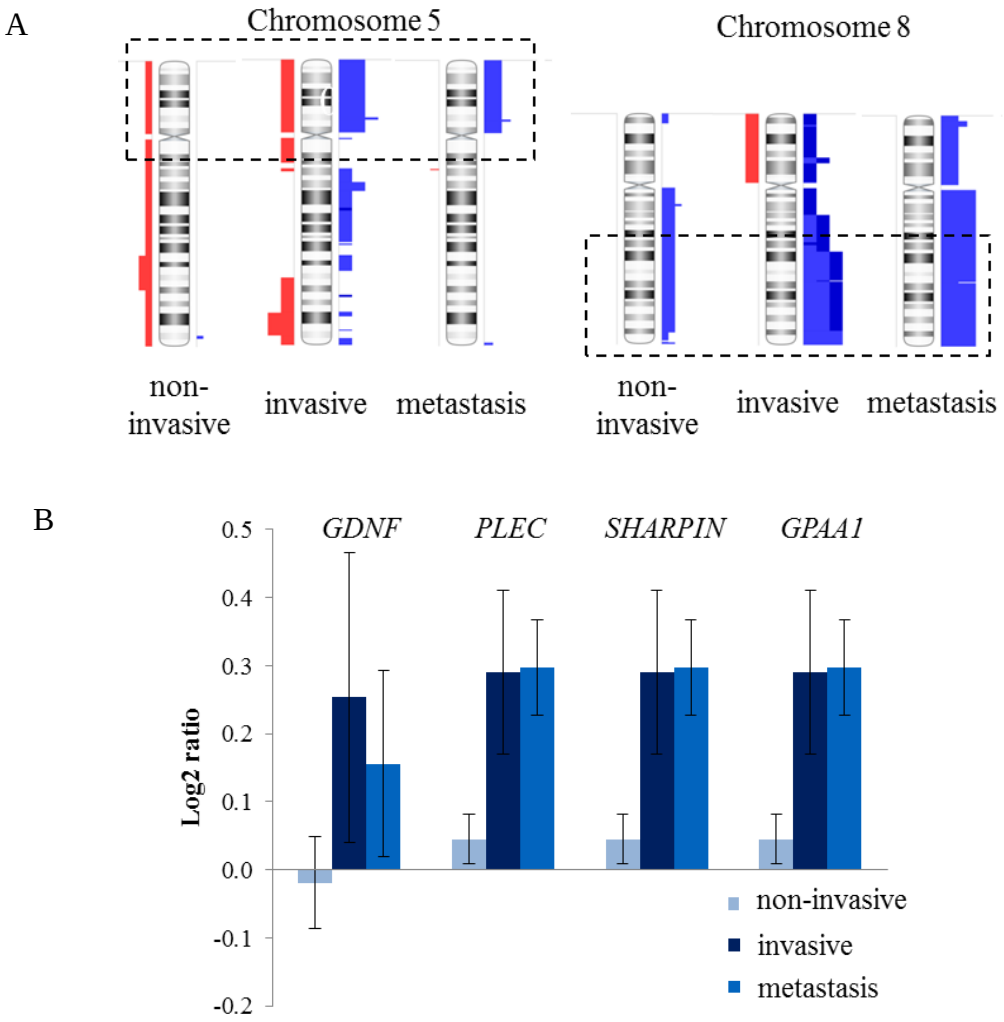

Figure 16. Summary of chromosome 5 and 8 copy number alterations in melanoma cell lines*. A.) Distribution of CN gains (blue colour) and CN losses (red colour) on chromosome 5 and 8 in non-invasive, invasive primary- and metastatic tumour derived melanoma cell lines. B.) CN changes of invasion-related candidate genes (GDNF (5p13.1), PLEC, SHARPIN and GPAA1 (8q24.3)) in melanoma cell lines.*

To validate our array CGH data, real time quantitative PCR method was performed using TaqMan® Copy Number Assays. Copy numbers of *COL1A2*, *RELN* and *GLIPR1* genes were determined. Pearson's correlations were then calculated between the array CGH data using the mean log2 ratios of probes covering the genes and the normalized copy numbers determined by qPCR method. Good concordance was found between the data derived from array CGH and qPCR methods. The correlation coefficients revealed moderate and strong correlation between our datasets; 0.659, 0.695 and 0.555, respectively (p=0.003, p=0.001, p=0.017).

Copy number alterations of candidate genes in melanoma tumour samples

In order to define the relevance of the invasion associated alterations in native melanoma tissues, we applied the Skin Cutaneous Melanoma dataset (TCGA, Provisional). We have to note that the publicly available array CGH data set were obtained mainly from metastatic melanoma tissue samples and no data are listed about the invasive property of the primary tumours in the database. On the other hand, the invasive property of primary melanoma cell lines that were used in our *in vitro* model systems cannot be precisely applied for melanoma tissues in the same context. As a systematic comparison is not possible between the public datasets and our results, we focused on candidate genes (*GDNF*, *GPAA1, PLEC* and *SHARPIN)* that exhibited copy number alterations in both invasive and metastatic melanoma cell lines. Notably, these genes exhibited copy number alterations exclusively in the metastatic tissues but not in the primary lesions. Interestingly, *GPAA1*, *PLEC* and *SHARPIN* genes were co-amplified in 26 metastatic melanomas out of the 366 samples. *GDNF* was found to be amplified to a lesser extent, in 14 metastatic tissues.

BRAF and NRAS mutation in association with invasion

We also aimed to confer genetic alterations related to *BRAF* and *NRAS* mutation status of cell lines and compare copy number changes associated with mutations of the invasive cells. Mutation status of the cell lines are shown in Table 2. The overall frequency of the $BRAF^{V600E}$ mutation was 68.4%, and $BRAF^{K601E}$ mutation was detected only in one cell line (WM1789). *NRAS* mutations (21.1%) were seen at lower frequency than *BRAF* mutations, and no cell line was mutated for both *BRAF* and *NRAS*.

According to the array CGH results, several CN alterations were associated with the presence of $BRAF^{V600E}$ mutation. Cell lines with $BRAF^{V600E}$ mutation had a higher frequency of 7q gain, including the *BRAF* gene located on 7q34. This locus showed copy number gain in 53.9% of

BRAF mutated cell lines, while only 20% of the wild-type cell lines exhibited alterations on 7q34. Other CN alterations associated with *BRAF*^{V600E} mutation were gains of 1q and 6p, whereas loss of 9p and 10p occurred more frequently in cell lines with wild-type *BRAF* (Figure 17A). Additionally, loss of 19p12 was seen only in *BRAF*^{V600E} mutated cell lines. On the other hand, loss of 4q was associated with *NRAS* mutations. Losses of 4q22.1-q22.2 and 4q31.3 were seen in all *NRAS* mutated cell lines, while these losses were detected with significantly lower frequency in wild-types (p=0.0032 and p=0.0018, respectively).

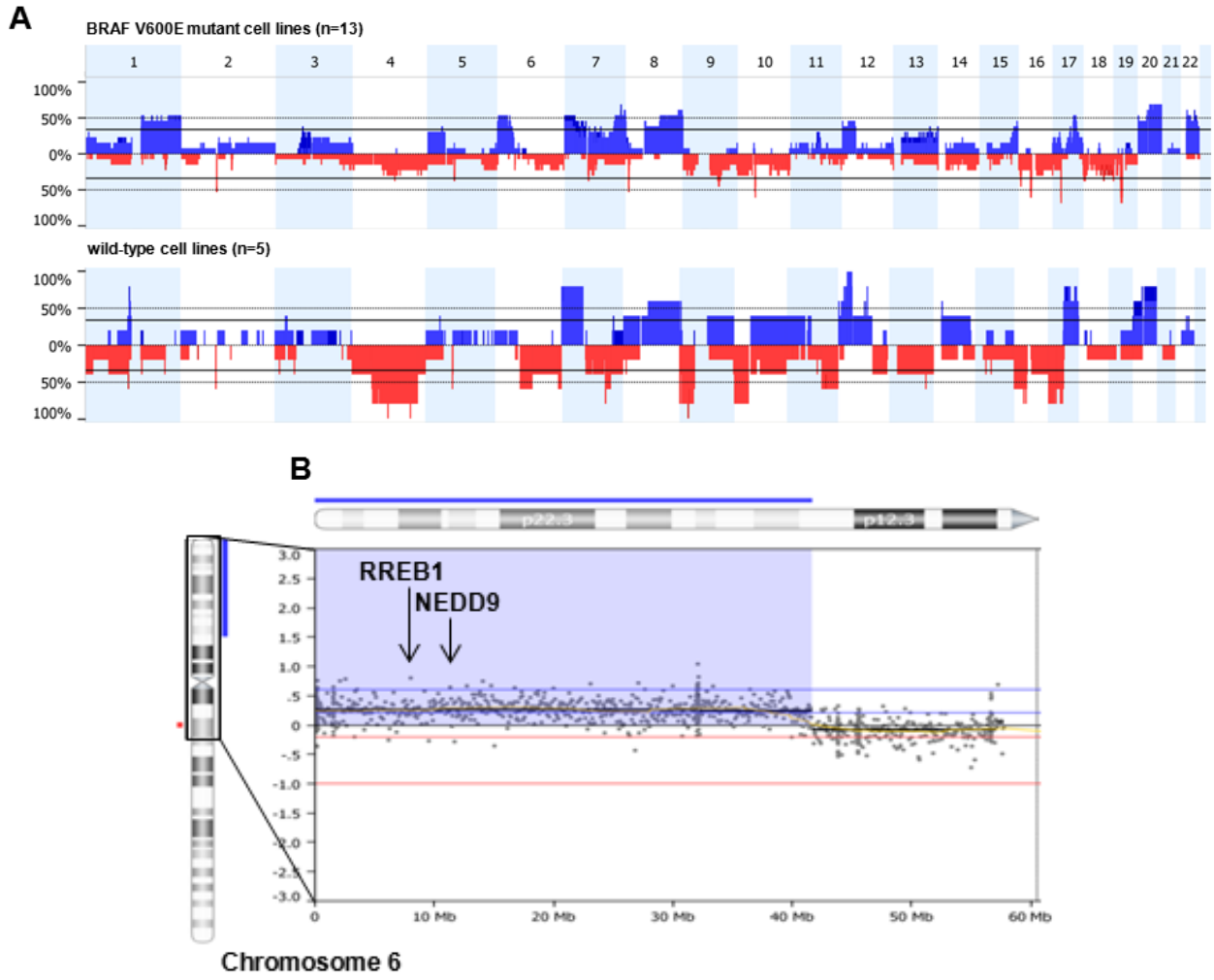

Figure 17. Summary of array CGH data of BRAF^{V600E} mutated and wild-type melanoma cell lines. *(A) Frequency of DNA copy number changes in BRAF mutated (n=13) and wild-types (n=5) melanoma cell lines. Clones are arranged from chromosome 1 to 22. Red colour represents copy number losses, and blue colour represents copy number gains. (B) Array CGH results of chromosome 6p gain targeting the RREB1 and NEDD9 genes in the invasive, BRAF^{V600E} mutant HT199 cell line.*

Invasive cell lines with *BRAF*^{V600E} mutation (WM983A, HT199) showed copy number gain of 6p25.3-p22.3 targeting *RREB1* (6p25) and *NEDD9* (6p24) genes (Figure 17B), whereas gain of 7p was characteristic for invasive cell lines with wild-type *BRAF* gene (WM3211, WM1366).

Relative mRNA expression of candidate genes

To examine the possible effect of CN alterations on the gene expression, we performed real time PCR experiments and determined the relative mRNA level of 14 candidate genes (*GDNF, PTPN12, ADAM22, FZD1, TFPI2, GNG11, COL1A2, SMURF1, VGF, RELN, GPAA1, PLEC, SHARPIN*). Seven of these genes were either up- or down-regulated in the same way as it was expected from of gene copy numbers based on array CGH data (Figure 18A). Relative mRNA expression of *FZD1* and *SMURF1* genes were significantly lower in invasive cell lines compared to non-invasive ones. By correlating the log2 transformed relative expression levels with array CGH results (log2 ratios), we identified 4 genes (*PTPN12*, *ADAM22*, *FZD1* and *SMURF1*) that relative mRNA level was significantly correlated with CN changes (Figure 18B).

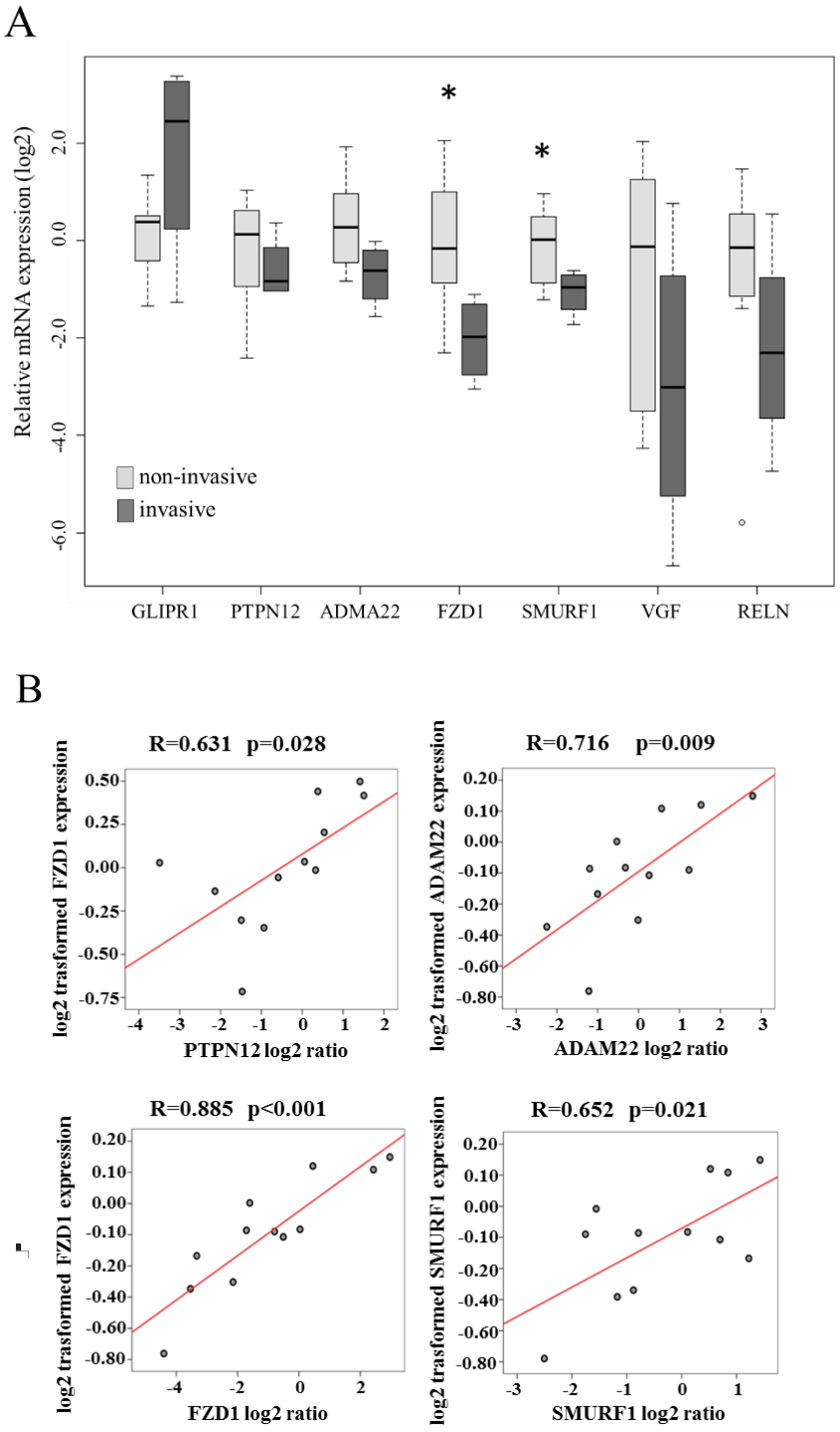

Figure 18. Relative expression of seven genes by real-time quantitative PCR. *(A) Comparison of the relative mRNA expressions (log2) of the non-invasive and invasive cell lines. The data are presented as mean ±SD of non-invasive (N=8) and invasive (N=4) cell lines (three replicates/sample). *Expression was significantly higher in non-invasive cell lines than in the invasive cells (P<0.05). (B) Correlation analysis between log2 transformed expression levels and array CGH results (log2 ratios). Pearson's correlation coefficients (R) are shown in the graphs (P<0.05).*

Phenotypic characterization of selected invasive cells

To further analyse the invasion-related genetic and epigenetic alterations in melanoma cells, we established four invasive cell subpopulations (WM983A-INV, WM1366-INV, WM3211-INV and WM793B-INV) using Matrigel coated invasion chambers.

Selected invasive melanoma cells differed from the original cell lines in morphology. Invasive cells were flatter, and more spindle-shaped than the original cell lines (Figure 19).

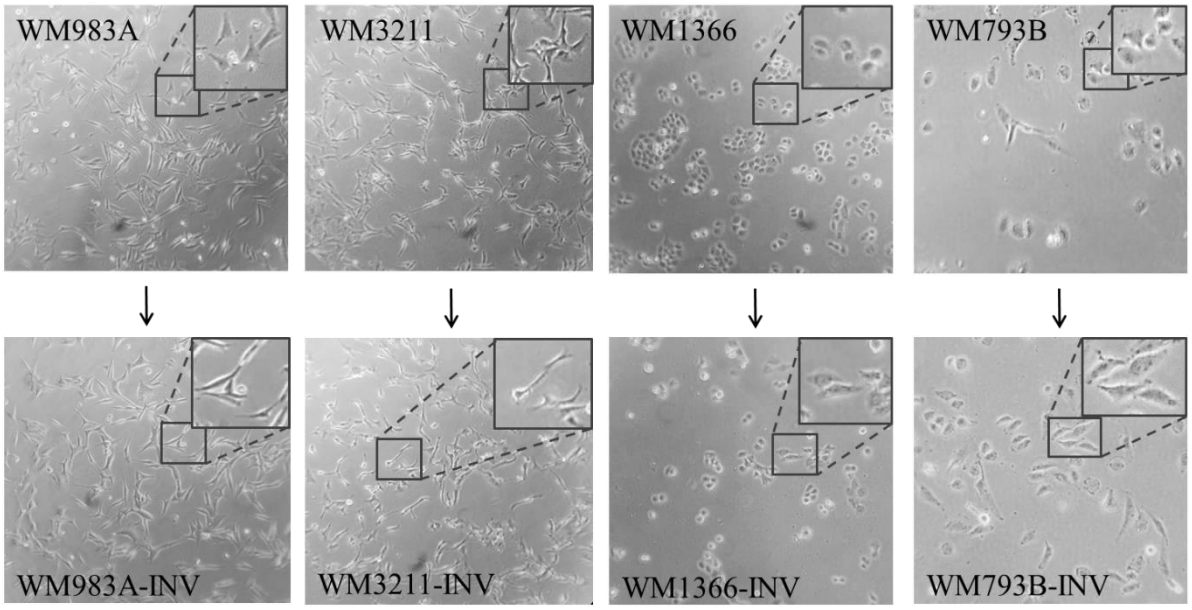

Figure 19. Morphological feature of the original (WM983A, WM3211, WM1366 and WM793B) and the selected invasive cells (WM983A-INV, WM3211-INV, WM1366-INV and WM793B-INV). *Inserts of each cell lines shows magnification of representative cells.*

Based on further invasion experiments, the selected cell lines had significantly higher invasive potential compared to the original cell lines ($p < 0.05$) (Figure 20A). On the other hand, since invasive cells have been described to have lower proliferation rate than proliferative cell populations, we aimed to determine the proliferation rate of the selected invasive cells, and compared that to the original cell lines [74]. The proliferation rate was lower of the invasive cell lines than the original cell lines, however, the difference was not statistically significant (Figure 20B).

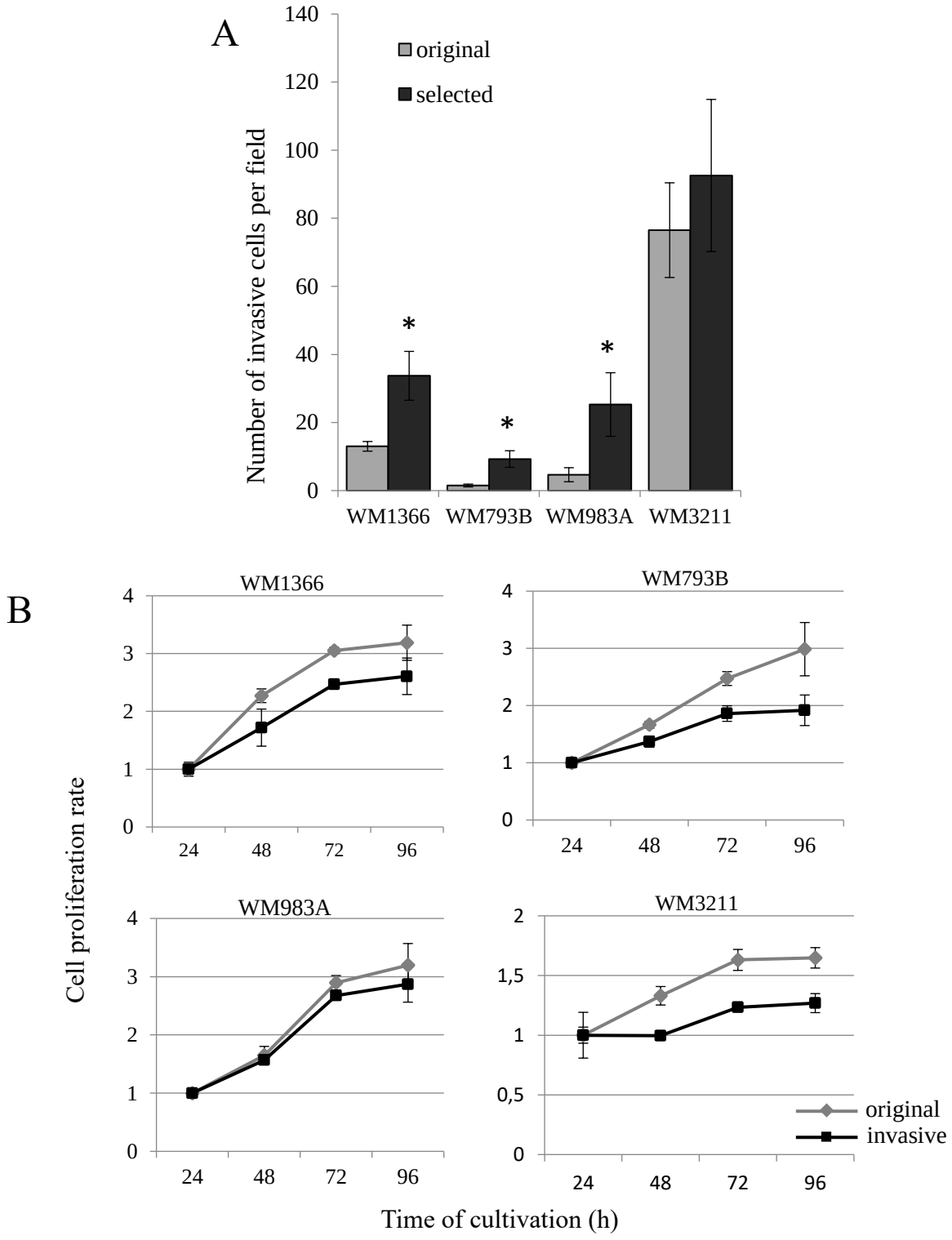

Figure 20. Phenotypic characterization of the selected invasive cells compared to the original cell lines. *(A) Invasive potential and (B) proliferation rate of the original and selected invasive melanoma cell lines. The data are presented as the mean ±SD of three independent experiments. The asterisk indicates statistically significant difference (Mann-Whitney-Wilcoxon test: P<0.05).*

Genetic profile of the selected invasive cells

Array CGH analyses were performed on the 4 selected invasive cell lines (WM983A-INV, WM3211-INV, WM1366-INV and WM793B-INV) and compared to the original cell lines to identify specific invasion related chromosomal alterations. Based on this comparison, CN alterations located on 1p, 2q and 8q were present at higher frequencies in the *in vitro* selected invasive cells compared to the original cell lines (Figure 21A). Detailed log2 ratios of the candidate genes located on these chromosomal regions are presented on Figure 21B including *GPAA1*, *MMP16*, *RHOC* and *PDK1* genes.

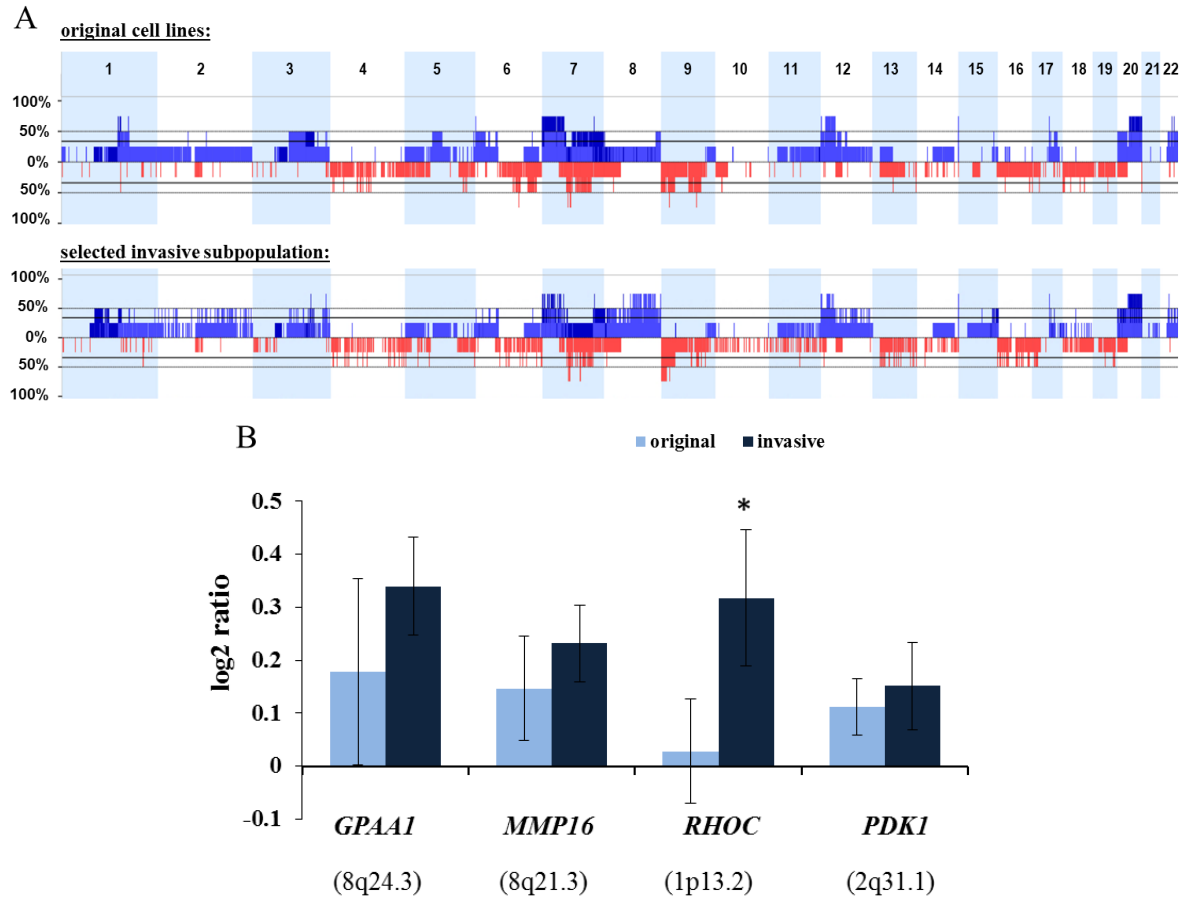

Figure 21. Summary of array CGH results of 4 melanoma cell lines and the corresponding selected subpopulations. *(A) Frequency of DNA copy number changes of four original (WM983A, WM793B, WM1366 and WM3211) and the selected invasive subpopulations (WM983A-INV, WM793B-INV, WM1366-INV and WM3211-INV). Red indicates copy number (CN) losses and blue represents CN gains. (B) Relative CN changes (log2 ratio) of four candidate genes in the original and in the in vitro selected invasive cells. The localizations of genes are in parentheses. The asterisk indicates statistically significant difference (P<0.05).*

Methylation profile of the selected invasive cells

Invasion related methylation changes in selected invasive cells

To define the methylation patterns of the melanoma cell lines, we used Illumina Infinium Human Methylation 450K BeadChip array specific for more than 450,000 methylation sites, within and outside of CpG islands. This methylation profiling platform allowed to compare epigenome-wide data of selected invasive melanoma cell subpopulations (WM983A-INV, WM793B-INV, WM1366-INV, WM3211-INV) to the original cell lines (WM983A, WM793B, WM1366, WM3211). Altogether, we identified 1,249 regions with significant differences at the methylation levels between the invasive and the original cell lines. Globally, hypermethylated DMRs (n=1,216) were more predominant than the hypomethylated DMRs (n=33) with a total of 8,733 and 165 CpG sites, respectively. The full list of hyper- and hypomethylated DMRs and CpG sites are shown in Supplementary Table 2 and 3, respectively.

The hypermethylated CpG probes (DMPs) exhibited enrichment for CpG islands. On the other hand, the array probe distributions of the hypomethylated DMPs were mostly detected in 2 kb (CpG shores) or more than 4 kb region (open seas) from the promoter CpGs islands (Figure 22).

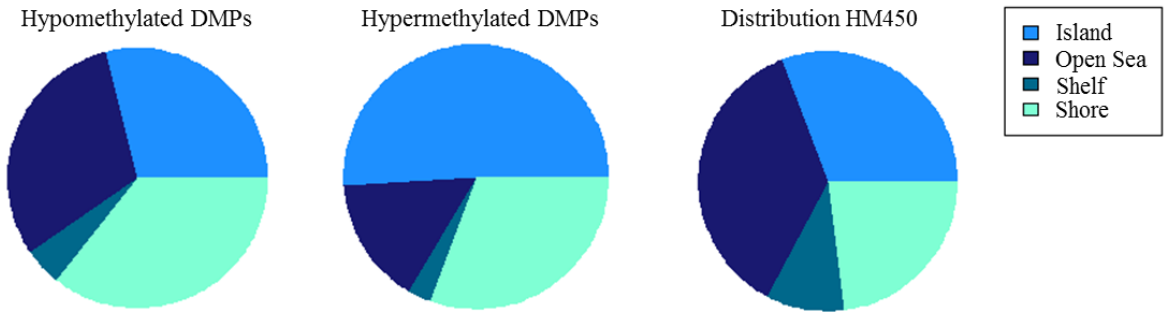

Figure 22. Distribution of the DMPs according to the CpG islands (island, "open sea", shelf and shore). *The total bead array probe distribution (HM450) is shown as reference.*

Comparison the distribution of all bead array (HM450) probes, marked enrichments of both the hyper– and hypomethylated DMPs were mainly observed within 3 kb distance from the transcription start sites (TSSs) of the corresponding coding genes (Figure 23).

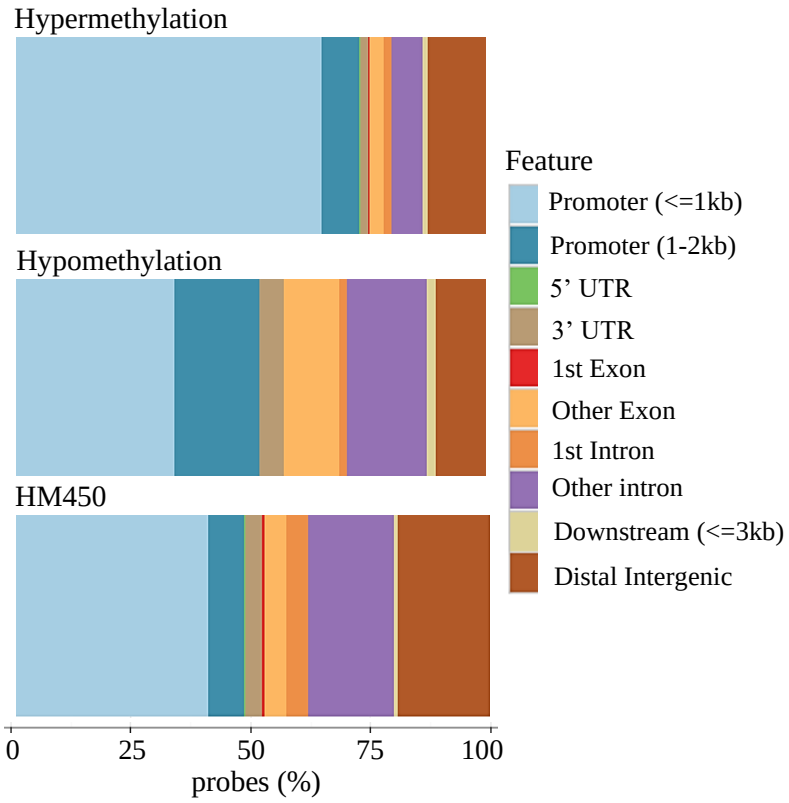

Figure 23. Differentially methylated probe (DMP) position relative to the genes (promoter, UTRs, intron/exon). *Hyper– and hypomethylated DMPs were detected predominantly within 3 kb distance from the transcription start sites (TSSs) of the related genes. The total bead array probe distribution (HM450) is shown as a reference.*

While the hypermethylated DMPs showed marked increase within the closer promoter regions, within 1kb distance to their annotated TSS, the hypomethylated DMPs were enriched in the distant (1-2 kb) promoter region (Figure 24). We detected significant difference in the GC content between hypermethylated probes and all bead array (HM450) probes (Figure 25). Furthermore, we observed significant difference in the GC content between hypermethylated probes and all bead array (HM450) probes (Figure 26).

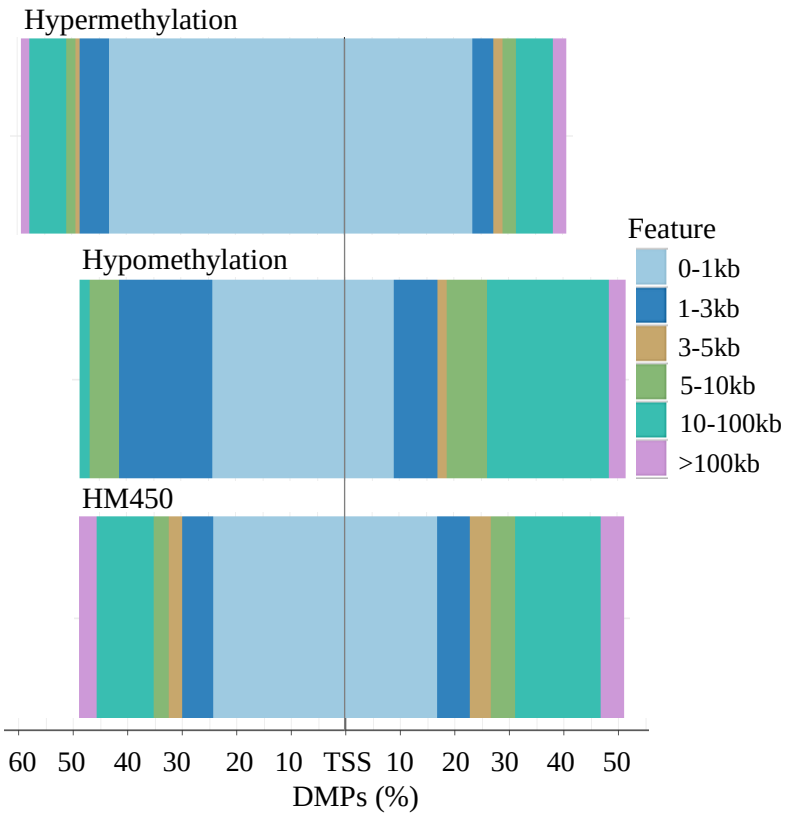

Figure 24. Differentially methylated probe (DMP) position relative to the distance to transcription start sites (TSSs). *Hypermethylated DMPs showed increase within 1kb distance to their annotated TSS, while the hypomethylated DMPs were enriched in the distant (1-2 kb) promoter region. The total bead array probe distribution (HM450) is shown as a reference.*

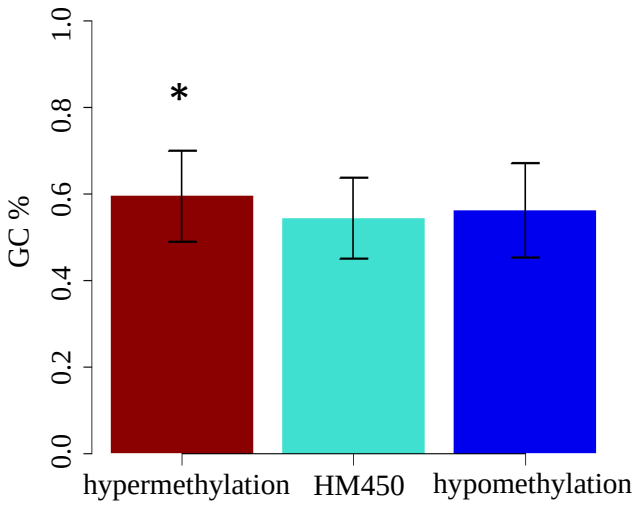

Figure 25. The GC content of hypermethylated and hypomethylated probes. *The total bead array probe distribution (HM450) is shown as a reference. The error bars mark the standard deviations. The asterisk indicates statistical significance (P<0.05)*

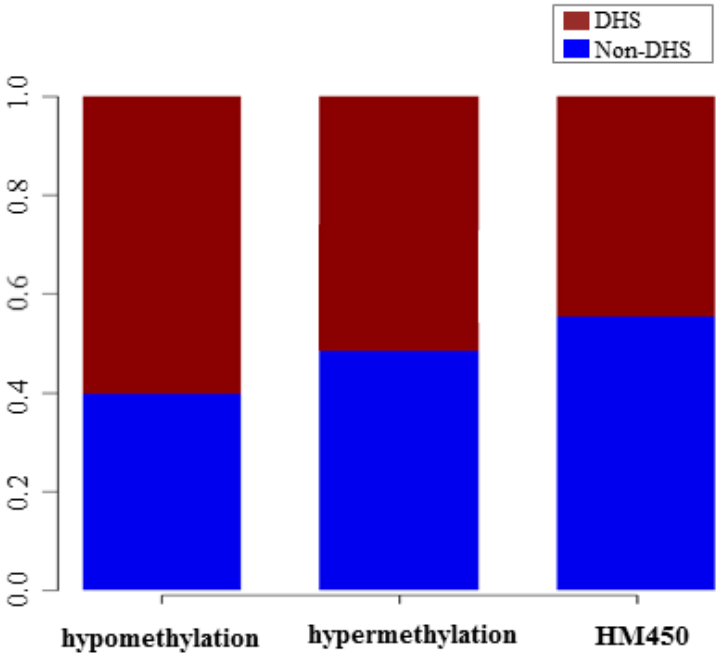

Figure 26. Differentially methylated probe (DMP) position relative to DNAse I hypersensitivity sites (DHSs). *The total bead array probe distribution (HM450) is shown as a reference.*

We applied more stringent criteria to determine significant DMRs with increased $\Delta\beta_{mean}$ >10% between the invasive and the original cell lines. As a result, we identified the 416 DMRs with 1,982 DMPs (corresponding to 384 genes) with hypermethylation in the selected invasive population, and only one DMR with 3 DMPs (corresponding to one gene) were hypomethylated (Supplementary Table 2 and 3). The top significant DMR presented with 15 differentially methylated probes and showing more than 20% included the *BAALC* gene with its corresponding non-coding RNA (ncRNA) pair, *BAALC-AS2* (FDR= 1.61E-11; Benjamini Hochberg procedure adjusted). Notably, several significant DMRs simultaneously covering coding genes and their corresponding ncRNAs were found such as *KIRREL3-AS3, CACNA1C-AS1, GCSAML-AS1, KCNAB1-AS2, BAALC-AS2, HOXC13-AS, BOK-AS1, PAX6-AS1, SHANK2-AS1, UNC5B-AS1, RUNX1-IT1, HOXB-AS1,* and *MCF2L-AS1* (Supplementary Table 3). We also identified genes with well-known functions in melanomas (e.g., *MITF, CYP27A1* and *GRIA2*) among the significant DMRs.

We performed pathway analysis using EnrichR web application on our predefined gene list ranked by the $\Delta\beta_{mean}$ methylation differences and compared to the WikiPathways June 2017 Release elements as an input. Applying FDR<0.05 (Benjamini Hochberg procedure adjusted) as a cut-off and considering pathways presented with at least 5 genes, we found that hypermethylation mostly affected the neural crest differentiation pathway (WP2064; *NOTCH3, PAX7*, *HEY2, MITF, FGFR2, FGFR3, RHOB, MSX2, TLX2,* and *ZIC5* genes) and the regulation of actin cytoskeleton pathway (WP51; e.g., *MOS, GSN, ACTN1, WASF2,* and *VAV1* genes) (Table 5).

Table 5. Enrichment analysis of significant hypermethylated DMPs meeting the criteria of mean Δβ > 0.1.

Term	P-value	Combined score	Genes
Neural Crest Differentiation_Homo sapiens_WP2064	2.86E-05	20.11953	*NOTCH3, MSX2, TLX2, PAX7, HAND1, HEY2, MITF, ZIC5, FGFR3, FGFR2, RHOB*
Regulation of Actin Cytoskeleton_Homo sapiens_WP51	0.009862	9.681106	*MOS, GSN, ACTN1, PAK6, PIP4K2C, FGFR3, WASF2, FGFR2, VAV1*
Ectoderm Differentiation_Homo sapiens_WP2858	0.048743	4.810694	*GRAMD1B, SHH, ZBTB16, PAX6, NR2F2, MZF1, FGFR2*

Integration of methylation and gene expression profiles

To investigate the functional relevance of the DNA methylation changes observed in the selected invasive cells, we performed integrative analysis of the DNA methylation data and gene expression alterations. The analysis involved all DMPs that passed the criteria for significant DMRs (FDR<0.05, Benjamini Hochberg procedure adjusted) without $\Delta\beta_{mean}$ cut-off.

We identified a total of 886 significantly correlated CpG sites corresponding to 392 individual genes between DNA methylation and gene expression, of which 220 showed negative, whereas 172 genes exhibited positive correlation (Supplementary Table 4). Although both the negatively and positively correlated CpGs exhibited enrichment for the closer promoter regions (Figure 27A), the increase was remarkable for differential methylation that exhibited negative correlation with the gene expression. If we compared the negatively correlated CpGs to the Infinium HumanMethylation450 BeadChip probes, we observed an enrichment within 1 kb distance up– and downstream from the transcription start sites (TSSs) of the corresponding coding genes, while the positively correlated CpGs were enriched in 1-3 kb downstream from the TSSs (Figure 27B). Interestingly, CpG island shore hypermethylation was associated with decreased expression level in case of four DMRs corresponding to *RHOB*, *ID4*, *ST8SIA1*, and *GRIA2* genes (Figure 28).

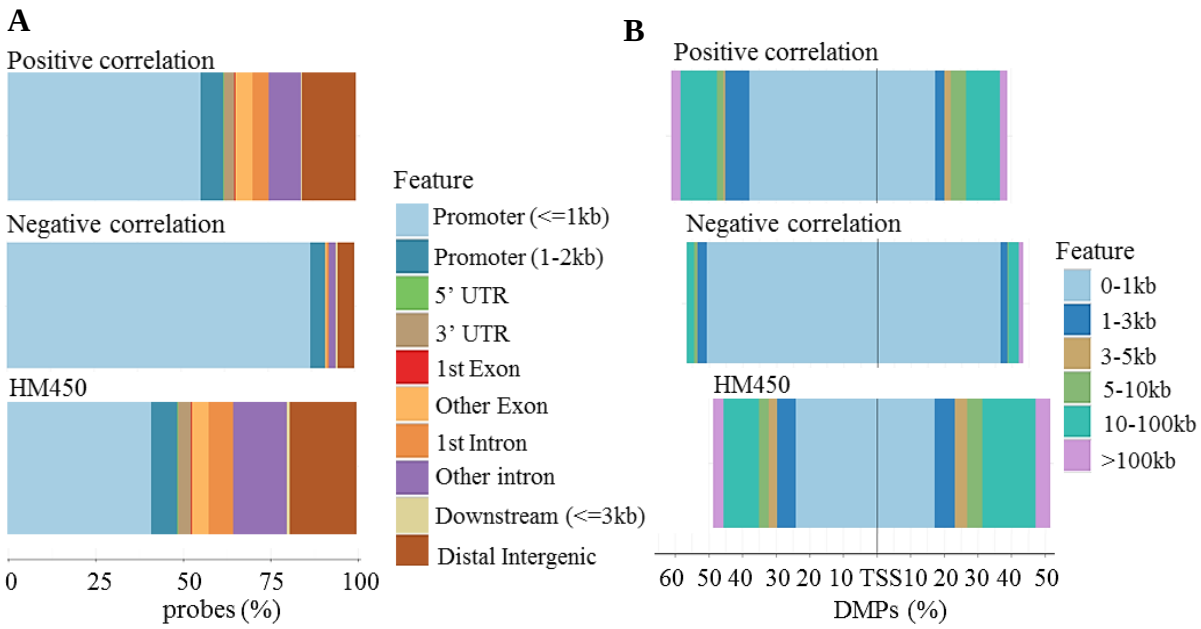

Figure 27. Integration of methylation and gene expression profiles related to melanoma invasiveness. *(A) Positively and negatively correlated probes relative to the genes (promoter, UTRs, or intron/exon) and (B) the distance to transcription start sites (TSSs). The total bead array probe distribution (HM450) is shown as a reference.*

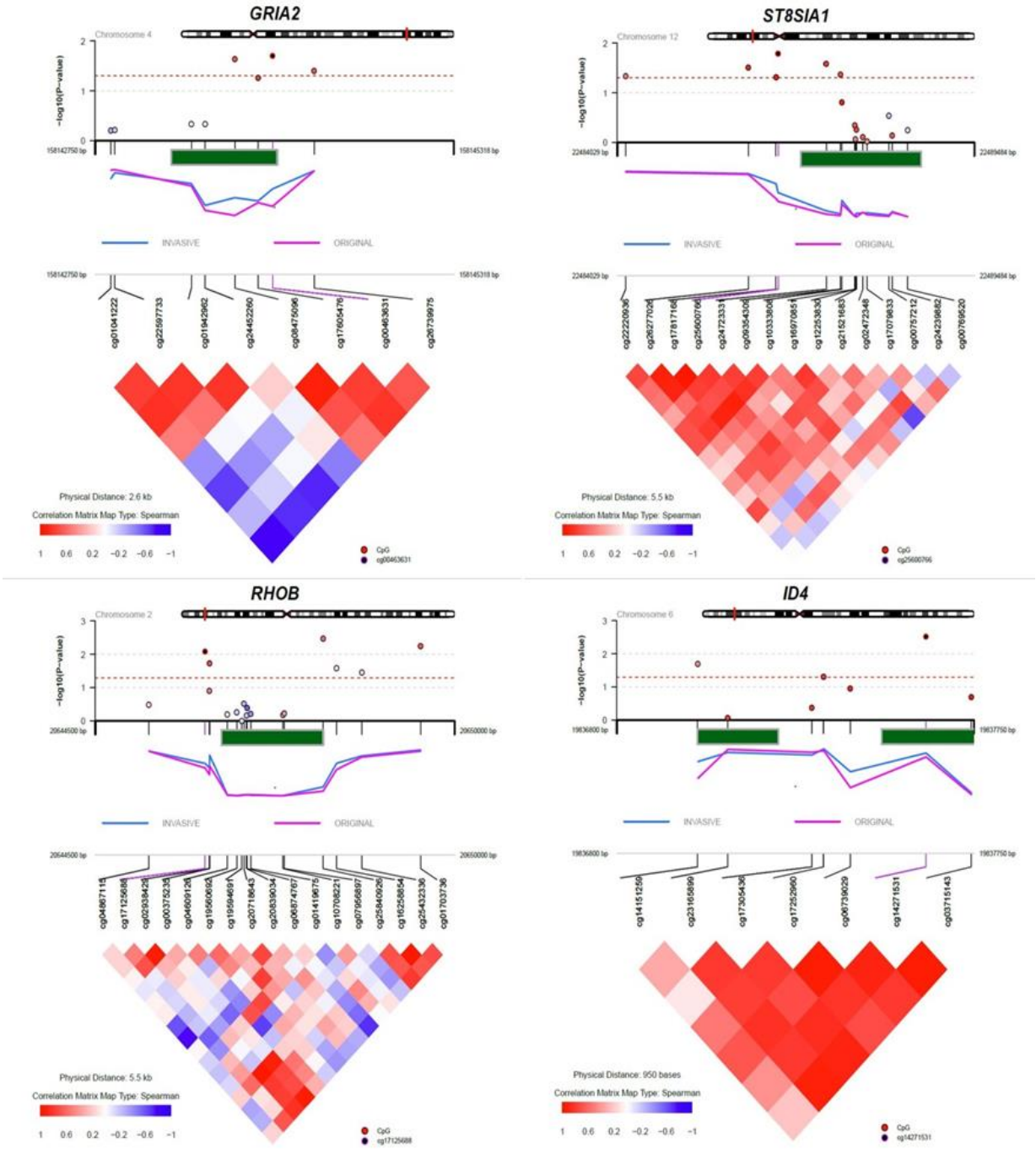

Figure 28. Visualization of DNA co-methylation patterns at CpG shores in invasive melanoma cell lines. *Co-methylation plots show the p values of the methylation difference between the selected invasive and the original cell lines for differentially methylated regions (DMRs). The reference probe is highlighted in black, the rest of the circles are marked according to Spearman correlation coefficients among probes. Blue and the violet lines represent the methylation level of the invasive and original cell lines, respectively. The green horizontal line shows the position of CpG island of the region.*

Furthermore, we applied more stringent criteria for the correlation analysis to increase the relevance of DNA methylation changes into gene expression differences: genes with 1-fold expression differences (log2 fold change > ±0.5) between the invasive and the original cell lines were correlated to DMPs of $\Delta\beta_{mean}$ >10% (Table 6). As demonstrated in Figure 29, majority of the genes were negatively correlated, i.e. hypermethylation was associated with decreased gene expression (*IL12RB2, LYPD6B, CHL1, SLC9A3, BAALC, FAM213A, SORCS1, GPR158, FBN1,* and *ADORA2B*; lower right segment, Figure 29), while a few genes exhibited positive correlation between hypermethylation and increased gene expression (*MCC, PTCHD4, EGFR, RBP4* and *FAR2*; upper right segment, Figure 29). Additionally, two hypomethylated genes revealed significant correlation with either upregulation (*NNMT*; upper left segment; Figure 29) or downregulation (*NBPF8*; lower left segment; Figure 29) of gene expression.

Real time quantitative PCR analyses were performed to confirm the relative gene expression levels of candidate genes significantly correlated with DNA methylation (*MITF, TERC, CDH13, PAX6, RHOB, HCK, NNMT, PMEL, EDNRB, ID4, EGFR, LEF1* and *ST8SIA1*). The qRT-PCR results were consistent with the microarray expression data, and robust correlation was observed in the majority of the tested transcripts ($0.74 \leq R \leq 1.00$, P-value ≤ 0.05). The relative expression levels are shown in Supplementary Table 5.

Table 6. Significant correlation between differentially methylated probes (DMPs) and gene expression data

Chr.	start	end	Nearest gene symbol	Nearest TSS	Mean Δß	Mean logFC	P-value	R[a]
Negative correlation								
chr1	67772986	67772987	*IL12RB2*	*IL12RB2*	0.13	-0.73	1.95E-02	-0.79
chr2	149895023	149895024	*LYPD6B*	*LYPD6B*	0.14	0.70	3.54E-02	-0.74
chr3	238618	238619	*CHL1*	*CHL1*	0.13	-0.65	1.40E-02	-0.81
chr5	497639	497640	*SLC9A3*	*PP7080*	0.13	-0.60	2.07E-02	-0.79
chr5	497397	497398	*SLC9A3*	*PP7080*	0.10	-0.60	4.04E-02	-0.73
chr8	104153592	104153593	*BAALC*	*BAALC*	0.25	-0.79	2.40E-02	-0.77
chr8	104153637	104153638	*BAALC*	*BAALC*	0.32	-0.79	3.42E-02	-0.74
chr8	104153767	104153768	*BAALC*	*BAALC*	0.20	-0.79	2.33E-02	-0.78
chr8	104153627	104153628	*BAALC*	*BAALC*	0.36	-0.79	4.11E-02	-0.73
chr8	104153643	104153644	*BAALC*	*BAALC*	0.36	-0.79	3.02E-02	-0.76
chr10	82167774	82167775	*FAM213A*	*FAM213A*	0.18	-0.89	3.41E-03	-0.89
chr10	82167757	82167758	*FAM213A*	*FAM213A*	0.17	-0.89	2.57E-03	-0.90
chr10	108924867	108924868	*SORCS1*	*SORCS1*	0.19	-0.94	1.64E-02	-0.80
chr10	25464418	25464419	*GPR158*	*GPR158*	0.13	-0.53	3.58E-03	-0.88
chr10	82167764	82167765	*FAM213A*	*FAM213A*	0.16	-0.89	1.38E-03	-0.92
chr11	114165661	114165662	*NNMT*	*NNMT*	-0.13	0.94	4.01E-02	-0.73
chr15	48938576	48938577	*FBN1*	*FBN1*	0.12	0.73	6.12E-03	-0.86
chr15	48938239	48938240	*FBN1*	*FBN1*	0.11	0.73	4.66E-03	-0.87
chr15	48938370	48938371	*FBN1*	*FBN1*	0.11	0.73	3.70E-03	-0.88
chr17	15848264	15848265	*ADORA2B*	*ADORA2B*	0.15	-0.61	3.02E-03	-0.89
chr17	15848828	15848829	*ADORA2B*	*ADORA2B*	0.10	-0.61	2.08E-04	-0.96
chr17	15848253	15848254	*ADORA2B*	*ADORA2B*	0.185	-0.609	6.03E-04	-0.94
Positive correlation								
chr1	147737024	147737025	*NBPF8*	NA	-0.14	-0.81	3.62E-02	0.74
chr5	112824765	112824766	*MCC*	*MCC*	0.21	0.76	1.10E-02	0.83
chr6	48036605	48036606	*PTCHD4*	*PTCHD4*	0.15	0.58	4.16E-02	0.73
chr6	48036409	48036410	*PTCHD4*	*PTCHD4*	0.13	0.58	3.79E-04	0.95
chr6	48036280	48036281	*PTCHD4*	*PTCHD4*	0.10	0.58	5.02E-05	0.97
chr7	54956598	54956599	*EGFR*	*EGFR*	0.27	0.63	1.24E-02	0.82
chr10	95326178	95326179	*RBP4*	*RBP4*	0.22	0.51	2.40E-02	0.78
chr12	29376483	29376484	*FAR2*	*FAR2*	0.11	0.97	3.55E-02	0.74

[a]Correalation Coefficient

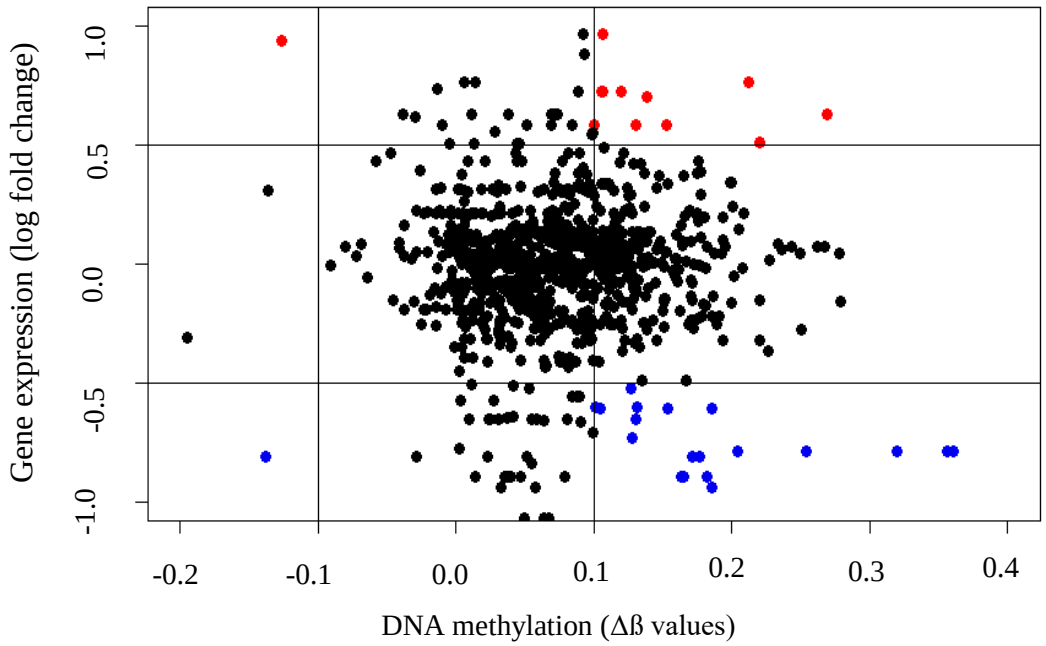

Figure 29. A starburst plot corresponding to correlation analysis between DNA methylation and gene expression changes. *The filtered mean log expression and methylation data are shown in a correlation plot (1-fold expression differences between the invasive and the original cell lines were correlated to DMPs of Δβmean >10%). Probes with increased gene expression are shown in red, and probes with decreased expression are highlighted in blue.*

Invasion related methylation changes in melanoma tumour samples

To validate our results of methylation changes observed in the selected invasive cells, we compared our findings with publicly available melanoma dataset of the TCGA-SKMC cohort. First, we determined the methylation changes present in the TCGA metastatic melanomas (n=349) versus tissues of primary sites (n=88). Altogether 879 genes (corresponding to 1,984 differentially methylated regions) exhibited significant differences between the metastatic and primary melanomas of the TCGA cohort. The full list of the differentially methylated regions is shown in Supplementary Table 6. Notably, the number of differentially methylated genes is much higher compared to our results, which is expected, as the metastatic melanomas are known to harbour more alterations that of being representative of not only for the metastatic

potential but also the heterogeneity of the metastatic tissues represented by different locations such as lymph node, skin bone and distant organs. Nevertheless, 28 genes out of our differentially methylated 385 genes showed overlap to the TCGA metastatic melanomas. Remarkably, several of the overlapping genes between the 2 datasets have already well-established role in in invasion and metastasis formation, of which includes *TP73, HOXD13, PAX6, ITPKA, NR2F2, SLC17A7, SPTBN1, AHNAK, CCL23, NFE2L3*, and *SLC9A* [107, 136]. Furthermore, 10 out of the 28 genes seem to have a role in the transcriptomic reprogramming during early invasion: the methylation changes of *CBFA2T3, TP73, CTSK, NAV2, PAX6, ARHGAP22, SDK1, ATP11A, RASA3*, and *SLC9A3* showed significant correlation with gene expression changes.

However, this comparison has the limitation that later metastatic events are not necessarily characteristic for those arise at the early stages of invasion [137, 138]. For this reason, we aimed to concentrate on the 88 primary melanoma tissues and used Clark staging as the most relevant clinical parameter to differentiate between locally invasive (Clark stage-5, n=20) and early stage (all the Clark stages below V, n=41) referred as less invasive. We identified 448 differentially methylated genes (corresponding to 1269 probes) seem to have a role during early invasion represented by the Clark staging system (Supplementary Table 7). Of note, 18 out of the 385 genes in our dataset show overlap with the TCGA (e.g., *MECOM*, *CHD5*, *TRIM55*, *FZD6*, *TPBG*, and *TRPC4*).

Comparing our data with the TCGA, the most interesting finding is the hypermethylation of *ARHGAP22* and *NAV2* genes that were commonly presented in locally invasive primary melanomas as well as during metastasis.

Expression of DNMTs, UHRFs and TETs in selected invasive cells

To investigate the possible biological background of different methylation patterns between the selected invasive and the original cell lines, we analysed the relative mRNA expression of the DNA methyltransferases (DNMT1, DNMT13A, and DNMT13B), the ubiquitin-like protein containing PHD and RING finger domains 1 and 2 (UHRF1 and UHRF2) and the TET methylcytosine dioxygenase enzymes (TET1 and TET2), all playing a crucial role in the maintaining and removing of epigenetic marks. We observed that each of the selected invasive cells had decreased DNMT1 and DNMT3B expression compared to the original cell lines (Figure 30).

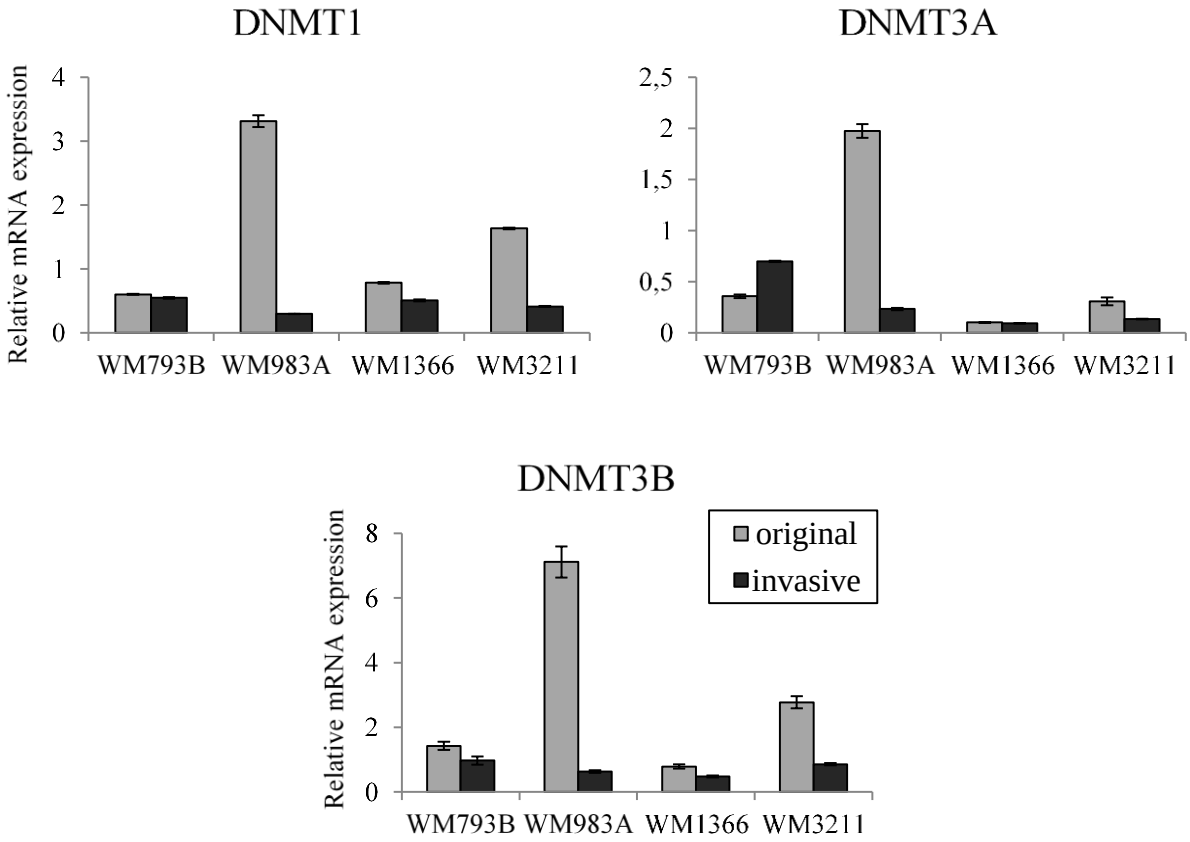

Figure 30. Comparison of the relative mRNA expressions of DNMTs in the original and the selected invasive melanoma cell lines by real-time quantitative PCR*. In case of WM983A, WM1366 and WM3211, selected invasive cells had decreased DNMT1 and DNMT3B expression compared to the original cell lines. The data are presented as mean ± SD (three triplicates/samples).*

UHRF1 and *UHRF2* genes also showed downregulation in invasive cells compared to the original cell lines (Figure 31). Additionally, the expression levels of TET1 and TET2 were also remarkably lower in two of the four invasive cells (WM983A-INV and WM3211-INV) than in the original cell lines (Figure 32). Unexpectedly, TET2 down-regulation was associated with hypermethylation at the *TET2* gene promoter region in the invasive subpopulation (Figure 33).

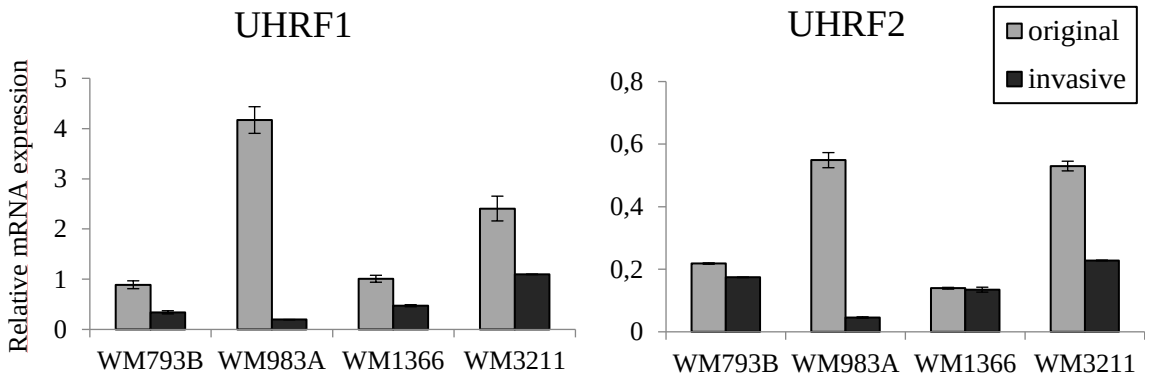

Figure 31. Comparison of the relative mRNA expressions of UHRFs in the original and the selected invasive melanoma cell lines by real-time quantitative PCR*. Both UHRF1 and UHRF2 genes showed downregulation in invasive cells compared to the original cell lines. The data are presented as mean ± SD (three triplicates/samples).*

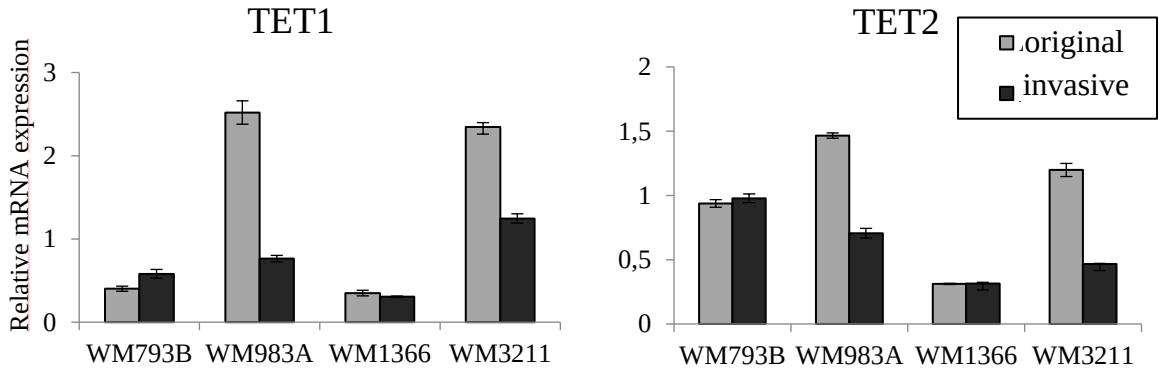

Figure 32. Comparison of the relative mRNA expressions of TET genes in the original and the selected invasive melanoma cell lines*. The data are presented as mean ± SD (three triplicates/samples).*

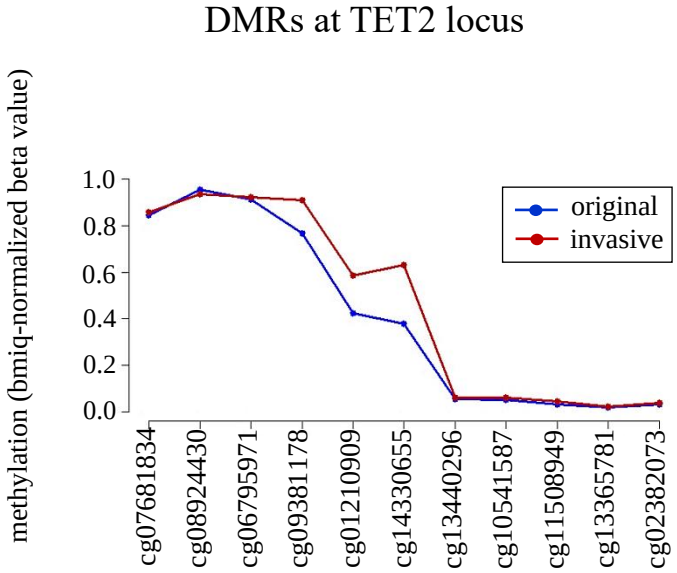

Figure 33. Comparison of the methylation level of TET2 gene in the original and the selected invasive melanoma cell lines. *Line plot of significantly differentially methylated region at TET2 gene in the invasive (red line) and the original cell lines (blue line).*

Discussion

Cytogenetic heterogeneity resulting from chromosomal instability is a major driving force of melanoma progression [55]. Invasion is one of the first steps of metastasis formation in primary tumours; however, insufficient data are available on the genetic and epigenetic alterations involved in this initial process in melanoma.

During this study, our major goal was to define genetic, gene expression and DNA methylation alterations associated with melanoma cell invasion. First, we examined the invasive property of 12 primary tumour and 6 metastasis originated melanoma cell lines and defined the genomic alterations of all by array CGH. In overall, the pattern of genomic alterations was in close agreement with previously published data [56, 139-142]. Gains of whole chromosomes or chromosome arms were observed across the 1q, 6p, 7, 8q, 17q, 20 and 22q regions, whereas losses were frequently found on chromosomes 6q, 9p and 10p. CN changes of several well-known oncogenes (*EGFR*, *NEDD9*, *MYC* and *BRAF*) and tumour suppressor genes (*CDKN2A*, *CDKN2B*) related to melanoma progression were detected [143-147]. Based on our invasion assay experiments on melanoma cell lines, we were able to group the cell lines according to their invasive capacity. One of our main goals was to identify the invasive potential of multiple primary melanomas derived melanoma cell lines and compare the CN changes between the invasive and non-invasive subgroups. We found several CN alterations that were uniquely detected only in the invasive cell lines. Loss of 7q appeared to associate with invasive behaviour; targeting genes whose deletion or down-regulation can potentially increase melanoma cell invasion (e.g., *PTPN12*, *ADAM22*, *FZD1*, *TFPI2*, *GNG11*, *COL1A2*, *SMURF1*, *VGF* and *RELN*).

In association with the mRNA expression analyses, downregulation of *PTPN12*, *ADAM22*, *FZD1*, *SMURF1*, *VGF* and *RELN* genes was characteristic for the invasive cell lines compared to non-invasive ones. Although alterations of these genes have already been reported in a

variety of invasive tumours, but we were the first to describe that the structural and functional alterations of these genes have fundamental role in melanoma invasion. [148-155].

We observed that gain of the *GLIPR1* gene was specifically characteristic for invasive cell lines. The mRNA expression level of *GLIPR1* gene was notably higher in invasive cell lines than in non-invasive lines confirming that upregulation of the gene is associated with increased invasive potential in melanoma [156]. According to previous studies, after the translocation of the GLIPR1 (GLI pathogenesis-related 1) protein to the cell surface, the soluble N-terminal domain of the molecule is exposed to the extracellular space, which can lead to invasion [154, 155].

We also aimed to identify CN alterations that are specific for invasive primer melanoma and present in the metastasis-derived cell lines. We found that gains of the *GDNF* (5p13.1), *GPAA1*, *PLEC* and *SHARPIN* (8q24.3) genes were detected in invasive and in metastatic cell lines as well, indicating the possible role of these genes both in invasion and in metastasis formation. In addition, these genes showed copy number alterations also in metastatic melanoma tissues of the TCGA (Provisional) melanoma dataset, supporting the relevance of these genes during the progression, metastasis formation of melanoma cells. Results of previous studies have shown that upregulation of the *GDNF* (glial cell derived neurotrophic factor) gene can induce proliferation and invasion of melanoma cells through activating the MAPK and PI3K pathways [157, 158]. The overexpression of *GPAA1* (glycosylphosphatidylinositol anchor attachment 1) could induce tumour invasion as well [159, 160]. Plectin (PLEC) is a multifunctional plakin protein that is essential for the integrity of skin, skeletal and cardiac muscle; it can regulate actin assembly and cell migration [161]. In addition, a recent study demonstrated the role of overexpressed SHARPIN (SHANK-associated RH domain interactor) in the activation of NFκB pathway and its downstream targets affecting cell invasion and metastasis [162]. The

function of GPAA1, PLEC and SHARPIN in association with melanoma invasion and metastasis formation has not been mentioned previously.

Through DNA copy-number profiling, we also aimed to determine genetic changes related to the *BRAF* and *NRAS* mutation status of melanoma cell lines. Previous studies indicated that *BRAF* mutation is present in approximately half of the melanomas [59, 163, 164], and it seems to be an early event through melanoma progression (high frequency in benign nevi) suggesting additional cooperative events associated with oncogenesis [163, 165, 166]. According to our array CGH results, $BRAF^{V600E}$ mutation was associated with the gain of the *BRAF* gene on 7q34 in 53.9% of the cell lines, concordantly with previous studies [141, 167]. Copy number gains of 1q, 6p, and loss of 19p12 were characteristic in $BRAF^{V600E}$ mutated cell lines, in a good agreement with the literature [142]. Copy number alteration associated with *NRAS* mutations was detected only on chromosome arm 4q, similarly to former study [167].

Several investigations have shown the role of $BRAF^{V600E}$ mutation during melanoma invasion and metastasis formation [2, 168, 169]. In our study, two out of the four invasive cell lines carried *BRAF* mutation. The comparison of CN alterations in invasive *BRAF* mutant and wild-type cell lines resulted in that gain of 6p25.3-p22.3 was present specifically in invasive cell lines with *BRAF* mutation, including *NEDD9* (6p24) and *RREB1* (6p25) genes. The copy number change of *RREB1* is a well-known alteration in melanoma, this gene has a very important role in melanoma diagnosis, it is a target of multiprobe FISH to differentiate cutaneous nevi from melanoma [170]. Amplification of the *NEDD9* gene also correlates with melanoma metastasis by promoting elongated movement and invasion of melanoma cells [37, 171]. It is important to note, that alteration of *NEDD9* in association with *BRAF* mutation was not described previously.

Our systematic comparison of CN alterations between cell lines with different invasive properties revealed several remarkable genomic alterations in invasive melanoma cells. CN

alterations of various invasion-related genes were observed for the first time in *in vitro* invasive melanoma cell lines. Furthermore, our data highlight the possible role for the gain of *GDNF*, *GPAA1*, *PLEC* and *SHARPIN* genes in metastasis formation as well. Our genomic analysis of human melanoma cell lines and the classification of CN alterations associated with melanoma invasiveness thus provide novel candidate genes for further functional studies.

We also aimed to select invasive cells *in vitro* from the original cell lines and analysed their invasion-associated DNA methylation changes, which followed by functional analysis of the observed changes at mRNA expression level. A number of studies have indicated that several tumour suppressor genes are silenced by DNA methylation in malignant melanoma compared to normal melanocytes or nevi [172-174]. Levy et al. have been described the relevance of MITF activity in melanocyte precursors arising from neural-crest progenitor cells, as well as the role of *MITF* gene downregulation in advanced melanoma [175]. Additionally, Lauss et al. indicated that the downregulation of *MITF* in late-stage melanomas may be regulated by hypermethylation [103]. MITF (microphthalmia-associated transcription factor) has been extensively studied in the context of master-regulator of melanin-production, suppression of invasion and regulation of the proliferative phenotype in melanoma cells [79, 103, 176, 177]. Its methylation change was also observed in melanoma brain metastases, suggesting its role not only in invasion property, but also in metastasis formation [107, 108]. In accordance with previous studies, selected invasive melanoma cells showed hypermethylation of *MITF* that may directly affect MITF expression, giving a functional role of the detected epigenetic change. Additionally, pathway analysis of hypermethylated genes in the invasive cells revealed a significant enrichment of the neural crest differentiation pathway (WP2064).

Several studies have pointed out that different biological behaviours of melanomas are associated with distinct methylation subgroups [107, 110, 178, 179]. Altered gene expression in correlation with methylation changes in potential DNA methylation biomarkers of melanoma

(e.g., *TFI2, HCK, MGMT* and *TP73*) were also observed in the selected invasive cells. The methylation changes of the aforementioned genes have been described in association with advanced clinical stage, shorter overall survival and the presence of metastasis, and it seems that, according to our results, these genes have a potential role in the earlier invasion steps of primary melanoma cells [98, 179-181].

In agreement with the widely accepted assumption that increased DNA methylation of certain promoters causes deregulation of the corresponding genes, based on the correlation analysis we performed between our methylation and gene expression microarray data, we observed a negative correlation between the methylation and gene expression for several promoters such as *FBN1*, *ADORA2B,* and *CHL1*. It was reported that hypermethylation is associated with the deregulation of fibrillin-1 (FBN1; a major component of microfibrils), and it can mediate cell adhesion in melanoma cells [182]. ADORA2B has been identified as specific receptor for 5'-methylthioadenosine (MTA) that can affect cell invasiveness in melanoma cells [183]. Neural cell adhesion molecule L1 (CHL1) has diverse functions including different signal transduction pathways and plays important role in various human cancers [184]. *CHL1* is frequently down-regulated in different types of tumours, and it is verified to inhibit invasive growth and able to suppress further metastatic spread [185]. Down-regulation of *CHL1* in association with methylation change was also observed in melanoma cells by Chatterjee et al. indicating that differentially methylated *CHL1* is a marked alteration in melanoma cells as well [186].

While previous studies have shown that DNA hypermethylation at gene promoters is associated with the silencing of gene expression, recent studies have shown that the methylation of the gene body is positively correlated with transcription [93, 187, 188]. Similar to these observations, hypermethylation in the gene body potentially plays a role in the upregulation of *EGFR* and *RBP4* genes in the selected invasive cell populations. The role of EGFR in a range of neoplasms including melanoma is well-known, in association with tumour progression and

metastasis [147, 189, 190]. Based on our results, methylation of *EGFR* gene body in correlation with upregulated expression was characteristic for the invasive cells. Epigenetic activation of *EGFR* upon resistance development to BRAF inhibitors has been previously described in melanoma, *EGFR* showed methylation difference in metastatic cell lines compared to its matched primary cell lines as well [186, 191]. The role of EGFR expression in melanoma cells is controversial, its association with the outcome of melanoma and with specific pathological features is disapproved, however, a high percentage of primary and metastatic melanoma tissues shows EGFR positivity [192, 193]. It is suggested that the functional relevance of the EGFR-mediated signalling is depending on stimulation of the ERK and AKT pathways by EGF [193]. On the other hand, RBP4 (retinol binding protein 4) is the major transporter for vitamin A/retinol acid (RA) in serum [194]. Recent studies indicated that RBP4 serum levels might be a biomarker in colorectal cancer, its overexpression was also associated with ovarian cancer cell migration [195, 196]. However, its function in melanoma has not been observed previously.

In addition, we also found that increased *NNMT* (nicotinamide N-methyltransferase) gene expression was significantly associated with hypomethylation in the invasive cells. The expression of *NNMT* has been shown to be essential in cellular invasion and migration; however, it has not been previously identified in melanoma cells [197, 198].

To obtain insights into the possible clinical relevance of the DNA methylation changes identified in our *in vitro* invasion model, we compared our results to the publicly available 450k TCGA-SKCM datasets involving more than 400 melanoma samples with the vast majority being metastatic melanomas and the representative for heterogeneous anatomic locations.

Based on this analysis we identified several methylation changes that can have functional role in melanoma tumour samples, including *HOXD13*, being the member of the well-known master regulators of developmental processes, and involved both in oncogenesis and tumour suppression [199]. In addition, we recognized further 8 differentially methylated members of

the HOX gene family including *HOXA5, HOXB1, HOXB2, HOXB3, HOXB4, HOXC5, HOXC9,* and *HOXD11*. Hypermethylation of homeobox genes are frequent in several cancers, however, elevated methylation level does not consequently associated with the reduced expression of the downstream genes, as well as differentially methylated homeobox genes are not shown to be down-regulated in our invasive cells [107, 200-202]. Differentially methylated *HOXA5* and *HOXD11* was found as a specific alteration in melanoma brain metastasis, and hypermethylation of *HOXD9* were described in lymph node metastasis with shorter overall survival [105, 107, 109]. It is suggested that methylation pattern of homeobox genes can be specific to melanoma cells, and it is a possible approach to use epigenetic biomarker panels including homeobox genes in diagnosis, prediction and prognosis [200, 203].

The most interesting finding between our results and the TCGA melanoma data is the hypermethylation of *ARHGAP22* and *NAV2* promoter regions that are commonly presented in locally invasive primary melanomas as well as during metastasis. Both *ARHGAP22* and *NAV2* (neuron navigator 2) have been identified to be involved in cell migration of different tumour types including melanoma [204-206]. NAV2 has several functional domains, which play key roles in the regulation of cytoskeletal remodelling and cell migration facilitating tumour invasion and metastasis [207, 208]. Furthermore, a recent study suggested that NAV2 might contribute to melanoma invasion by epithelial–mesenchymal transition through the GSK-3β/β-catenin-SNAI2 pathway [209]. ARGHAP22 is a member of Rho GTPases that regulate the cytoskeleton-dependent processes during migration and invasion [210]. Silencing of *ARHGAP22* results in increased number of elongated cells in melanoma cell lines, and can regulate the mesenchymal-amoeboid transition [37]. The switch between mesenchymal and amoeboid types of movement, allowing metastatic tumour cells to adapt their morphology and movement in different microenvironments [37]. Our results indicate the relevance of

methylation mediated gene expression changes of *ARHGAP22* and *NAV2* during the invasion of primary tumours, and also during invasion-related melanoma progression.

DNA methylation pattern is processed by an enzyme family, the DNA methyl transferases (DNMTs), including DNMT1, the major enzyme involved in the inheritance of methylation pattern, and DNMT3A and DNMT3B, which are predominantly catalyse *de novo* DNA methylation [211, 212]. In our study, *DNMT1* and *DNMT3B* had decreased expression levels in the selected invasive cells, which might suggest global hypomethylation patterns, however, the invasive subpopulations were characterized by preferential hypermethylation. Recent studies indicated that increased expression of UHRF1 and/or UHRF2 negatively regulates de novo DNA methylation and contributes to global DNA hypomethylation by promoting DNMT3A degradation in cancer cells; while their decreased expression has been observed to correlate with hypermethylation pattern in different tumours [213, 214]. Consistent with the recent findings, both *UHRF1* and *UHRF2* genes showed downregulation in invasive cells, however, we did not observe a significant correlation with the expression of DNA methyltransferases. The relationship between *UHRFs* gene expression and methylation pattern is well defined in melanoma cells as well, however, this mechanism need additional investigations [186]. On the other hand, DNA methylation is not an irreversible event as it was described earlier, and the family of TET enzymes are involved in removing this epigenetic mark [215-218]. An interesting finding in this study was the hypermethylation at *TET2* gene along with decreased mRNA expression in the invasive subpopulation of the melanoma cell lines, which may be due to the down-regulation of the *TET1* and *TET2* genes. Interestingly the hypermethylation of *TET2* promoter region along with the downregulation of gene was characteristic for the invasive melanoma cell population, which may contribute to the accumulation of 5mC and therefore, plays a role in the global hypermethylation pattern of melanoma invasiveness; this observation need further investigations.

Overall, we found aberrant methylations of multiple genes in the *in vitro* selected invasive melanoma cells and a cohort of hypermethylated genes with decreased gene expression. Our results indicate the relevance of hypermethylated pattern in invasive melanoma cells, which might associate with the early invasion steps of melanoma.

Summary

Invasion of cells is the first step during metastasis formation, resulting in cell migration through tissue compartments. It is well known that cancer-related genes play a fundamental role during tumorigenesis and lead to cellular plasticity which promotes invasion. Our aim was to identify novel genetic and epigenetic markers on invasive melanoma cells.

Matrigel invasion chambers were used to determine the invasive properties of cell lines originated from primary and metastatic melanomas. We applied array comparative genomic hybridisations (CGH) to define the chromosome copy number alterations (CNAs). To explore the DNA methylation landscape of invasive melanoma cells we applied Illumina BeadChip assays, to define the gene expression pattern we used Affymetrix Human Gene 1.0 microarrays. Based on our results, we observed that the invasive primary cell lines harbour CNAs with high frequencies, including the loss of 7q and gain of 12q regions. Beside these alterations, gain of the *GDNF* (5p13.1), *GPAA1*, *PLEC* and *SHARPIN* (8q24.3) genes were significantly more frequent in invasive cells compared to the non-invasive ones. Importantly, copy number gains of these genes were also found in cell lines originated from metastases, suggesting their role in melanoma metastasis formation. On the other hand, our data revealed predominantly hypermethylated genes in the invasive cells. Integrative analysis of the methylation and gene expression profiles resulted in a cohort of hypermethylated genes with decreased expression. We also identified hypermethylation of the promoter regions of the *ARHGAP22* and *NAV2* genes that are commonly altered in locally invasive primary melanomas as well as during metastasis which might have important role during melanoma progression.

In our study we summarized genetic and epigenetic differences related to melanoma invasion and we assume that those alterations may contribute to the aggressive phenotype of human melanoma cells.

Összefoglalás

A tumorsejtek inváziója a metasztázis képzés első lépése, melynek során a sejtek képesek a környező szövetek infiltrációjára. Tekintettel arra, hogy a sejtek invazív képességéhez különböző molekuláris eltérések járulhatnak hozzá, célul tűntük ki a daganat progresszióban meghatározó szerepet játszó invazív melanoma sejtek genetikai és epigenetikai eltéréseinek vizsgálatát melanoma sejtvonal modell rendszerekben.

A sejtek invazív képességének meghatározásához Matrigel inváziós kamrát használtunk. Az invazív sejtek genetikai eltéréseinek elemzéséhez array komparatív genom hibridizációt alkalmaztunk (CGH). A sejtek metilációs mintázatának elemzéséhez Illumina Infinium array-t használtunk, a génexpressziós változásokat Affymetrix Human Gene 1.0 ST array-vel határoztuk meg. A primer tumor eredetű invazív sejtvonalak szignifikáns eltérései a 7q deléció és a 12q amplifikációja voltak. Továbbá, az invazív sejtvonalakban szignifikánsan magasabb volt a *GDNF* (5p13.1), *GPAA1*, *PLEC* és *SHARPIN* (8q24.3) gének kópiaszáma a nem invazív sejtvonalakhoz hasonlítva. Ezeknek a géneknek az eltérései a metasztázis eredetű sejtvonalakban is jelen voltak, ami a metasztázis képzésben betöltött lehetséges szerepükre utal. Továbbá megfigyeltük, hogy az invazív sejteket főként hipermetilált mintázat jellemzi. A DNS metiláció eredményeit és a génexpressziós profilt integrálva kimutattuk, hogy a hipermetilált gének egy csoportjára csökkent génexpresszió jellemzi. Számos olyan metilációs eltérést is azonosítottunk, melyek szerepet játszhatnak a melanoma progressziójában, beleértve az *ARHGAP22* és *NAV2* gének promóter hipermetilációját, melyek eltérést mutattak az invazív tulajdonsággal jellemzett primer melanoma és a metasztázis mintákban is. A dolgozat részletes elemzést ad az invazív melanoma sejtek genetikai és epigenetikai eltéréseiről, továbbá eredményeink hozzájárulhatnak a melanoma sejtek agresszív viselkedésének megértéséhez.

References

1. Dunki-Jacobs, E.M., G.G. Callender, and K.M. McMasters, *Current management of melanoma.* Curr Probl Surg, 2013. **50**(8): p. 351-82.
2. Orgaz, J.L. and V. Sanz-Moreno, *Emerging molecular targets in melanoma invasion and metastasis.* Pigment Cell Melanoma Res, 2013. **26**(1): p. 39-57.
3. Paluncic, J., et al., *Roads to melanoma: Key pathways and emerging players in melanoma progression and oncogenic signaling.* Biochim Biophys Acta, 2016. **1863**(4): p. 770-784.
4. Svedman, F.C., et al., *Stage-specific survival and recurrence in patients with cutaneous malignant melanoma in Europe - a systematic review of the literature.* Clin Epidemiol, 2016. **8**: p. 109-22.
5. Rozeman, E.A., et al., *Advanced Melanoma: Current Treatment Options, Biomarkers, and Future Perspectives.* Am J Clin Dermatol, 2018. **19**(3): p. 303-317.
6. Ferlay, J., et al., *Cancer incidence and mortality worldwide: sources, methods and major patterns in GLOBOCAN 2012.* Int J Cancer, 2015. **136**(5): p. E359-86.
7. Ferlay, J.E., M; Lam, F; Colombet, M; Mery, L; Piñeros, M; Znaor, A; Soerjomataram, I; Bray F *Global Cancer Observatory: Cancer Today. Lyon, France: International Agency for Research on Cancer.* 2018; Available from: https://gco.iarc.fr/today, accessed 28 October 2019].
8. Eggermont, A.M., A. Spatz, and C. Robert, *Cutaneous melanoma.* Lancet, 2014. **383**(9919): p. 816-27.
9. Rastrelli, M., et al., *Melanoma: epidemiology, risk factors, pathogenesis, diagnosis and classification.* In Vivo, 2014. **28**(6): p. 1005-11.
10. Siegel, R.L., K.D. Miller, and A. Jemal, *Cancer Statistics, 2017.* CA Cancer J Clin, 2017. **67**(1): p. 7-30.
11. Forsea, A.M., et al., *Melanoma incidence and mortality in Europe: new estimates, persistent disparities.* Br J Dermatol, 2012. **167**(5): p. 1124-30.
12. Russak, J.E. and D.S. Rigel, *Risk factors for the development of primary cutaneous melanoma.* Dermatol Clin, 2012. **30**(3): p. 363-8.
13. Whiteman, D.C., C.A. Whiteman, and A.C. Green, *Childhood sun exposure as a risk factor for melanoma: a systematic review of epidemiologic studies.* Cancer Causes Control, 2001. **12**(1): p. 69-82.
14. Elwood, J.M. and J. Jopson, *Melanoma and sun exposure: an overview of published studies.* Int J Cancer, 1997. **73**(2): p. 198-203.
15. Leonardi, G.C., et al., *Cutaneous melanoma: From pathogenesis to therapy (Review).* Int J Oncol, 2018. **52**(4): p. 1071-1080.
16. Ross, M.I. and J.E. Gershenwald, *Evidence-based treatment of early-stage melanoma.* J Surg Oncol, 2011. **104**(4): p. 341-53.
17. Chapman, P.B., et al., *Improved survival with vemurafenib in melanoma with BRAF V600E mutation.* N Engl J Med, 2011. **364**(26): p. 2507-16.
18. Balch, C.M., et al., *Final version of 2009 AJCC melanoma staging and classification.* J Clin Oncol, 2009. **27**(36): p. 6199-206.
19. Hodi, F.S., et al., *Improved survival with ipilimumab in patients with metastatic melanoma.* N Engl J Med, 2010. **363**(8): p. 711-23.
20. Griewank, K.G., *Biomarkers in melanoma.* Scand J Clin Lab Invest Suppl, 2016. **245**: p. S104-12.

21. Topalian, S.L., et al., *Survival, durable tumor remission, and long-term safety in patients with advanced melanoma receiving nivolumab.* J Clin Oncol, 2014. **32**(10): p. 1020-30.
22. Blank, C.U., et al., *CANCER IMMUNOLOGY. The "cancer immunogram".* Science, 2016. **352**(6286): p. 658-60.
23. Gray-Schopfer, V., C. Wellbrock, and R. Marais, *Melanoma biology and new targeted therapy.* Nature, 2007. **445**(7130): p. 851-7.
24. Bailey, C.M., J.A. Morrison, and P.M. Kulesa, *Melanoma revives an embryonic migration program to promote plasticity and invasion.* Pigment Cell Melanoma Res, 2012. **25**(5): p. 573-83.
25. Bertolotto, C., *Melanoma: from melanocyte to genetic alterations and clinical options.* Scientifica (Cairo), 2013. **2013**: p. 635203.
26. Testa, U., G. Castelli, and E. Pelosi, *Melanoma: Genetic Abnormalities, Tumor Progression, Clonal Evolution and Tumor Initiating Cells.* Med Sci (Basel), 2017. **5**(4).
27. Sommer, L., *Generation of melanocytes from neural crest cells.* Pigment Cell Melanoma Res, 2011. **24**(3): p. 411-21.
28. Mort, R.L., I.J. Jackson, and E.E. Patton, *The melanocyte lineage in development and disease.* Development, 2015. **142**(4): p. 620-32.
29. Lin, J.Y. and D.E. Fisher, *Melanocyte biology and skin pigmentation.* Nature, 2007. **445**(7130): p. 843-50.
30. Shain, A.H. and B.C. Bastian, *From melanocytes to melanomas.* Nat Rev Cancer, 2016. **16**(6): p. 345-58.
31. van Zijl, F., G. Krupitza, and W. Mikulits, *Initial steps of metastasis: cell invasion and endothelial transmigration.* Mutat Res, 2011. **728**(1-2): p. 23-34.
32. Gout, S., P.L. Tremblay, and J. Huot, *Selectins and selectin ligands in extravasation of cancer cells and organ selectivity of metastasis.* Clin Exp Metastasis, 2008. **25**(4): p. 335-44.
33. Valastyan, S. and R.A. Weinberg, *Tumor metastasis: molecular insights and evolving paradigms.* Cell, 2011. **147**(2): p. 275-92.
34. Fidler, I.J., *The pathogenesis of cancer metastasis: the 'seed and soil' hypothesis revisited.* Nat Rev Cancer, 2003. **3**(6): p. 453-8.
35. Horejs, C.M., *Basement membrane fragments in the context of the epithelial-to-mesenchymal transition.* Eur J Cell Biol, 2016. **95**(11): p. 427-440.
36. Gaggioli, C. and E. Sahai, *Melanoma invasion - current knowledge and future directions.* Pigment Cell Res, 2007. **20**(3): p. 161-72.
37. Sanz-Moreno, V., et al., *Rac activation and inactivation control plasticity of tumor cell movement.* Cell, 2008. **135**(3): p. 510-23.
38. Sahai, E. and C.J. Marshall, *Differing modes of tumour cell invasion have distinct requirements for Rho/ROCK signalling and extracellular proteolysis.* Nat Cell Biol, 2003. **5**(8): p. 711-9.
39. Parri, M., et al., *EphA2 reexpression prompts invasion of melanoma cells shifting from mesenchymal to amoeboid-like motility style.* Cancer Res, 2009. **69**(5): p. 2072-81.
40. Hegerfeldt, Y., et al., *Collective cell movement in primary melanoma explants: plasticity of cell-cell interaction, beta1-integrin function, and migration strategies.* Cancer Res, 2002. **62**(7): p. 2125-30.
41. Gandalovicova, A., et al., *Cell polarity signaling in the plasticity of cancer cell invasiveness.* Oncotarget, 2016. **7**(18): p. 25022-49.
42. Kalluri, R. and R.A. Weinberg, *The basics of epithelial-mesenchymal transition.* J Clin Invest, 2009. **119**(6): p. 1420-8.

43. Pearlman, R.L., et al., *Potential therapeutic targets of epithelial-mesenchymal transition in melanoma.* Cancer Lett, 2017. **391**: p. 125-140.
44. Li, F.Z., et al., *Phenotype switching in melanoma: implications for progression and therapy.* Front Oncol, 2015. **5**: p. 31.
45. Giampieri, S., et al., *Localized and reversible TGFbeta signalling switches breast cancer cells from cohesive to single cell motility.* Nat Cell Biol, 2009. **11**(11): p. 1287-96.
46. Ridley, A.J., et al., *Cell migration: integrating signals from front to back.* Science, 2003. **302**(5651): p. 1704-9.
47. Sanz-Moreno, V. and C.J. Marshall, *The plasticity of cytoskeletal dynamics underlying neoplastic cell migration.* Curr Opin Cell Biol, 2010. **22**(5): p. 690-6.
48. Aladowicz, E., et al., *Molecular networks in melanoma invasion and metastasis.* Future Oncol, 2013. **9**(5): p. 713-26.
49. Wolf, K., et al., *Compensation mechanism in tumor cell migration: mesenchymal-amoeboid transition after blocking of pericellular proteolysis.* J Cell Biol, 2003. **160**(2): p. 267-77.
50. Yamazaki, D., S. Kurisu, and T. Takenawa, *Involvement of Rac and Rho signaling in cancer cell motility in 3D substrates.* Oncogene, 2009. **28**(13): p. 1570-83.
51. Charras, G.T., et al., *Reassembly of contractile actin cortex in cell blebs.* J Cell Biol, 2006. **175**(3): p. 477-90.
52. Sanz-Moreno, V., et al., *ROCK and JAK1 signaling cooperate to control actomyosin contractility in tumor cells and stroma.* Cancer Cell, 2011. **20**(2): p. 229-45.
53. Sabeh, F., R. Shimizu-Hirota, and S.J. Weiss, *Protease-dependent versus -independent cancer cell invasion programs: three-dimensional amoeboid movement revisited.* J Cell Biol, 2009. **185**(1): p. 11-9.
54. Van Goethem, E., et al., *Matrix architecture dictates three-dimensional migration modes of human macrophages: differential involvement of proteases and podosome-like structures.* J Immunol, 2010. **184**(2): p. 1049-61.
55. Shain, A.H., et al., *The Genetic Evolution of Melanoma from Precursor Lesions.* N Engl J Med, 2015. **373**(20): p. 1926-36.
56. Kabbarah, O., et al., *Integrative genome comparison of primary and metastatic melanomas.* PLoS One, 2010. **5**(5): p. e10770.
57. Beadling, C., et al., *KIT gene mutations and copy number in melanoma subtypes.* Clin Cancer Res, 2008. **14**(21): p. 6821-8.
58. Ball, N.J., et al., *Ras mutations in human melanoma: a marker of malignant progression.* J Invest Dermatol, 1994. **102**(3): p. 285-90.
59. Davies, H., et al., *Mutations of the BRAF gene in human cancer.* Nature, 2002. **417**(6892): p. 949-54.
60. Wu, H., V. Goel, and F.G. Haluska, *PTEN signaling pathways in melanoma.* Oncogene, 2003. **22**(20): p. 3113-22.
61. Sharpless, E. and L. Chin, *The INK4a/ARF locus and melanoma.* Oncogene, 2003. **22**(20): p. 3092-8.
62. Kamb, A., et al., *Analysis of the p16 gene (CDKN2) as a candidate for the chromosome 9p melanoma susceptibility locus.* Nat Genet, 1994. **8**(1): p. 23-6.
63. Govindarajan, B., et al., *Malignant transformation of melanocytes to melanoma by constitutive activation of mitogen-activated protein kinase kinase (MAPKK) signaling.* J Biol Chem, 2003. **278**(11): p. 9790-5.
64. van den Hurk, K., et al., *Genetics and epigenetics of cutaneous malignant melanoma: a concert out of tune.* Biochim Biophys Acta, 2012. **1826**(1): p. 89-102.

65. Gray-Schopfer, V.C., S. da Rocha Dias, and R. Marais, *The role of B-RAF in melanoma.* Cancer Metastasis Rev, 2005. **24**(1): p. 165-83.
66. Huntington, J.T., et al., *Overexpression of collagenase 1 (MMP-1) is mediated by the ERK pathway in invasive melanoma cells: role of BRAF mutation and fibroblast growth factor signaling.* J Biol Chem, 2004. **279**(32): p. 33168-76.
67. Jiang, K., et al., *Akt mediates Ras downregulation of RhoB, a suppressor of transformation, invasion, and metastasis.* Mol Cell Biol, 2004. **24**(12): p. 5565-76.
68. Dankort, D., et al., *Braf(V600E) cooperates with Pten loss to induce metastatic melanoma.* Nat Genet, 2009. **41**(5): p. 544-52.
69. Shain, A.H., et al., *Genomic and Transcriptomic Analysis Reveals Incremental Disruption of Key Signaling Pathways during Melanoma Evolution.* Cancer Cell, 2018. **34**(1): p. 45-55 e4.
70. Zeng, H., et al., *Bi-allelic Loss of CDKN2A Initiates Melanoma Invasion via BRN2 Activation.* Cancer Cell, 2018. **34**(1): p. 56-68 e9.
71. Krauthammer, M., et al., *Exome sequencing identifies recurrent somatic RAC1 mutations in melanoma.* Nat Genet, 2012. **44**(9): p. 1006-14.
72. Bastian, B.C., *The molecular pathology of melanoma: an integrated taxonomy of melanocytic neoplasia.* Annu Rev Pathol, 2014. **9**: p. 239-71.
73. Ungefroren, H., D. Witte, and H. Lehnert, *The role of small GTPases of the Rho/Rac family in TGF-beta-induced EMT and cell motility in cancer.* Dev Dyn, 2018. **247**(3): p. 451-461.
74. Hoek, K.S., et al., *In vivo switching of human melanoma cells between proliferative and invasive states.* Cancer Res, 2008. **68**(3): p. 650-6.
75. Hoek, K.S., et al., *Metastatic potential of melanomas defined by specific gene expression profiles with no BRAF signature.* Pigment Cell Res, 2006. **19**(4): p. 290-302.
76. Eichhoff, O.M., et al., *Differential LEF1 and TCF4 expression is involved in melanoma cell phenotype switching.* Pigment Cell Melanoma Res, 2011. **24**(4): p. 631-42.
77. Holmquist, L., T. Lofstedt, and S. Pahlman, *Effect of hypoxia on the tumor phenotype: the neuroblastoma and breast cancer models.* Adv Exp Med Biol, 2006. **587**: p. 179-93.
78. de Visser, K.E., A. Eichten, and L.M. Coussens, *Paradoxical roles of the immune system during cancer development.* Nat Rev Cancer, 2006. **6**(1): p. 24-37.
79. Verfaillie, A., et al., *Decoding the regulatory landscape of melanoma reveals TEADS as regulators of the invasive cell state.* Nat Commun, 2015. **6**: p. 6683.
80. Nallet-Staub, F., et al., *Pro-invasive activity of the Hippo pathway effectors YAP and TAZ in cutaneous melanoma.* J Invest Dermatol, 2014. **134**(1): p. 123-32.
81. Sanchez, I.M. and A.E. Aplin, *Hippo: hungry, hungry for melanoma invasion.* J Invest Dermatol, 2014. **134**(1): p. 14-16.
82. Plass, C., *Cancer epigenomics.* Hum Mol Genet, 2002. **11**(20): p. 2479-88.
83. Doerfler, W., *DNA methylation and gene activity.* Annu Rev Biochem, 1983. **52**: p. 93-124.
84. Visone, R., et al., *DNA methylation of shelf, shore and open sea CpG positions distinguish high microsatellite instability from low or stable microsatellite status colon cancer stem cells.* Epigenomics, 2019. **11**(6): p. 587-604.
85. Rodriguez, J., et al., *Chromosomal instability correlates with genome-wide DNA demethylation in human primary colorectal cancers.* Cancer Res, 2006. **66**(17): p. 8462-9468.
86. Ogoshi, K., et al., *Genome-wide profiling of DNA methylation in human cancer cells.* Genomics, 2011. **98**(4): p. 280-7.

87. Kader, F., M. Ghai, and L. Maharaj, *The effects of DNA methylation on human psychology.* Behav Brain Res, 2018. **346**: p. 47-65.
88. Kulis, M., et al., *Intragenic DNA methylation in transcriptional regulation, normal differentiation and cancer.* Biochim Biophys Acta, 2013. **1829**(11): p. 1161-74.
89. Varley, K.E., et al., *Dynamic DNA methylation across diverse human cell lines and tissues.* Genome Res, 2013. **23**(3): p. 555-67.
90. Jones, P.A. and G. Liang, *Rethinking how DNA methylation patterns are maintained.* Nat Rev Genet, 2009. **10**(11): p. 805-11.
91. Herceg, Z. and P. Hainaut, *Genetic and epigenetic alterations as biomarkers for cancer detection, diagnosis and prognosis.* Mol Oncol, 2007. **1**(1): p. 26-41.
92. Hansen, K.D., et al., *Increased methylation variation in epigenetic domains across cancer types.* Nat Genet, 2011. **43**(8): p. 768-75.
93. Sigalotti, L., et al., *Epigenetics of human cutaneous melanoma: setting the stage for new therapeutic strategies.* J Transl Med, 2010. **8**: p. 56.
94. Schinke, C., et al., *Aberrant DNA methylation in malignant melanoma.* Melanoma Res, 2010. **20**(4): p. 253-65.
95. Guo, Y., J. Long, and S. Lei, *Promoter methylation as biomarkers for diagnosis of melanoma: A systematic review and meta-analysis.* Journal of Cellular Physiology, 2018.
96. *Genomic Classification of Cutaneous Melanoma.* Cell, 2015. **161**(7): p. 1681-96.
97. Lauss, M., et al., *Consensus of Melanoma Gene Expression Subtypes Converges on Biological Entities.* J Invest Dermatol, 2016. **136**(12): p. 2502-2505.
98. Micevic, G., N. Theodosakis, and M. Bosenberg, *Aberrant DNA methylation in melanoma: biomarker and therapeutic opportunities.* Clin Epigenetics, 2017. **9**: p. 34.
99. Tanemura, A., et al., *CpG island methylator phenotype predicts progression of malignant melanoma.* Clin Cancer Res, 2009. **15**(5): p. 1801-7.
100. de Unamuno Bustos, B., et al., *Aberrant DNA methylation is associated with aggressive clinicopathological features and poor survival in cutaneous melanoma.* Br J Dermatol, 2018. **179**(2): p. 394-404.
101. Fratta, E., et al., *Promoter methylation controls the intratumoral heterogeneity of Cancer/Testis antigens expression in human cutaneous melanoma: Immunotherapeutic implications of epigenetic drugs.* Environmental and Molecular Mutagenesis, 2006. **47**(6): p. 453-453.
102. Sigalotti, L., et al., *Epigenetic drugs as pleiotropic agents in cancer treatment: Biomolecular aspects and clinical applications.* Journal of Cellular Physiology, 2007. **212**(2): p. 330-344.
103. Lauss, M., et al., *Genome-Wide DNA Methylation Analysis in Melanoma Reveals the Importance of CpG Methylation in MITF Regulation.* J Invest Dermatol, 2015. **135**(7): p. 1820-8.
104. Maio, M., et al., *Epigenetic targets for immune intervention in human malignancies.* Oncogene, 2003. **22**(42): p. 6484-6488.
105. Orozco, J.I.J., et al., *Epigenetic profiling for the molecular classification of metastatic brain tumors.* Nat Commun, 2018. **9**(1): p. 4627.
106. Jin, S.G., et al., *The DNA methylation landscape of human melanoma.* Genomics, 2015. **106**(6): p. 322-30.
107. Marzese, D.M., et al., *Epigenome-wide DNA methylation landscape of melanoma progression to brain metastasis reveals aberrations on homeobox D cluster associated with prognosis.* Hum Mol Genet, 2014. **23**(1): p. 226-38.

108. de Araujo, E.S., et al., *DNA Methylation Levels of Melanoma Risk Genes Are Associated with Clinical Characteristics of Melanoma Patients.* Biomed Res Int, 2015. **2015**: p. 376423.
109. Chatterjee, A., et al., *Genome-wide methylation sequencing of paired primary and metastatic cell lines identifies common DNA methylation changes and a role for EBF3 as a candidate epigenetic driver of melanoma metastasis.* Oncotarget, 2017. **8**(4): p. 6085-6101.
110. Cheng, P.F., et al., *Methylation-dependent SOX9 expression mediates invasion in human melanoma cells and is a negative prognostic factor in advanced melanoma.* Genome Biol, 2015. **16**: p. 42.
111. Rastrelli, M., et al., *Melanoma m1: Diagnosis and Therapy.* In Vivo, 2014. **28**(3): p. 273-85.
112. Shtivelman, E., et al., *Pathways and therapeutic targets in melanoma.* Oncotarget, 2014.
113. Friedl, P. and D. Gilmour, *Collective cell migration in morphogenesis, regeneration and cancer.* Nat Rev Mol Cell Biol, 2009. **10**(7): p. 445-57.
114. Ladanyi, A., et al., *Sex-dependent liver metastasis of human melanoma lines in SCID mice.* Melanoma Res, 1995. **5**(2): p. 83-6.
115. Lazar, V., et al., *Characterization of candidate gene copy number alterations in the 11q13 region along with BRAF and NRAS mutations in human melanoma.* Mod Pathol, 2009. **22**(10): p. 1367-78.
116. Timar, J., et al., *Two human melanoma xenografts with different metastatic capacity and glycosaminoglycan pattern.* J Cancer Res Clin Oncol, 1989. **115**(6): p. 554-7.
117. Mueller, B.M., et al., *Suppression of spontaneous melanoma metastasis in scid mice with an antibody to the epidermal growth factor receptor.* Cancer Res, 1991. **51**(8): p. 2193-8.
118. Bibikova, M., et al., *High density DNA methylation array with single CpG site resolution.* Genomics, 2011. **98**(4): p. 288-95.
119. Du, P., W.A. Kibbe, and S.M. Lin, *lumi: a pipeline for processing Illumina microarray.* Bioinformatics, 2008. **24**(13): p. 1547-8.
120. Pidsley, R., et al., *A data-driven approach to preprocessing Illumina 450K methylation array data.* BMC Genomics, 2013. **14**: p. 293.
121. Aryee, M.J., et al., *Minfi: a flexible and comprehensive Bioconductor package for the analysis of Infinium DNA methylation microarrays.* Bioinformatics, 2014. **30**(10): p. 1363-9.
122. Chen, Y.A., et al., *Discovery of cross-reactive probes and polymorphic CpGs in the Illumina Infinium HumanMethylation450 microarray.* Epigenetics, 2013. **8**(2): p. 203-9.
123. Teschendorff, A.E., et al., *A beta-mixture quantile normalization method for correcting probe design bias in Illumina Infinium 450 k DNA methylation data.* Bioinformatics, 2013. **29**(2): p. 189-96.
124. Du, P., et al., *Comparison of Beta-value and M-value methods for quantifying methylation levels by microarray analysis.* BMC Bioinformatics, 2010. **11**: p. 587.
125. Smyth, G.K., *Linear models and empirical bayes methods for assessing differential expression in microarray experiments.* Stat Appl Genet Mol Biol, 2004. **3**: p. Article3.
126. Peters, T.J., et al., *De novo identification of differentially methylated regions in the human genome.* Epigenetics Chromatin, 2015. **8**: p. 6.
127. Triche, *FDb.InfiniumMethylation.hg19: Annotation package for Illumina Infinium DNA methylation probes.* . R package version 2.2.0. , 2014.
128. Martin, T.C., et al., *coMET: visualisation of regional epigenome-wide association scan results and DNA co-methylation patterns.* BMC Bioinformatics, 2015. **16**: p. 131.

129. Chen, E.Y., et al., *Enrichr: interactive and collaborative HTML5 gene list enrichment analysis tool.* BMC Bioinformatics, 2013. **14**: p. 128.
130. Gao, J., et al., *Integrative analysis of complex cancer genomics and clinical profiles using the cBioPortal.* Sci Signal, 2013. **6**(269): p. pl1.
131. Cerami, E., et al., *The cBio cancer genomics portal: an open platform for exploring multidimensional cancer genomics data.* Cancer Discov, 2012. **2**(5): p. 401-4.
132. Colaprico, A., et al., *TCGAbiolinks: an R/Bioconductor package for integrative analysis of TCGA data.* Nucleic Acids Res, 2016. **44**(8): p. e71.
133. Oghabian, A., D. Greco, and M.J. Frilander, *IntEREst: intron-exon retention estimator.* BMC Bioinformatics, 2018. **19**(1): p. 130.
134. Fernandez-Jimenez, N., et al., *Accuracy in copy number calling by qPCR and PRT: a matter of DNA.* PLoS One, 2011. **6**(12): p. e28910.
135. Diskin, S.J., et al., *Copy number variation at 1q21.1 associated with neuroblastoma.* Nature, 2009. **459**(7249): p. 987-91.
136. Mayes, D.A., et al., *PAX6 suppresses the invasiveness of glioblastoma cells and the expression of the matrix metalloproteinase-2 gene.* Cancer Res, 2006. **66**(20): p. 9809-17.
137. Hunter, K.W., et al., *Genetic insights into the morass of metastatic heterogeneity.* Nat Rev Cancer, 2018. **18**(4): p. 211-223.
138. Werner-Klein, M., et al., *Genetic alterations driving metastatic colony formation are acquired outside of the primary tumour in melanoma.* Nat Commun, 2018. **9**(1): p. 595.
139. Stark, M. and N. Hayward, *Genome-wide loss of heterozygosity and copy number analysis in melanoma using high-density single-nucleotide polymorphism arrays.* Cancer Res, 2007. **67**(6): p. 2632-42.
140. Lin, W.M., et al., *Modeling genomic diversity and tumor dependency in malignant melanoma.* Cancer Res, 2008. **68**(3): p. 664-73.
141. Jonsson, G., et al., *Genomic profiling of malignant melanoma using tiling-resolution arrayCGH.* Oncogene, 2007. **26**(32): p. 4738-48.
142. Lazar, V., et al., *Marked genetic differences between BRAF and NRAS mutated primary melanomas as revealed by array comparative genomic hybridization.* Melanoma Res, 2012. **22**(3): p. 202-14.
143. Bis, S. and H. Tsao, *Melanoma genetics: the other side.* Clin Dermatol, 2013. **31**(2): p. 148-55.
144. Swick, J.M. and J.C. Maize, Sr., *Molecular biology of melanoma.* J Am Acad Dermatol, 2012. **67**(5): p. 1049-54.
145. Ghosh, P. and L. Chin, *Genetics and genomics of melanoma.* Expert Rev Dermatol, 2009. **4**(2): p. 131.
146. Miller, A.J. and M.C. Mihm, Jr., *Melanoma.* N Engl J Med, 2006. **355**(1): p. 51-65.
147. Rakosy, Z., et al., *EGFR gene copy number alterations in primary cutaneous malignant melanomas are associated with poor prognosis.* Int J Cancer, 2007. **121**(8): p. 1729-37.
148. Villa-Moruzzi, E., *Tyrosine phosphatases in the HER2-directed motility of ovarian cancer cells: Involvement of PTPN12, ERK5 and FAK.* Anal Cell Pathol (Amst), 2011. **34**(3): p. 101-12.
149. Lee, S.J., et al., *Over-expression of miR-145 enhances the effectiveness of HSVtk gene therapy for malignant glioma.* Cancer Lett, 2012. **320**(1): p. 72-80.
150. Planutis, K., et al., *Invasive colon cancer, but not non-invasive adenomas induce a gradient effect of Wnt pathway receptor frizzled 1 (Fz1) expression in the tumor microenvironment.* J Transl Med, 2013. **11**: p. 50.

151. Becker, J., et al., *Keratoepithelin reverts the suppression of tissue factor pathway inhibitor 2 by MYCN in human neuroblastoma: a mechanism to inhibit invasion.* Int J Oncol, 2008. **32**(1): p. 235-40.
152. Matise, L.A., et al., *Lack of transforming growth factor-beta signaling promotes collective cancer cell invasion through tumor-stromal crosstalk.* Breast Cancer Res, 2012. **14**(4): p. R98.
153. Sahai, E., et al., *Smurf1 regulates tumor cell plasticity and motility through degradation of RhoA leading to localized inhibition of contractility.* J Cell Biol, 2007. **176**(1): p. 35-42.
154. Mitra, A., et al., *Large isoform of MRJ (DNAJB6) reduces malignant activity of breast cancer.* Breast Cancer Res, 2008. **10**(2): p. R22.
155. Lin, Z.Y. and W.L. Chuang, *Genes responsible for the characteristics of primary cultured invasive phenotype hepatocellular carcinoma cells.* Biomed Pharmacother, 2012. **66**(6): p. 454-8.
156. Awasthi, A., et al., *Variable Expression of GLIPR1 Correlates with Invasive Potential in Melanoma Cells.* Front Oncol, 2013. **3**: p. 225.
157. Wiesenhofer, B., C. Weis, and C. Humpel, *Glial cell line-derived neurotrophic factor (GDNF) is a proliferation factor for rat C6 glioma cells: evidence from antisense experiments.* Antisense Nucleic Acid Drug Dev, 2000. **10**(5): p. 311-21.
158. Narita, N., et al., *Functional RET G691S polymorphism in cutaneous malignant melanoma.* Oncogene, 2009. **28**(34): p. 3058-68.
159. Chen, G., et al., *Enhanced expression and significance of glycosylphosphatidylinositol anchor attachment protein 1 in colorectal cancer.* Genet Mol Res, 2014. **13**(1): p. 499-507.
160. Wu, G., et al., *Overexpression of glycosylphosphatidylinositol (GPI) transamidase subunits phosphatidylinositol glycan class T and/or GPI anchor attachment 1 induces tumorigenesis and contributes to invasion in human breast cancer.* Cancer Res, 2006. **66**(20): p. 9829-36.
161. McInroy, L. and A. Maatta, *Plectin regulates invasiveness of SW480 colon carcinoma cells and is targeted to podosome-like adhesions in an isoform-specific manner.* Exp Cell Res, 2011. **317**(17): p. 2468-78.
162. Zhang, Y., et al., *Activation of nuclear factor kappaB pathway and downstream targets survivin and livin by SHARPIN contributes to the progression and metastasis of prostate cancer.* Cancer, 2014. **120**(20): p. 3208-18.
163. Pollock, P.M., et al., *High frequency of BRAF mutations in nevi.* Nat Genet, 2003. **33**(1): p. 19-20.
164. Safaee Ardekani, G., et al., *The prognostic value of BRAF mutation in colorectal cancer and melanoma: a systematic review and meta-analysis.* PLoS One, 2012. **7**(10): p. e47054.
165. Poynter, J.N., et al., *BRAF and NRAS mutations in melanoma and melanocytic nevi.* Melanoma Res, 2006. **16**(4): p. 267-73.
166. Machnicki, M.M. and T. Stoklosa, *BRAF - A new player in hematological neoplasms.* Blood Cells Mol Dis, 2014.
167. Greshock, J., et al., *Distinct patterns of DNA copy number alterations associate with BRAF mutations in melanomas and melanoma-derived cell lines.* Genes Chromosomes Cancer, 2009. **48**(5): p. 419-28.
168. Gaggioli, C., et al., *Tumor-derived fibronectin is involved in melanoma cell invasion and regulated by V600E B-Raf signaling pathway.* J Invest Dermatol, 2007. **127**(2): p. 400-10.

169. Woods, D., et al., *Induction of beta3-integrin gene expression by sustained activation of the Ras-regulated Raf-MEK-extracellular signal-regulated kinase signaling pathway.* Mol Cell Biol, 2001. **21**(9): p. 3192-205.
170. Morey, A.L., et al., *Diagnosis of cutaneous melanocytic tumours by four-colour fluorescence in situ hybridisation.* Pathology, 2009. **41**(4): p. 383-7.
171. Kim, M., et al., *Comparative oncogenomics identifies NEDD9 as a melanoma metastasis gene.* Cell, 2006. **125**(7): p. 1269-81.
172. Bonazzi, V.F., et al., *Cross-platform array screening identifies COL1A2, THBS1, TNFRSF10D and UCHL1 as genes frequently silenced by methylation in melanoma.* PLoS One, 2011. **6**(10): p. e26121.
173. Koga, Y., et al., *Genome-wide screen of promoter methylation identifies novel markers in melanoma.* Genome Res, 2009. **19**(8): p. 1462-70.
174. Conway, K., et al., *DNA-methylation profiling distinguishes malignant melanomas from benign nevi.* Pigment Cell Melanoma Res, 2011. **24**(2): p. 352-60.
175. Levy, C., M. Khaled, and D.E. Fisher, *MITF: master regulator of melanocyte development and melanoma oncogene.* Trends Mol Med, 2006. **12**(9): p. 406-14.
176. Steingrimsson, E., N.G. Copeland, and N.A. Jenkins, *Melanocytes and the microphthalmia transcription factor network.* Annu Rev Genet, 2004. **38**: p. 365-411.
177. Dadras, S.S., et al., *A novel role for microphthalmia-associated transcription factor-regulated pigment epithelium-derived factor during melanoma progression.* Am J Pathol, 2015. **185**(1): p. 252-65.
178. Lauss, M., et al., *DNA methylation subgroups in melanoma are associated with proliferative and immunological processes.* BMC Med Genomics, 2015. **8**: p. 73.
179. Ecsedi, S., et al., *DNA methylation characteristics of primary melanomas with distinct biological behaviour.* PLoS One, 2014. **9**(5): p. e96612.
180. Lo Nigro, C., et al., *Methylated tissue factor pathway inhibitor 2 (TFPI2) DNA in serum is a biomarker of metastatic melanoma.* J Invest Dermatol, 2013. **133**(5): p. 1278-85.
181. Tuominen, R., et al., *MGMT promoter methylation is associated with temozolomide response and prolonged progression-free survival in disseminated cutaneous melanoma.* Int J Cancer, 2015. **136**(12): p. 2844-53.
182. Bax, D.V., et al., *Cell adhesion to fibrillin-1 molecules and microfibrils is mediated by alpha 5 beta 1 and alpha v beta 3 integrins.* J Biol Chem, 2003. **278**(36): p. 34605-16.
183. Limm, K., et al., *The metabolite 5'-methylthioadenosine signals through the adenosine receptor A2B in melanoma.* Eur J Cancer, 2014. **50**(15): p. 2714-24.
184. Yu, W., et al., *Overexpression of miR-21-5p promotes proliferation and invasion of colon adenocarcinoma cells through targeting CHL1.* Mol Med, 2018. **24**(1): p. 36.
185. Senchenko, V.N., et al., *Differential expression of CHL1 gene during development of major human cancers.* PLoS One, 2011. **6**(3): p. e15612.
186. Chatterjee, A., et al., *Marked Global DNA Hypomethylation Is Associated with Constitutive PD-L1 Expression in Melanoma.* iScience, 2018. **4**: p. 312-325.
187. Sarkar, D., et al., *Epigenetic regulation in human melanoma: past and future.* Epigenetics, 2015. **10**(2): p. 103-21.
188. Lister, R., et al., *Human DNA methylomes at base resolution show widespread epigenomic differences.* Nature, 2009. **462**(7271): p. 315-22.
189. Haydn, J.M., et al., *The MAPK pathway as an apoptosis enhancer in melanoma.* Oncotarget, 2014. **5**(13): p. 5040-53.
190. Uribe, P. and S. Gonzalez, *Epidermal growth factor receptor (EGFR) and squamous cell carcinoma of the skin: molecular bases for EGFR-targeted therapy.* Pathol Res Pract, 2011. **207**(6): p. 337-42.

191. Wang, J., et al., *Epigenetic changes of EGFR have an important role in BRAF inhibitor-resistant cutaneous melanomas.* J Invest Dermatol, 2015. **135**(2): p. 532-541.
192. Boone, B., et al., *EGFR in melanoma: clinical significance and potential therapeutic target.* J Cutan Pathol, 2011. **38**(6): p. 492-502.
193. Gross, A., et al., *Expression and activity of EGFR in human cutaneous melanoma cell lines and influence of vemurafenib on the EGFR pathway.* Target Oncol, 2015. **10**(1): p. 77-84.
194. Raghu, P. and B. Sivakumar, *Interactions amongst plasma retinol-binding protein, transthyretin and their ligands: implications in vitamin A homeostasis and transthyretin amyloidosis.* Biochim Biophys Acta, 2004. **1703**(1): p. 1-9.
195. Fei, W., et al., *RBP4 and THBS2 are serum biomarkers for diagnosis of colorectal cancer.* Oncotarget, 2017. **8**(54): p. 92254-92264.
196. Wang, Y. and Z. Zhang, *Adipokine RBP4 drives ovarian cancer cell migration.* J Ovarian Res, 2018. **11**(1): p. 29.
197. Chen, C., et al., *Nicotinamide N-methyltransferase: a potential biomarker for worse prognosis in gastric carcinoma.* Am J Cancer Res, 2016. **6**(3): p. 649-63.
198. Tang, S.W., et al., *Nicotinamide N-methyltransferase induces cellular invasion through activating matrix metalloproteinase-2 expression in clear cell renal cell carcinoma cells.* Carcinogenesis, 2011. **32**(2): p. 138-45.
199. Shah, N. and S. Sukumar, *The Hox genes and their roles in oncogenesis.* Nat Rev Cancer, 2010. **10**(5): p. 361-71.
200. Furuta, J., et al., *Silencing of Peroxiredoxin 2 and aberrant methylation of 33 CpG islands in putative promoter regions in human malignant melanomas.* Cancer Res, 2006. **66**(12): p. 6080-6.
201. Rauch, T.A., et al., *DNA methylation biomarkers for lung cancer.* Tumour Biol, 2012. **33**(2): p. 287-96.
202. Tommasi, S., et al., *Methylation of homeobox genes is a frequent and early epigenetic event in breast cancer.* Breast Cancer Res, 2009. **11**(1): p. R14.
203. Rodrigues, M.F., et al., *Methylation status of homeobox genes in common human cancers.* Genomics, 2016. **108**(5-6): p. 185-193.
204. Maes, T., A. Barcelo, and C. Buesa, *Neuron navigator: a human gene family with homology to unc-53, a cell guidance gene from Caenorhabditis elegans.* Genomics, 2002. **80**(1): p. 21-30.
205. Alinezhad, S., et al., *Validation of Novel Biomarkers for Prostate Cancer Progression by the Combination of Bioinformatics, Clinical and Functional Studies.* PLoS One, 2016. **11**(5): p. e0155901.
206. Liu, S., et al., *Genetic variants in the genes encoding rho GTPases and related regulators predict cutaneous melanoma-specific survival.* Int J Cancer, 2017. **141**(4): p. 721-730.
207. Stringham, E.G. and K.L. Schmidt, *Navigating the cell: UNC-53 and the navigators, a family of cytoskeletal regulators with multiple roles in cell migration, outgrowth and trafficking.* Cell Adh Migr, 2009. **3**(4): p. 342-6.
208. Tan, F., et al., *Neuron navigator 2 overexpression indicates poor prognosis of colorectal cancer and promotes invasion through the SSH1L/cofilin-1 pathway.* J Exp Clin Cancer Res, 2015. **34**: p. 117.
209. Hu, W., et al., *NAV2 facilitates invasion of cutaneous melanoma cells by targeting SNAI2 through the GSK-3beta/beta-catenin pathway.* Arch Dermatol Res, 2019. **311**(5): p. 399-410.
210. Pankova, K., et al., *The molecular mechanisms of transition between mesenchymal and amoeboid invasiveness in tumor cells.* Cell Mol Life Sci, 2010. **67**(1): p. 63-71.

211. Liu, X.D., et al., *[Relationship between DNMT1 and Methylation of SHP-1 Promoter 2 in K562 Cells].* Zhongguo Shi Yan Xue Ye Xue Za Zhi, 2018. **26**(2): p. 401-406.
212. Xi, Y.B., et al., *Radiomics signature: A potential biomarker for the prediction of MGMT promoter methylation in glioblastoma.* J Magn Reson Imaging, 2018. **47**(5): p. 1380-1387.
213. Jia, Y., et al., *Negative regulation of DNMT3A de novo DNA methylation by frequently overexpressed UHRF family proteins as a mechanism for widespread DNA hypomethylation in cancer.* Cell Discov, 2016. **2**: p. 16007.
214. Lu, H., et al., *Loss of UHRF2 expression is associated with human neoplasia, promoter hypermethylation, decreased 5-hydroxymethylcytosine, and high proliferative activity.* Oncotarget, 2016. **7**(46): p. 76047-76061.
215. Molognoni, F., et al., *Epigenetic reprogramming as a key contributor to melanocyte malignant transformation.* Epigenetics, 2011. **6**(4): p. 450-64.
216. Zhu, Y.B., et al., *A lncRNA-H19 transcript from secondary hair follicle of Liaoning cashmere goat: Identification, regulatory network and expression regulated potentially by its promoter methylation.* Gene, 2018. **641**: p. 78-85.
217. Ancey, P.B., et al., *TET-Catalyzed 5-Hydroxymethylation Precedes HNF4A Promoter Choice during Differentiation of Bipotent Liver Progenitors.* Stem Cell Reports, 2017. **9**(1): p. 264-278.
218. Gomes, C.B., et al., *TET2 Negatively Regulates Nestin Expression in Human Melanoma.* Am J Pathol, 2016. **186**(6): p. 1427-34.

Publications

UNIVERSITY of DEBRECEN

UNIVERSITY AND NATIONAL LIBRARY
UNIVERSITY OF DEBRECEN
H-4002 Egyetem tér 1, Debrecen
Phone: +3652/410-443, email: publikaciok@lib.unideb.hu

Registry number: DEENK/14/2020.PL
Subject: PhD Publikációs Lista

Candidate: Viktória Koroknai
Neptun ID: EBWBZY
Doctoral School: Doctoral School of Health Sciences
MTMT ID: 10044575

List of publications related to the dissertation

1. **Koroknai, V.**, Szász, I., Hernandez, V. H., Fernandez, J. N., Cuenin, C., Herceg, Z., Vízkeleti, L., Ádány, R., Ecsedi, S., Balázs, M.: DNA hypermethylation is associated with invasive phenotype of malignant melanoma.
Exp. Dermatol. [Epub ahead of print], 2019.
DOI: http://dx.doi.org/10.1111/exd.14047
IF: 2.868 (2018)

2. **Koroknai, V.**, Ecsedi, S., Vízkeleti, L., Kiss, T., Szász, I., Lukács, A., Papp, O., Ádány, R., Balázs, M.: Genomic profiling of invasive melanoma cell lines by array comparative genomic hybridization.
Melanoma Res. 2, 100-107, 2016.
DOI: http://dx.doi.org/10.1097/CMR.0000000000000227
IF: 2.615

List of other publications

3. Szász, I., **Koroknai, V.**, Kiss, T., Vízkeleti, L., Ádány, R., Balázs, M.: Molecular alterations associated with acquired resistance to BRAFV600E targeted therapy in melanoma cells.
Melanoma Res. 29 (4), 390-400, 2019.
DOI: http://dx.doi.org/10.1097/CMR.0000000000000588
IF: 2.381 (2018)

4. Balázs, M., **Koroknai, V.**, Szász, I., Ecsedi, S.: Detection of CCND1 Locus Amplification by Fluorescence In Situ Hybridization.
In: The Retinoblastoma Protein. Ed.: Pedro G. Santiago-Cardona, Springer Science+Business Media, New York, NY, 85-100, 2018.

UNIVERSITY of DEBRECEN

UNIVERSITY AND NATIONAL LIBRARY
UNIVERSITY OF DEBRECEN
H-4002 Egyetem tér 1, Debrecen
Phone: +3652/410-443, email: publikaciok@lib.unideb.hu

5. Vízkeleti, L., Kiss, T., **Koroknai, V.**, Ecsedi, S., Papp, O., Szász, I., Ádány, R., Balázs, M.: Altered integrin expression patterns revealed by microarray in human cutaneous melanoma.
Melanoma Res. 27 (3), 180-188, 2017.
IF: 3.135

6. Kiss, T., Ecsedi, S., Vízkeleti, L., **Koroknai, V.**, Emri, G., Kovács, N., Ádány, R., Balázs, M.: The role of osteopontin expression in melanoma progression.
Tumor Biol. 36 (10), 7841-7847, 2015.
DOI: http://dx.doi.org/10.1007/s13277-015-3495-y
IF: 2.926

7. Ecsedi, S., Hernandez, V. H., Lima, S. C., Vízkeleti, L., Tóth, R., Lázár, V., **Koroknai, V.**, Kiss, T., Emri, G., Herceg, Z., Ádány, R., Balázs, M.: DNA methylation characteristics of primary melanomas with distinct biological behaviour.
PloS One. 9 (5), e96612, 2014.
DOI: http://dx.doi.org/10.1371/journal.pone.0096612
IF: 3.234

8. Vízkeleti, L., Ecsedi, S., Rákosy, Z., Orosz, A., Lázár, V., Emri, G., **Koroknai, V.**, Kiss, T., Ádány, R., Balázs, M.: The role of CCND1 alterations during the progression of cutaneous malignant melanoma.
Tumor Biol. 33 (6), 2189-2199, 2012.
DOI: http://dx.doi.org/10.1007/s13277-012-0480-6
IF: 2.518

Total IF of journals (all publications): 19,677
Total IF of journals (publications related to the dissertation): 5,483

The Candidate's publication data submitted to the iDEa Tudóstér have been validated by DEENK on the basis of the Journal Citation Report (Impact Factor) database.

16 January, 2020

DEBRECENI EGYETEM Egyetemi és Nemzeti Könyvtár

Keywords

malignant melanoma, invasion, metastasis, selected invasive cells, BRAF mutation, array comparative genomic hybridization, copy number alteration, DNA methylation, differentially methylated regions

Kulcsszavak

malignus melanoma, inváció, metasztázis, szelektált invazív sejtek, BRAF mutáció, komparatív hibridizációs array, kópiaszám eltérés, DNS metiláció, régiószintű metilációs eltérések

Acknowledgements

First and foremost I wish to thank my supervisor Professor Margit Balázs , who has introduced me into the world of cancer research, and helped and guided my research during both my undergraduate and graduate research studies, and providing me the opportunity to learn a wide variety of molecular genetic techniques and different types of analysis.

I would like to express my thankfulness to Professor Róza Ádány for providing me the opportunity to work in the MTA-DE Public Health Research Group, as well as for all of her support during PhD study.

I am thankful for my colleagues István Szász, Tímea Kiss and Szilvia Ecsedi for their always generous help and their critique during my experiments.

I would like to acknowledge my colleagues of the Department of Preventive Medicine for their help during my experiments, especially to Györgyné Kovács for her assistance.

Finally, I would like to say special thanks to my family for their support and patient.

Financial supports

This research was supported by the Hungarian National Research Fund (OTKA K75191, OTKA K112327, and OTKA K81847) and the TÁMOP-4.2.2.A-11/1/KONV-2012–0031 project; the TÁMOP project is co-financed by the European Union and the European Social Fund. The work was co-financed by the European Union under the European Social Fund and European Regional Development Fund (GINOP-2.3.2-15-2016-00005). This research was also supported by ÚNKP-18-3 and ÚNKP-19-3 New National Excellence Programs of the Ministry of Human Capacities and by the IARC Postdoctoral Fellowship and Marie Curie Actions-People-COFUND.

Appendix

Supplementary Table 1 - Primer sequences used in RT-qPCR experiments

Gene	Primer sequence (5'-3')[1]	Amplicon size (bp)[2]
GNDF	F: GAAGCAGCAGTTACCAGACA	87
	R: GGAGCAGAAAGGACAGAGAAG	
PTPN12	F: GGTGCTGTGACCCAGAATAA	70
	R: CAGTACTAGTGGCAGCAGAAA	
ADAM22	F: GTGTCTTCCTGTGGCTTCTT	69
	R: CCTGAGCAAATAGTGCCTTCT	
FZD1	F: AAGACCGAGTGGTGTGTAATG	100
	R: AGCATCATGAAGAGGATGGTG	
TFPI2	F: GTCAGGGACTGGTTGAAGATT	100
	R: CTAGGCCCTGTGTTTCTTATGT	
GNG11	F: GTGCTACTCATCTTTGCTCACTA	60
	R: ACATCTGATACTCTCTGCTCTCT	
COL1A2	F: AGAGTGGAGCAGTGGTTACTA	100
	R: GATACAGGTTTCGCCAGTAGAG	
SMURF1	F: GGAGTCTTACCGCCAGATAATG	96
	R: CCACCGTAATCCAAACCTTCT	
VGF	F: TGTGTGAAGTGTGTCTGTCTC	74
	R: ATTCACAGCGACTTGGAGAG	
RELN	F: TCATGGCACCCATTGGTAAG	75
	R: CAGGATCCGTTGCAGATGATAG	
GPAA1	F: TGGGCCAAAGATATCGTCTTC	88
	R: TGACATTGACATCGTGGTAGG	
PLEC	F: GGCACTGCGTAGGAAATACA	100
	R: CTCGTTCAGCTGTTCCTTCTC	
SHARPIN	F: CCTTCCTGCACCTTCATCAAT	61
	R: TCTGGGTGCTACACATCTCA	
DNMT1	F: GATGTGGCGTCTGTGAGGT	60
	R: CCTTGCAGGCTTTACATTTCC	
DNMT3A	F: CCTGAAGCCTCAAGAGCAGT	94
	R: TGGTCTCCTTCTGTTCTTTGC	
DNMT3B	F: CAAATGGCTTCAGATGTTGC	67
	R: TCCTGCCACAAGACAAACAG	
TET1	F: GCTATACACAGAGCTCACAG	139
	R: GCCAAAAGAGAATGAAGCTCC	
TET2	F: CTTTCCTCCCTGGAGAACAGCTC	146
	R: TGCTGGGACTGCTGCATGACT	
UHRF1	F: CGTGGTCCAGATGAACTCC	193
	R: CACGTTGGCGTAGAGTTCC	
UHRF2	F: GGACCTTCCAATCAGCC	120

	R: TTCAAACCAAGCACCAA	
MITF	F: GTGTCACTGATCCACTCCTTTC	87
	R: CCGTCTCTTCCATGCTCATAC	
TERC	F: CCTAACTGAGAAGGGCGTAG	114
	R: TCTAGAATGAACGGTGGAAGG	
CDH13	F: AACGACAAGCTACGCTATGAG	95
	R: TTGCCCACTGCAGTTATGT	
PAX6	F: CAGCCAGACCTCCTCATACT	117
	R: CCCATTGGCTGACTGTTCAT	
NNMT	F: GAGGTGATCTCGCAAAGTTATTC	67
	R: TCGCCACCAGGGAGAAAAG	
EDNRB	F: CTGCTGCACATCGTCATTGAC	71
	R: GCTCCAAATGGCCAGTCCT	
HCK	F: CACACCAGGAATCAGGGAGG	88
	R: GCTGAGGTCTTCGTGGTGAA	
ST8SIA1	F: AGAGCATGTGGTATGACGGG	86
	R: GGGAGATTGCATCTGTGGGA	
RHOB	F: GTGTGTCTGTTCGACTCCCC	134
	R: AGGGATATCAAGCTCCCGCT	
ID4	F: CCGAGCCAGGAGCACTAGAG	116
	R: CTTGGAATGACGAATGAAAACG	
EGFR	F: TTTGCCAAGGCACGAGTAACAAGC	104
	R: ATTCCCAAGGACCACCTCACAGTT	
LEF1	F: CCGAAGAGGAAGGCGATTTAG	111
	R: CCTGAGAGGTTTGTGCTTGT	
PMEL	F: GTCAGCACCCAGCTTATCAT	97
	R: CAAGGACCACAGCCATCAA	
GAPDH	F: AGCCACATCGCTCAGACAC	66
	R: GCCCAATACGACCAAATCC	

[1]F: forward, R: reverse; [2]bp: base pair

Supplementary Table 2-7 are available at

https://onlinelibrary.wiley.com/doi/full/10.1111/exd.14047